Characterization of human bone marrow derived mesenchymal stem cells as a model for in vitro adipocytes studies

Inaugraldissertation

zur
Erlangung der Würde eines Doktors der Philosophie
vorgelegt der
Philosophisch-Naturwissenschaftlichen Fakultät der Universität Basel

von

Estelle Hirzel

aus Rapperswil, Kanton Bern

Grafenried, 2013

Genehmigt von der Philosophisch-Naturwissenschaftlichen Fakultät der Universität Basel auf Antrag von

Prof. Dr. Alex N. Eberle

Prof. Dr. Stephan Krähenbühl

Basel, den 18.10. 2011

Prof. Dr. Martin Spiess

Dekan

Psalm 103, 2

Table of content

Abbrevations

BAT	brown adipose tissue
BMI	body mass index: (kg body weight / height in meter^2)
C/EBP	CCAAT/enhancer-binding protein
CJ	cristae junction
CM	cristae membrane
CoQ	coenzyme Q
CuZnSOD	copper-zinc superoxide dismutase
cyt *c*	cytochrome *c*
Drp1	utropin
ECAR	extracellular acidification rate
ETC	electron transport chain
FAD / $FADH_2$	oxidized / reduced flavin adenine dinucleotide
FCCP	carbonyl cyanide 4-(trifluoromethoxy)phenylhydrazone
FFA	free fatty acid
Fis1	mitochondrial fission protein 1
GLUT4	glucose transporter type 4
GSH-PX	glutathione peroxidase
GSSG / GSH	oxidized / reduced glutathione
HAT	histone acetyl transferase
Hb	hemoglobin
hBM-MSC	human bone marrow derived mesenchymal stem cell
HDL	high-density lipoprotein
HSA	human serum albumin
IBM	inner boundary membrane
IGF	insulin growth factor
IL-6	interleukin-6
IMM	inner mitochondrial membrane
IMS	intermembrane space
IRe	insulin resistance
IRS	insulin receptor substrate
ISP	iron-sulfur protein / Rieske protein
LDL	low-density lipoprotein
MCP-1	monocyte chemoattractant protein 1

Mff	mitochondrial fission factor
Mfn1 / Mfn2	mitofusin 1 / mitofusin 2
MM	mitochondrial matrix
MMP	matrix metalloprotease
MnSOD	manganese superoxide dismutase
MOMP	mitochondrial outer membrane permeabilization
MSC	mesenchymal stem cell
mtDNA	mitochondrial DNA
Myf	myogenic factor
NAD+ / NADH	oxidized / reduced nicotinamide adenine dinucleotide
NFκB	Nuclear factor NF-kappa-B
NR	nuclear receptor
OMM	outer mitochondrial membrane
Opa1	mitochondrial dynamin-like 120 kDa protein
oxphos	oxidative phosphorylation
PGC-1α	Peroxisome proliferator-activated receptor gamma coactivator 1-alpha
PI3K	phosphoinositide 3-kinase
PPARγ	peroxisome proliferator-activated receptor gamma
Q_i / Q_o	inner / outer side of the IMM
ROS	reactive oxygen species
SCAT	subcutaneous adipose tissue
SIRT	NAD-dependent deacetylase sirtuin
SOD	superoxide dismutase
SRC	steroid receptor coactivator
STAT3	signal transducer and activator of transcription 3
T2DM	type 2 diabetes mellitus
TG	triglyceride
TLR4	toll-like receptor 4
TNFα	tumor necrosis factor alpha
TPP	triphenylphosphonium cation
tRNA	transfer RNA
UCP1	uncoupling protein 1
VAT	visceral adipose tissue

WAT	white adipose tissue

1 Summary

Overweight and obesity are major problems of public health in many countries worldwide. Overweight can cause severe diseases such as type II diabetes mellitus, hypertension, stroke, heart failure and several types of cancer. In addition, inflammatory cytokines and oxidative stress are increased in overweight people. Reactive oxygen species have been shown to cause insulin resistance (IRe) *in vitro* and IRe has been reported to correlate with a decrease in antioxidative capacity.

To support research in this relevant field of our society, a good *in vitro* model for adipocytes and adipogenesis is necessary. However, most *in vitro* studies about adipocyte function are currently done with murine cell lines. These models have the disadvantages that they may not reflect the (patho-)physiologic situation in humans because of species differences. Another problem resides in major physiologic differences between immortalized and primary cells, particularly in view of their reaction to oxidative stress. As elevated oxidative stress is supposed to contribute to the development of type II diabetes mellitus (T2DM) in obese people, it might be advantageous to apply antioxidant treatments for these patients.

In this thesis two studies are presented. In the first study, human bone marrow derived mesenchymal stem cells (hBM-MSCs) are described and investigated as a model for (primary) adipocytes and adipogenesis. In the second study hBM-MSC derived adipocytes were treated with the well-characterized antioxidants MitoQ, resveratrol and curcumin and the effects of these substances on different mitochondrial parameters were determined.

In the first study, hBM-MSCs were grown to confluence and adipocyte differentiation was induced by differentiation medium. Cell number and protein content, fat accumulation, production of reactive oxygen species (ROS), cellular oxygen consumption, mitochondrial mass and morphology were assessed during a differentiation period of 22 days. The cell number did not change but the protein content increased markedly during adipogenesis, indicating that the cell mass increased over time. ROS production was measured with two different assays showing either oxidizing or reducing radicals. Both methods showed an increase in ROS, indicating that overall oxidative stress increased during adipocyte differentiation. Oxygen consumption of intact cells was measured with a Seahorse

flux analyzer. Basal respiration as well as leak respiration and uncoupled oxygen consumption increased during adipogenesis. This result suggests an increase in mitochondrial mass. Therefore, mitochondrial content in a defined cytoplasmic volume was quantified using confocal microscopy. A distinct elevation of mitochondrial mass during adipocyte differentiation was observed. Mitochondrial morphology also changed during the differentiation process. During adipocyte differentiation mitochondria built a tight network while electron microscopy revealed that their inner morphology and cristae structure did not change.

In the second study, the effects of MitoQ, resveratrol and curcumin on ROS production, oxygen consumption, glycolysis and intracellular ATP content were assessed. All three substances were used at non-toxic concentrations. MitoQ lowered ROS production of oxidizing and reducing radicals, resveratrol and curcumin only decreased reducing and oxidizing radicals, respectively. The immediate effect of these antioxidants on oxygen consumption was measured in an Oxygraph; respiration after 24 h treatment was assessed with a Seahorse flux analyzer. Upon addition, all substances tested slightly decreased oxygen consumption. However, after 24 h only MitoQ inhibited the respiration. Intracellular ATP content did not change in response to any treatment.

In coclusion, hBM-MSC derived adipocytes are an interesting model for human fat cells *in vitro*. They efficiently differentiated into fat cells and shared many, but not all characteristics with the murine cells lines commonly used in this research. In fact, these cultured hBM-MSCs are one of the closest models to the human adipose tissue for *in vitro* studies.

MitoQ, resveratrol and curcumin acted as antioxidants in this cell type. In contrast to resveratrol and curcumin, MitoQ seemed to impair mitochondrial function but intracellular ATP levels did not change. Thus, all three antioxidants tested are interesting candidates for lowering oxidative stress and possibly preventing insulin resistance in obesity.

2 Introduction

2.1 Adipose tissue, Obesity and Adipocytes

2.1.1 Obesity

Overweight and obesity, meaning excessive body fat, are a major threat to public health in many countries. Overweight is defined as a body mass index (BM I) > 25, obesity as BMI > 30 and morbid obesity as BMI > 35. The BMI is calculated as (body weight in kilogram) / (height in meters)^2. Especially in the USA the prevalence of overweight has reached an alarming extent. In 2008 68% of adults were overweight, 34% were obese and 14% were morbidly obese [1]. The prevalence for abdominal obesity in children adolescents aged 2-19 years increased from 10.5% in the period between 1988-1994 to 19% in the period from 2003-2004. Obesity is influenced by genetics, maternal and perinatal factors and sex. However, the main contributor to the development of obesity is an imbalance between food intake and energy expenditure. The global increase in the prevalence of obesity is mainly due to an unhealthy change in lifestyle. People shift to energy-dense food which is rich in fat and sugar and become more sedentary. Thus, at the same time energy intake increases and expenditure decreases. Social stigmatization and disability cause high psychological strain to the patients [2]. Guh *et al.* [3] published a meta-analysis investigating the prevalence of overweight and obese people to several diseases compared to the lean population. They reported an increase in the risk for endometrial cancer, colorectal cancer, pancreatic cancer, hypertension, stroke, asthma and heart failure. The most prominent risk was T2DM which was 6.7-fold increased in obese men and even 12.4-fold in obese women [3]. The metabolic syndrome is a metabolic derailment and another consequence of insulin resistance and / or visceral adipositas.

According to the American Heart Association there are five criteria of metabolic syndrome: central adiposity (waist circumference in women $\geq$89 cm and in men $\geq$101 cm); reduced HDL (“good cholesterol”, in women $\leq$50 mg/l and in men $\leq$40 mg/l); high blood pressure (systolic $\geq$130 mm Hg or diastolic $\geq$85 mm Hg); elevated fasting plasma glucose (>100 mg/l or T2DM) and fasting blood triglycerides >150 mg/dl. The metabolic syndrome is diagnosed if at least three of these criteria are present [4].

Thus obesity is not only a cosmetic problem but also a disease causing severe co-morbidities and huge costs to health care.

2.1.2 White and brown adipose tissue

There are two types of adipocytes originating from the two types of adipose tissue, namely brown and white adipose tissue (BAT and WAT). They are characterized by different morphology and function.

The predominant site of triglyceride (TG) storage and lipolysis is WAT. White adipocytes usually contain a big lipid droplet which occupies about 90% of the cytoplasm and have a diameter between 20 μM and 200 μM. WAT contains its own population of resident macrophages, called adipose tissue macrophages (ATM). The degree of macrophage infiltration and the levels of inflammatory cytokines and chemokines positively correlate with obesity and IRe [2]. Brown adipose tissue is responsible for non-shivering thermogenesis whereby the energy of fatty acid oxidation is used to produce heat through mitochondrial uncoupling by the UCP1 protein, which is characteristic for brown adipocytes [5].

Brown adipocytes have a high content of mitochondria and store lipid in many small droplets [5]. Small mammals have BAT during their whole life to protect them against cold [6]. It was assumed for a long time that in humans BAT is almost exclusively present in infants and very rare in adults [7]. Three recent human studies showed that also adults have BAT deposits [8-10]. In lean subjects cold induced glucose uptake was four fold higher than overweight people [9]. This result shows that BAT has the same function in small animals and humans.

Brown and white adipocytes are both derived from mesenchymal stem cells (MSCs). MSCs can give rise to osteoblasts, white pre-adipocytes or Myf+ progenitor cells. The white pre-adipocytes differentiate into white adipocytes while the Myf+ cells can differentiate into brown adipocytes or skeletal muscle cells. In contrast to the progenitor of brown adipocytes, white pre-adipocytes express PPARγ and CD24 but no Myf. After chronic exposure to cold brown adipocytes which did not originate from Myf+ progenitor cells were detected in WAT. Such cells are also called “brite” or “beige” adipocytes [11].

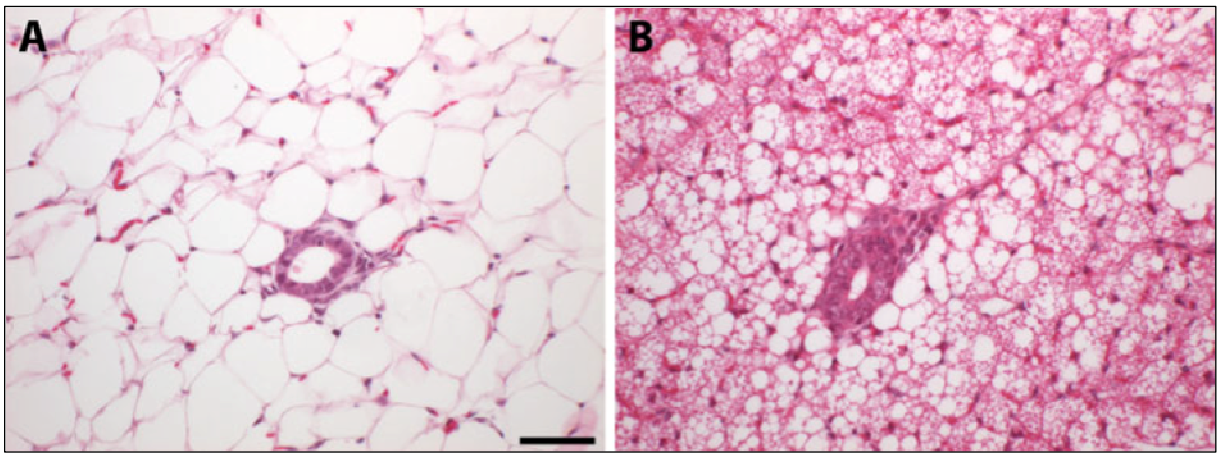

Fig. 1. White and brown adipose tissue.
Adipose tissue of a mouse mammary gland. A) White adipose tissue. B) Brown adipse tissue. Hovey, R. J Mammary Gland Biol Neoplasia, **15**, 279 (2010).

Adipose tissue serves as storage of fuel, plays an important role in thermoregulation as it can produce heat via non-shivering thermogenesis (production of heat instead of ATP by mitochondria due to uncoupling) and protects the inner organs. The most important function of adipocytes is their ability to store excessive energy as triglycerides. The adipocyte is the only cell type which is able to synthesize TGs from free fatty acids (FFAs) via de novo lipogenesis. FFAs are taken up through specific transport proteins and are esterified with glycerol to form TGs which are stored in intracellular lipid droplets. If FFAs as needed as fuels on the body, TGs can be broken down via lipolysis and FFAs are released into the circulation. Adipocytes respond to anabolic and catabolic hormones such as insulin, insulin growth factor (IGF), glucagon and catecholamines. Adipocytes also synthesize and secrete proteins called adipokines including pro-inflmmatory cytokines, growth factors, complement factors and non-protein products such as fatty acids, steroid hormones, prostaglandins and retinoids. Beside adipocytes, fat tissue also contains other cell types like pre-adipocytes (mesenychymal stem cells located in adipose tissue), endothelial cells, macrophages, lymphocytes and neurons [2].

2.1.3 Adipocyte differentiation

In both types of adipocytes the key regulator of differentiation is peroxisome proliferator-activated receptor gamma (PPARγ). PPARγ is a ligand dependent

transcription factor belonging to the nuclear receptors (NRs). It regulates expression of target genes upon binding to PPARγ binding elements (PPREs) after dimerization with retinoid X receptors (RXRs).

PPARγ controls the expression of genes involved in the key functions of adipocytes such as lipid transport, lipid metabolism, fatty acid uptake, recycling of intracellular fatty acids, lipolysis, insulin signaling and adipokine production. Insulin sensitivity can be regulated by PPARγ via expression of adipokines. Adiponectin which increases insulin sensitivity is elevated by PPARγ, while resistin and TNFα which both decrease insulin sensitivity are down-regulated [11].

In general nuclear receptors regulate transcription together with co-regulators. These proteins may affect chromatin structure or build a bridge between NRs and the basal transcription machinery but do not bind to DNA themselves. The co-regulators p300 and CBP are histone acetyl transferases (HATs) which can acetylate nucleosomal histones in target genes of PPARγ, thus altering chromatin structure and accessibility for the transcription machinery. Interactions between NRs and co-regulators can be regulated by ligands, for example the co-activator steroid receptor coactivator-1 (SRC-1). SRC-1, SRC-2 and SRC-3 can all interact with PPARγ [11]. SRC-1 and SRC-2 both control energy balance in adipose tissue. SRC-1 increases energy expenditure via fatty acid oxidation in BAT while SRC-2 leads to an increase in TGs and a decrease in FFAs in WAT by activation of PPARγ [11]. SRC-$1^{-/-}$ mice have reduced energy expenditure and are therefore prone to obesity. SRC-$2^{-/-}$ mice show reduced weight gain, improved glucose tolerance and insulin sensitivity as they have hyperactive BAT with increased adaptive thermogenesis [12]. The effects of SRC-1 and SRC-2 are mainly mediated by PGC-1α, another co-activator of PPARγ. SRC-3 knockout mice exhibit reduced weight gain what may be due to a defect of adipocytes differentiation and fat accumulation [13].

As mentioned before, PGC-1α binds to PPARγ but it also interacts with other transcription factors involved in metabolism [11]. PGC-1α knockout mice show reduced expression of mitochondrial genes in BAT, muscle and brain resulting in impaired response to cold exposure and starvation [14, 15]. Puigserver *et al.* [16] have shown before that PGC-1α is a cold co-activator and regulates adaptive thermogenesis via expression of several mitochondrial genes like UCP1 (uncoupling protein 1) in brown adipose tissue [16]. PGC-1α is a target gene of PPARγ itself [17]

and enhances PPARγ mediated UCP1 expression [16]. Thus, PGC-1α is important for oxidative metabolism ad fat function [11].

Beside PPARγ the other key transcription family for adipocytes is the CCAAT/enhancer-binding proteins C/EBPα, -β and -δ. The rapid expression of C/EBPβ and -δ is the initial event after induction of the differentiation process in response to adipogenic signals. C/EBPδ induces the expression of PPARγ, thus, initiating adipogenesis. C/EBPβ stops cell proliferation and induces C/EBPα which in turn leads to expression of GLUT4, a glucose transporter needed for the metabolic action of insulin. Over-expression of C/EBPβ or -δ in pre-adipocytes enhances adipogenesis while embryonic fibroblasts from C/EBPβ$^{-/-}$ or C/EBPδ$^{-/-}$ mice show impaired adipogenesis compared to wildtype mice [18].

2.1.4 Adipose tissue and inflammation

WAT exerts important endocrine and immune functions by secreting adipokines including inflammatory cytokines and proteins involved in regulating actions of insulin and food intake. Obesity is characterized by chronic systemic inflammation and disturbed reaction to insulin. The most important adipokines secreted by WAT are TNFα, IL-6, adiponectin and leptin. TNFα is the major mediator of inflammation and IRe in obesity. Free fatty acids, which are elevated in obesity, can bind to toll-like receptor 4 (TLR4) present in adipocytes and macrophages. TLR4 is part of innate immunity and triggers an inflammatory response. Adipose tissue of obese individuals contains more T cells and macrophages than that of lean people. The reason for increased macrophage infiltration may be due to increased necrotic cell death of adipocytes as clustering of macrophages was observed around necrotic cells [19]. The adipokines TNFα, IL-6, leptin and adiponectin are discussed below in more detail.

As mentioned above, in adipose tissue TNFα is secreted mainly by macrophages [20] but also by adipocytes [21]. Adipocytes express the TNFα receptor [22]. TNFα induces IRe, lipolysis, leptin production and suppresses lipogenesis and pre-adipocyte differentiation *in vitro* [23, 24] and decreases adiponectin expression and secretion [25]. In adipose tissue of genetically obese mice TNFα is over-expressed. In obese humans expression of TNFα is elevated and can be decreased by weight

loss [26]. Neutralization of TNFα in genetically obese rats leads to an increase in insulin sensitivity [21] and mice lacking TNFα are protected against obesity-induced IRe [27]. In contrast to WAT, TNFα induces apoptosis in BAT [28]. TNFα also elevates the secretion of leptin [29].

IL-6 is expressed by macrophages [19] and adipocytes which contribute to approximately 1/3 of circulating IL-6 in obese individuals [20]. An IL-6 overload leads to insulin resistance [30]. IL-6 increases leptin expression and decreases adiponectin expression and secretion in adipocytes [25].

Leptin is mainly produced by adipocytes [25]. Together with adiponectin it is the most abundantly expressed adipokine in fat tissue [31]. Leptin acts in the central nervous system and is an important negative regulator of appetite [32]. Adults with leptin deficiency show increased appetite and obesity what can be treated by supplementing leptin [33]. Leptin serum levels are proportional to overall adipose mass in mice and humans [34] and systemic hyper-leptinemia leads to a decrease in obesity [35]. Leptin stimulates the proliferation and differentiation of monocytes [25] and increases the production of TNFα and IL-6 by monocytes and macrophages [36].

Adiponectin has insulin sensitizing effects which seem to be mediated by an increase in fatty acid oxidation [37]. Serum levels of adiponectin are markedly decreased in people with visceral obesity and IRe even though it is mainly produced in adipocytes [38] and its synthesis can be induced by weight loss [39]. Adiponectin decreases the TNFα concentration in plasma [40]. In contrast to leptin, adiponectin inhibits T cell proliferation and activation [41] and decreases production of TNFα by macrophages[42].

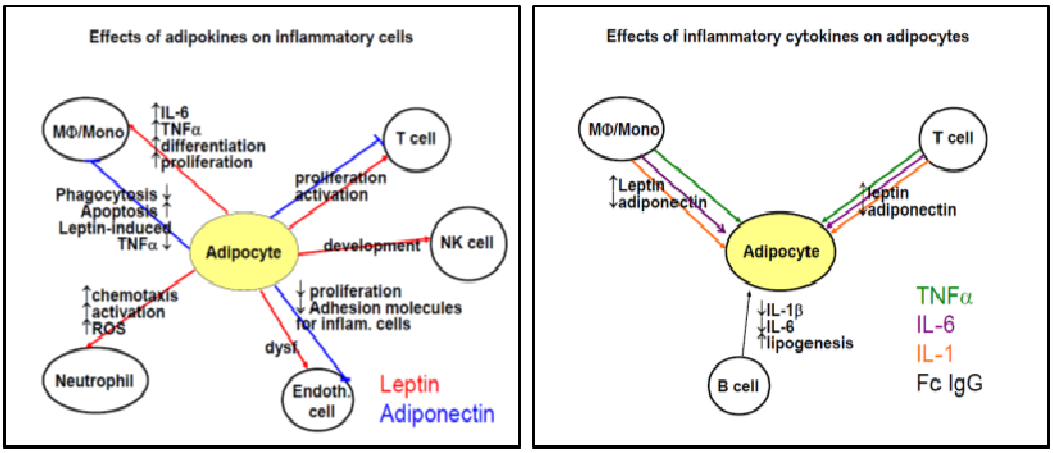

Fig. 2. Effects of adipokines on inflammatory cells and vice versa.

2.1.5 Subcutaneous and visceral adipose tissue

Subcutaneous (SCAT) and visceral adipose tissue (VAT) show differences in adipocyte morphology, endocrine profile and their association in metabolic complications like IRe and metabolic syndrome [43].

The adipose tissue around the organs in mesentery and omentum is called visceral or intra-abdominal fat. It accounts for about 10-20% of total adipose tissue in men and for 5-8% in women. Visceral fat increases with age. Subcutaneous fat tissue is located in the subcutaneous area and accounts for about 80% of total fat tissue [44]. Fat tissue contains bigger and smaller adipocytes. The younger, smaller adipocytes absorb FFAs and TGs, thus, acting as a buffer after meals. They are more insulin-sensitive and take up FFAs and TGs more efficiently than big adipocytes and therefore prevent deposition of FFAs and TGs in other tissues. Large adipocytes are more insulin-resistant and hyperlipolytic as they are also resistant to the anti-lipolytic effect of insulin. Visceral adipose tissue contains more large adipocytes while SCAT contains small adipocytes [45, 46]. Visceral fat is more innervated and vascularized than SCAT. Most studies show higher infiltration of inflammatory cells including macrophages in VAT than SCAT, but there are also contradictory reports [43]. In contrast to SCAT, VAT is drained directly through the portal vein to the liver. Therefore, FFAs and fat tissue derived cytokines directly induce hepatic immune mechanisms [43].

Visceral and subcutaneous adipose tissues show differences in cytokine secretion. Adiponectin and pro-inflammatory cytokines show higher expression in VAT while leptin is mainly produced in SCAT [43]. Dolinková *et al.* [47] showed increased expression of pro-inflammatory and adipogenic genes and lower expression of lipogenic and insulin signaling genes in obese compared to lean women. There were significant differences in gene expression between VAT and SCAT but both fat depots contributed to the inflammatory state in obesity [47].

Amongst other groups, Fox *et al.* [48] reported in a large study that the prevalence for metabolic complications like hypertension, high HDL, impaired fasting plasma glucose, T2DM and metabolic syndrome in men and women are more strongly associated with VAT than SCAT [48]. Another big clinical study which included young men only reported the opposite. They showed that SAT correlated more strongly with

IRe than VAT [49]. However, in the general opinion VAT is regarded as more harmful than SCAT.

2.1.6 Obesity, oxidative stress and mitochondrial dysfunction

Obese people and patients suffering from T2DM have increased levels of glucose and free fatty acids in the plasma. *In vitro* increased concentrations of glucose or FFA lead to elevated ROS production in muscle, adipocytes, pancreatic β-cells and other cell types [50].

High amounts of substrates cause a reduced state of the electron carriers of the electron transport chain. This condition dramatically increases ROS production [50]. Fridlyand *et al.* proposed that insulin resistance could be a protective mechanism to prevent oxidative stress [51]. Over-expression of antioxidant enzymes in transgenic mice is protective against β-cell dysfunction and IRe. High FFA concentrations lead to lipid accumulation in myocytes what has been proposed to be critical for the development of IRe and T2DM [52]. Thus, oxidative stress plays an important role in the development of these consequences of obesity [50].

Lipid-induced IRe may arise because β-oxidation provides reducing equivalents to the ETC, thus, competing with glucose [53] or due to an increase in ROS production through the mechanism mentioned before. In pancreatic β-cells an increase in glucose concentration stimulates glycolysis, thus, providing high levels of reduced ETC equivalents. In consequence ADP concentrations decrease what leads to insulin secretion. Therefore, high glucose concentrations lead to increased ROS production in β-cells causing potentially causing cellular damage [50]. Patients suffering from diabetes often have mutations in mtDNA of β-cells that lead to defective insulin secretion, cell apoptosis and a decrease in β-cells mass [54].

Normally, the insulin receptor autophosphorylates after binding insulin. Receptor phosphrylation allows association of insulin receptor substrate (IRS) with phosphoinositide 3-kinase (PI3K) resulting in translocation of cytoplasmic vesicles containing GLUT4 to the cell membrane. There these vesicles allow glucose uptake [55]. Glycolysis is stimulated after receptor activation, thus, leading to increased ROS production because more substrate is available for the ETC. *In vitro* oxidative stress

can lead to activation of multiple signaling cascades including kinases which increase serine phosphorylation of the insulin receptor and IRS-1 and IRS-2. This reduces downstream signaling resulting in inactivation of PI3K and decreases glucose uptake, thus, preventing oxidative damage to the cell. However, there are no similar mechanisms in endothelial and mesangial cells and neurons. Therefore, mitochondrial overproduction of superoxide due to substrate over-load can lead to oxidative damage [50].

White adipocytes from genetically overweight and diabetic *ob/ob* mice show a decrease in mitochondrial content of about 50% compared to the wild-type [56]. In leptin receptor deficient *db/db* mice fed a high fat diet, about half of the genes involved in mitochondrial ATP production and energy uncoupling are decreased when compared to *db/db* mice fed a normal diet or to *db/+* mice [57]. In morbidly obese patients expression of PGC-1α is reduced in adipose tissue [58]. A total deficiency of both transcription factors PGC-1α and PGC-1β completely prohibits mitochondrial biogenesis and respiration which are linked to adipocytes differentiation [59]. Song *et al.* [60] elucidated oxidative stress, antioxidant capacity and DNA damage in patients with newly diagnosed diabetes and impaired glucose regulation. They reported that patients with impaired glucose regulation have reduced superoxide dismutase (SOD) activity in erythrocytes and slight damage in DNA. Subjects with diabetes showed an increase in lipid oxidation products in plasma, lower plasma antioxidant capacity and erythrocyte SOD activity. Insulin resistance correlated with lipid peroxidation and was associated with lower SOD activity and overall antioxidative capacity [60].

2.2 Mitochondria

Over the last 150 years, numerous reports in the scientific literature appeared describing mitochondria in various tissues. Morphologically, they were described as threads or mitos in Greek. Other reports characterized them as grains or chondros. Since the 1850s the term mitochondria has been used for these organelles. Mitochondria are responsible for many vital functions, mainly oxidative phosphorylation, Krebs cycle, β-oxidation of fatty acids as well as controlling of apoptosis in higher eukaryotes [61].

2.2.1 Mitochondrial morphology

Two membranes surround mitochondria: the outer mitochondrial membrane (OMM) and the inner mitochondrial membrane (IMM) [61]. The IMM encloses the mitochondrial matrix (MM) which contains metabolic enzymes and multiple copies of the mitochondrial DNA (mtDNA). The mtDNA encodes 37 proteins and polypeptides [62] but most mitochondrial proteins are encoded in the nucleus and are imported from the cytosol. The mtDNA encodes for 22 tRNAs (transfer RNAs), the 12S and 16S ribosomal RNAs, the subunits I, II and III of cytochrome *c* oxidase, cytochrome b, ATP-synthase subunits 6 [62] and 8 [63], subunits of NADH dehydrogenase ND1, ND2, ND3, ND4, ND4L, ND5 [64] and ND6 [65]. For humans, around 4500 proteins are assumed to be mitochondrial, amongst them 1589 are identified experimentally or by homology, the others are predicted [66]. The compartment between the OMM and the IMM is called the intermembrane space (IMS). In many cases, mitochondria form tubular structures which show interactions with the endoplasmatic reticulum (ER) and the cytoskeleton [67].

In the IMM two regions can be distinguished: the inner boundary membrane (IBM) which runs parallel to the OMM and the cristae membrane (CM) forming the cristae structures [61]. Palade [68] was the first who showed mitochondria as an organelle surrounded by a double membrane with convolutions formed by the IMM. Later, mitochondria were shown to exhibit tubular, lamellar and even triangle-shaped structures depending on the physiological stage and developmental stage [69].

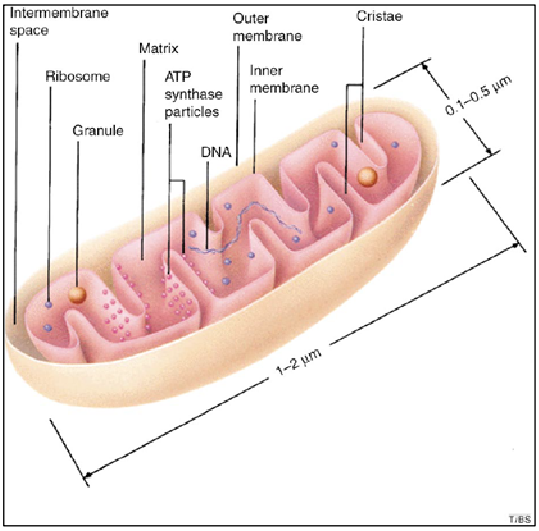

Fig. 3. Baffle model of a mitochondrium
Lodish, H. et al. Molecular Cell Biology (3rd ed.), 1999

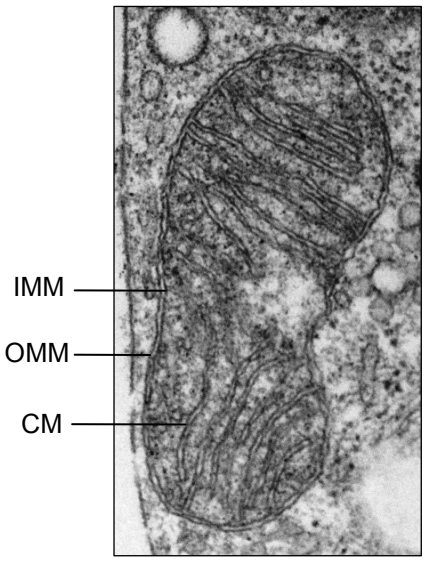

Fig. 4. Electron microscopy picture of a mitochondrium.
IMM: inner mitochondrial membrane
OMM: outer mitochodrial membrane
CM: cristae membrane

Several models regarding the IMM structures have been proposed. Palade suggested a model in which cristae are regarded as invaginations of the IMM with wide openings [68, 70], later called the “baffle model”. Sjöstrand suggested the septa model, meaning sheets of the IMM span through the MM, thus, building different compartments [71]. The baffle model was the one which gained general acceptance and entered the textbooks. Using very thin serial sections of mitochondria, small tubular structures which connected cristea with the IBM were visualized by other groups. These structures were named pediculi cristea meaning cristae feet [61]. In the 1990s Mannella *et al.* [67, 72-74] applied electron tomography to determine the structure of isolated mitochondria. With this technique, a three dimensional reconstruction of rather thick sections allows a precise spatial view of the specimen. For this a series of electron micrographs is taken over a wide range of angels and a three dimensional view is reconstructed by computational analysis. Mannella could show in several studies that cristea are attached to the IBM by narrow openings which they called cristae junctions (CJs) [67, 72-74]. Cristae junctions appear as narrow tubular, ring- or slot-like structures with diameters between 12-40 nm [67, 75, 76]. Williams [77] and Tedeschi [78] concluded that according to this new model proton flow is localized and kinetically controlled in contrast to the original description of delocalized proton flow by Mitchell [79].

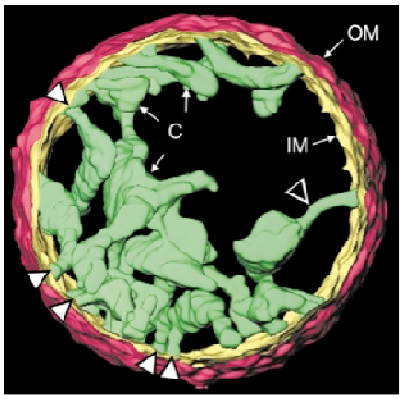

Fig. 5. Tomography of isolated rat-liver mitochondrion.
Frey, T. TIBS **25** (2000)

Computer simulations indicated that ADP depletion could occur within large cristae compartments due to limitation of diffusion by CJs, thus, ADP depletion would lower local ATP production [80]. Hackenbrock [81] was the first to show that the morphology of the IMM is highly dependent on the respiratory state.

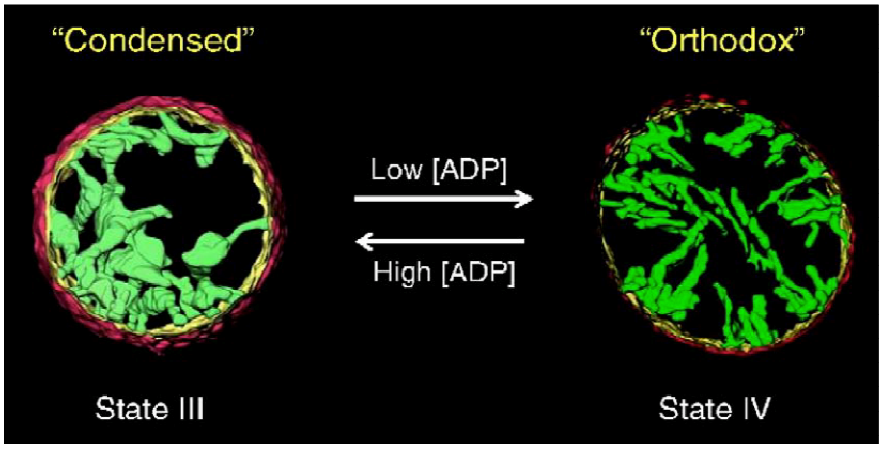

Fig. 6. Mitochondrial morphology in dependence of the bioenergetic state.
Manella, C. Biochimica et Biophysica Acta, **1763,** 542 (2006)

In state 3, when ADP is present in excess, isolated rat liver mitochondria were in the condensed state showing large swollen cristae. In state 4 when ADP becomes limiting, the intracristal volume became clearly smaller, what is characteristic for the orthodox state [81]. This morphological change may be initiated to optimize diffusion, thus, avoiding a decrease in local ATP production [82]. In summary, the bioenergetic state clearly influences mitochondrial ultrastructure [61].

2.2.2 Fission and fusion

Recordings in living cells revealed that mitochondria are capable of varying their shape and size. These changes in the mitochondrial network are the result of constant fusion and fission [83]. Knocking out the proteins responsible for these two processes is lethal for the cell [84, 85]. Mitochondria are exposed to high oxidative stress causing damage to mtDNA, proteins and lipids. It is thought that mitochondria can repair and replenish these damages from the healthy pool by circulating through the mitochondrial network [86, 87]. This hypothesis is supported by the observation that oxidized proteins accumulate when fission is blocked [88]. Loss of proteins responsible for the fission / fusion process leads to a decrease or total loss of mtDNA [83].

In mammals, the major fusion proteins are mitofusin 1 and mitofusin 2 (Mfn1 and Mfn2) and the mitochondrial dynamin-like 120 kDa protein (Opa1). The major fission proteins are utropin (Drp1), mitochondrial fission factor (Mff) and mitochondrial fission protein 1 (Fis1). Mitofusins 1/2, Opa1 and Drp1 are large GTPases. The complexes responsible for the membrane fusion and fission are formed by homo- and heteromeric self-assembly [83].

2.2.2.1 Mitochondrial fusion

Mitofusins are located in the OMM and are primarily responsible for OMM fusion. They have two membrane-spanning domains and both termini are in the cytosol. Mitofusins form oligomers with each other both on the same (*cis* manner) and on a different (*trans* manner) mitochondrium to tether mitochondria together. In mammals, the ratio and the tethering capabilities of Mfn1 and Mfn2 differ among cell types. This may explain the variation of the mitochondrial network phenotypes among cell types [83].

The major protein for IMM fusion, Opa1, has multiple isoforms which are located in the IMM and the IMS. In *in vitro* fusion assays Mgm1, the yeast analogue of Opa1, acts both in *cis* and *trans* manners [83]. Defects in IMM fusion result in normal OMM structure enclosing multiple IMM-bound matrices [89]. Thus, OMM and IMM fusion seem to be distinct processes [83]. In yeast, Ugo1 is a protein suggested to

coordinate the fusion of both membranes, however, until now no mammalian ortholog has been identified even though there is predicted to be one [83].

2.2.2.2 Mitochondrial fission

In mammals Drp1 is localized in the cytosol and is enriched at constriction sites of mitochondrial fission. Drp1 forms curved filaments in the GDP-bound state and spiral structures in the GTP-bound state [90]. In yeast the spirals of the GTP-bound Dnm1, the Drp 1 analog, form at the constriction sites of mitochondria and the formation of these spirals is also able to constrict liposomes [91]. Knock out of Drp1 or Dnm1 results in elongated mitochondria [85, 92]. Fis1 is located in the OMM, has the C-terminus in the IMS and the N-terminus in the cytosol. At least in yeast it acts as the mitochondrial receptor for Dnm1 [93]. The OMM protein Mff has recently been shown to be required for fission in mammals. It is suggested to act as a scaffold for other proteins involved in the fission process [94].

2.2.3 Mitochondria and apoptosis

Mitochondria are the major regulator in apoptosis and they undergo drastic morphological changes during this process [95]. They are involved both in caspase-dependent and caspase-independent pathways. An important step in the apoptotic process is the permeabilization of the OMM and the subsequent release of pro-apoptotic proteins, amongst others cytochrome *c* (cyt *c*). There seems to be complete release of cyt *c*, even though it is estimated that more than 85% of cyt *c* is stored in the intracristal space. An extensive remodeling of the IMM occurs after induction of apoptosis leading to increased accessibility of cyt *c*. Cytochorome *c* then triggers caspase activation in the major apoptotic pathway [61].

Mitochondrial outer membrane permeabilization (MOMP) for cyt *c* release and fragmentation of tubular mitochondria appear almost simultaneously. It was suggested that MOMP and Drp1 mediated fission are separate events during apoptosis and that Drp1 is only necessary for cyt *c* release but not for the release of other pro-apoptotic proteins [95]. Mitochondrial fragmentation seems to be dispensable as in Drp1 knockout cells cyt *c* release and apoptosis take place while

the tubular appearance of mitochondria remains [85]. As apoptosis is almost always accompanied by mitochondrial fragmentation, there should be a reason for this phenomenon. Brooks *et al.* showed that proteins involved in fission and fusion interact with the MOMP-directing Bcl-2 proteins [96]. Bcl-2 proteins are critical regulators of cell survival and regulate many processes including calcium metabolism, autophagy, insulin secretion and cell cycle control [95]. However, the morphological changes resulting from these interactions are not consistent with the fragmentation-MOMP time axis [95]. A new theory suggests that mitochondrial fragmentation is the result of the regulatory functions of Bcl-2 proteins rather than having a direct role in mitochondrial permeabilization and apoptosis [97].

2.2.4 Oxidative phosphorylation

In animal cells most of the energy is generated in the mitochondria through the process of oxidative phosphorylation (oxphos). In 1961 Peter Mitchell [98] proposed the chemiosmotic theory, the mechanistic principle of oxphos. In his theory he explained for the first time the coupling between respiration and ATP synthesis in mitochondria. He showed that the ratio of ATP / ADP, representing phosphorylation efficiency of ADP and phosphate to ATP, is proportional to a proton gradient causing a difference in pH and an electrical potential. Nowadays, the electrical potential across the IMM is referred as mitochondrial membrane potential or delta psi ($\Delta\Psi$). Mitchell concluded that the electrochemical gradient is the driving force for phosphorylation and that a charge-impermeable membrane is required for coupling of the system. This implicates that coupling varies with the extent of leakiness [98].

Today the mechanism of oxphos is well known. During this process, electrons produced by oxidation of NADH (reduced nicotinamide adenine dinucleotide) are passed along four respiratory enzyme complexes located in the inner mitochondrial membrane. NADH is generated by the oxidation of nutrients, for example glucose. Passage of electrons along these complexes releases energy which is used to translocate protons from the mitochondrial matrix into the intermembrane space. The electrons are finally transferred to molecular oxygen to produce water consuming protons from the matrix side. The resulting electrochemical gradient across the IMM

stores the energy and is used by the ATP synthase to make ATP from ADP and phosphate [99].

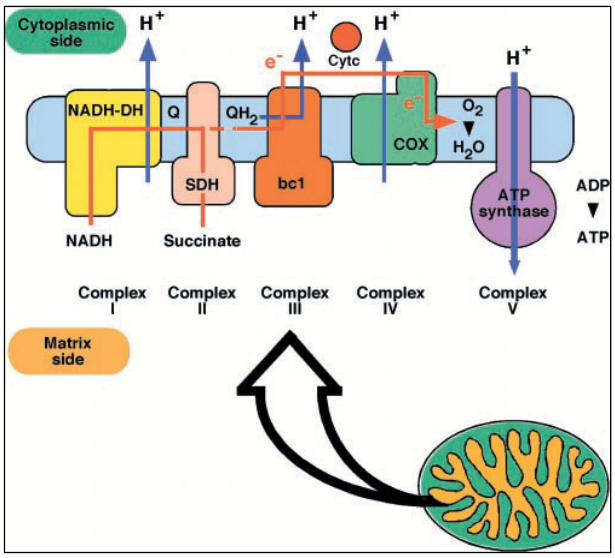

Fig. 7. The electron transport chain
Saraste, M. Science, **283**, 1488 (1999)

Complex I or NADH:ubiquinone oxidoreductase is the largest of all respiratory complexes and has a L-shaped structure. In mammals it consists of 42 or 43 different subunits and its size is comparable to the one of ribosomes [100]. Complex I oxidizes NADH to NAD+ and transfers electrons to ubiquinone, also called coenzyme Q (CoQ). The energy liberated from this reaction is used to translocate one proton across the IMM [99].

Complex II also called succinate:ubiquinone reductase or succinate dehydrogenase is part of the Krebs cycle and transfers electrons from succinate to ubiquinone without pumping electrons across the IMM. Succinate dehydrogenase oxidizes succinate to fumarate and thereby reduces covalently bound FAD (flavin adenine dinucleotide) to $FADH_2$. FDH_2 transfers its electrons to ubiquinone [101].

Complex III or cytochrome bc_1 delivers electrons from ubiquinone to cytochrome *c*. It is the best understood of all respiratory enzymes. The mammalian form of complex III consists of eleven subunits but only three of them carry redox centers. These three subunits are cytochrome b containing two hemes, a membrane-anchored FeS protein (iron-sulfur protein ISP) called Rieske protein carrying a Fe_2S_2 center and a cytochrome c_1 [102]. Ubiquinone is lipid soluble and can move within the membrane. The redox reactions of quinol imply protonation and deprotonation. These reactions

are topologically organized in a way that oxidation of ubiquiol results in active transport of protons across the IMM. The reactions of quinols require two active sites, one for oxidation and release of protons from ubiquinol at the outer side of the membrane (Q_o) and one for reduction of ubiquinone. Reduction of ubiquinone is coupled to the uptake of protons from the inner side of the membrane (Q_i) [99]. Cristal structures confirmed the presence of two active sites. The Q_o site is located between ISP and cytochrome b close to the outer site of the IMM. The Q_i site is in the cytochrome b subunit in the matrix side of the membrane [103]. The Q_o site is near the b_L heme (low redox potential) and the Q_i site is near the b_H heme (high redox potential). The mechanism by which Complex III transfers protons across the membrane is called Q-cycle. A quinol can donate two electrons. The first electron is transferred to the Rieske center and from there to cytochrome c_1, which reduces cytochrome *c*. The second electron is transferred along the hemes b_L and b_H to Q_i. This transfer generates part of the proton motive force of this complex due to the difference in the redox potential of the two hemes. After oxidation of two quinols at the Q_o site, two electrons are transferred to the Q_i site and reduce another quinone. Thus, two protons are transferred across the IMM for every electron delivered to cytochrome *c* [99].

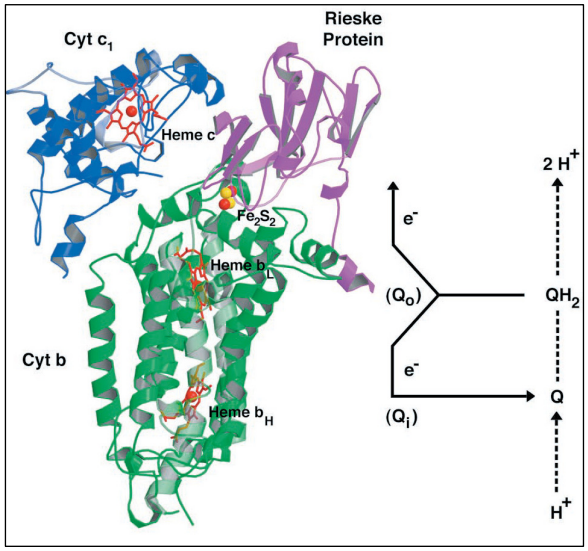

Fig. 8. Complex III and the Q-cycle
Saraste, M. Science, **283**, 1488 (1999)

Complex IV or cytochrome *c* oxidase is the last complex in the electron transport chain (ETC) and catalyzes the final step, the transfer of electrons to molecular oxygen, thus, producing water. The bovine cytochrome *c* oxidase consists of 13 subunits. Subunit I, II and III are coded in mtDNA and form the functional core of the

enzyme. Cyt *c* is a water soluble hemoprotein and donates electrons to complex IV at the cytoplasmic side of the IMM. The electrons are transferred to the active site of cytochrome *c* oxidase which contains a heme iron and a copper. There they are used to reduce oxygen to water. Four electrons and four protons from the MM are transferred to oxygen to produce two water molecules. The same channels which are used to take up protons to reduce oxygen are used to pump electrons across the IMM. One proton is translocated per electron which is transferred to complex IV [99].

Complex V or ATP-synthase (F_1F_0 ATPase) is functionally reversible. It can either synthesize ATP from ADP and phosphate using the proton gradient across the IMM or it can hydrolyze ATP to pump protons against the electrochemical gradient. The bovine complex V has a size of more than 500 kDa [104]. The enzyme consists of two main sectors, the F_0 part in the IMM and the F_1 part located in the matrix side of the membrane. The F_0 sector contains the proton channel and the F_1 the catalytic sector which synthesizes ATP. A stalk consisting of two parallel structures connects the parts [104]. The F_0 sector consists of one a, two b and 9-12 c subunits. The b subunits build a stalk and connect F_0 and F_1 [105]. The three-dimensional structure of this complex enzyme is becoming increasingly clear. In 2009 John Walker [106], one of the main contributors regarding complex V characterization, published the x-ray structure of the remaining unresolved parts of the stator. With this report, his group completed the three-dimensional structure of the membrane extrinsic part of bovine ATP-synthase [106].

The F_1 sector contains five different subunits: α, β, γ, δ and ε in a stochiometry of 3 : 3 : 1 : 1 :1. The β-subunit is the only catalytic one, although the α-subunit is homologous. Each of the three β-subunits has three catalytic sites. Boyer *et al.* [107] proposed a binding exchange mechanism in which each catalytic site of one β-subunit passes through the three different states “empty”, “loose” and “tight”. These terms correspond to an empty state, one with bound ADP and phosphate and one with tightly bound ATP. At any moment, each of the three catalytic sites of one subunit would be in a different state. Binding of ADP and phosphate as well as release of ATP require energy, formation of ATP does not [107].

F_0 and F_1 both contain a rotor, consisting of the c subunits and the γ and ε subunits, respectively. The subunits a and b and the αβ-hexamer are referred as stators. F_0 and F_1 rotate in opposite directions to generate a torque which is required for ATP synthesis. Yasuda *et al.* [108] fixed the stator of the isolated F_1 part of the enzyme on

a glass surface and attached a microfilament at the γ subunit. With this assay they could detect rotary steps of 120° [108]. Isolated F_1 is also called F_1-ATPase as in the absence of F_0 it hydrolizes ATP and rotates in the reverse direction [105].

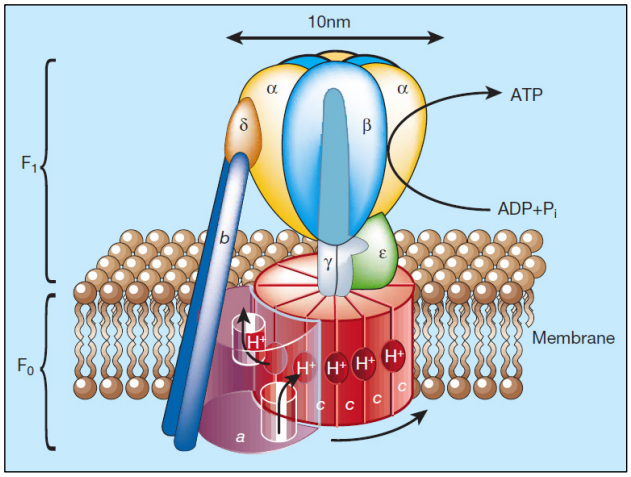

Fig. 9. ATP-synthase
Schnitzer, M. Nature, **410**, 878 (2001)

2.2.5 Mitochondria and oxidative stress

2.2.5.1 Chemistry of free oxygen radicals

Cells are challenged with several reactive oxygen species (ROS) which are generated within are generated intracellular and may have deleterious effects on proteins, lipids and carbohydrates. Thus, cells evolved multiple defense mechanisms to avoid oxidative damage. The free cellular ROS are composed by superoxide (O_2^-•), hydroxyl radical (•OH) and hydrogen peroxide (H_2O_2). In contrast to the other molecules, hydrogen peroxide is not a radical as it does not contain an unpaired electron.

Superoxide is a good reductant but poor oxidant radical. It can lead to the formation of other ROS as hydroxyl radical, hydrogen peroxide and perhydroxyl (HO_2•) which is much stronger oxidative than superoxide itself. At a neutral or higher pH superoxide is catalyzed to hydrogen peroxide by superoxide dismutase. Superoxide is an unavoidable by-product of oxidative phosphorylation and is formed by reduction of molecular oxygen.

Formation of superoxide $O_2 + e^- \rightarrow O_2^-$•

Hydrogen peroxide is considered the most potent oxidant in cells as its half-life time is extremely short. Hydroxyl radicals react with different molecules amongst other with lipids by removal or addition of unsaturated bonds. In cells hydroxyl is mainly derived from four reactions: the Fenton reaction, the Haber-Weiss reaction, via oxygen metabolism and with reduced metal ions, for example copper. The reaction occurring in oxygen metabolism may be the most important one in aerobic biological systems.

Fenton reaction	$Fe^{2+} + H_2O_2 \rightarrow Fe^{3+} + \bullet OH + OH^-$
Haber-Weiss reaction	$O_2^-\bullet + H_2O_2 \rightarrow O_2 + H_2O + \bullet OH$
Reaction with reduced metal ions	$Cu^+ + H_2O_2 \rightarrow Cu^{2+} + \bullet OH + OH^-$
Oxygen metabolism	$O_2 + H_2O \rightarrow HO_2\bullet + OH^-$

The major source of hydrogen peroxide is the reaction catalyzed by superoxide dismutase but it is also formed when two superoxide radicals (usually formed in oxygen metabolism) react together. Hydrogen peroxide cannot oxidize many organic molecules in an aqueous environment as it is not reactive enough. But it can generate hydroxyl radicals upon reaction with metals as shown above [109].

Reaction of superoxide dismutase	$O_2^-\bullet + 2H^+ \rightarrow H_2O_2 + O_2$
Oxygen metabolism	$O_2^-\bullet + O_2^-\bullet + 2H^+ \rightarrow H_2O_2 + O_2$

2.2.5.2 Cellular sources of free radicals

Superoxide generation is unavoidably generated by ETC and happens due to the reduction of oxygen to water at complex IV, thus the main source of ROS are mitochondria. High amounts of superoxide are produced when the electron carriers of the electron transport chain are in a reduced state, i.e. when the intracellular ADP levels are low (state 4 respiration) [110] or when the electron transport chain is

running at its maximal capacity. An increase in reduced carrier of the ETC occurs through increasing production of reducing equivalents or a decreased capacity of these carriers. ROS formation is increased after incubation with elevated concentrations of glucose or free fatty acids in adipocytes, pancreatic β cells, muscle and other cells [50]. Various catalytic cytosolic enzymes contribute to the generation of O_2^-•, •OH and mainly H_2O_2 [111]. Xanthine oxidase is another source of superoxide. It can reduce cytochrome *c* and plays an important role in ischaemic injury. Under ischaemic conditions xanthine dehydrogenase acts as an oxidase and leads to the production of superoxide [109].

2.2.5.3 Defense systems against oxidative stress

The cellular defense against oxidative damage consists of non-enzymatic compounds and antioxidant enzymes. Non-enzymatic antioxidants include vitamin C, vitamin E, vitamin A, glutathione, α-lipoic acid, CoQ and some minerals. Vitamin E is located in lipoproteins, cell membranes and extracellular fluids. It terminates lipid peroxidation processes as it can convert O_2^-• and •OH into less reactive forms. Vitamin C is hydrophilic and directly scavenges ROS and lipoid hydroperoxides. It is found in high concentrations in the adrenal and pituitary glands, liver, brain, spleen and pancreas. Vitamin C can restore oxidized vitamin E to its antioxidant state. Vitamin A is located in cellular membranes. It is lipophilic and can scavenge free radicals. Vitamin A prevents lipid and DNA oxidation [112]. Coenzyme Q is the only soluble antioxidant which is synthesized endogenously and not taken up by food. It is part of the ETC but beside the inner mitochondrial membrane it is also found in extramitochondrial membranes. In its reduced form ubiquinol, it protects membranes and lipoproteins from protein oxidation and lipid peroxidation [113]. Reduced glutathione (GSH) is one of the most important cellular antioxidant. It is the tripeptide γ-glutamyl-cysteine-glycine and generally has an intracellular concentration of approximately 0.5 mM but it can reach up to 10 mM. GSH can react with many oxidizing compounds such as O_2^-•, •OH and H_2O_2. It donates a hydrogen atom to free radicals, mainly hydroxyl and carbon radicals, thus, neutralizing the highly reactive •OH. After oxidation, two GSH molecules can form a sulfate bond, thus, resulting in GSSG. This oxidized form is restored under oxidation of NADPH to two reduced GSH [109].

$2GS\bullet \rightarrow GSSG$ $GSSG + NADPH \rightarrow 2GSH + NADP$

The enzymatic antioxidant systems mainly consist of two superoxide dismutase isoforms, catalase and glutathione peroxidase (GSH-PX). SOD was first described by McCord and Fridovich [114] and is present in all oxygen respiring species. SOD catalyzes the reaction of two superoxide radicals to hydrogen peroxide and molecular oxygen.

SOD reaction $O_2^{-}\bullet + O_2^{-}\bullet + 2H^{+} \rightarrow H_2O_2 + O_2$

The manganese (MnSOD) isoform is present in mitochondria while the copper-zinc (CuZnSOD) is located in the cytosol [109, 112]. The MnSOD appears as a tetramer while the CuZnSOD isoform is a dimer. Biosynthesis positively correlates with tissue oxygen. The highest levels of SOD are found in adrenal gland, liver, kidney and spleen [112].

Catalase and glutathione peroxidase catalyze the reaction of superoxide derived hydrogen peroxide to water. Catalase is ubiquitously expressed but the highest levels are found in the kidney, red blood cells, liver and especially in its peroxisomes. If hydrogen peroxide levels are low, catalase mainly catalyzes organic peroxide but at high concentration of hydrogen peroxide this radical is mainly catalyzed.

Catalase reaction $H_2O_2 \rightarrow 2H_2O + O_2$

Glutathione peroxidase is located in the cytosol the mitochondrial matrix and reduces hydrogen peroxide and organic hydroperoxides to water [109]. McCay *et al.* were the first to describe a protective effect of in lipid peroxidation [115].

2.2.5.4 Cellular damage by reactive oxygen species

Oxidative damage to proteins can lead to denaturation and aggregation. These aggregates may be caused by •OH and consist of crosslinked proteins rather than non-specific aggregation of protein fragments. Oxidation causes conformational changes in protein structure, thus, promoting protein degradation. Free radicals can also change the structure of lipids and therefore disrupt the structure of the

membrane bilayers. Oxidized lipids are a major source of other cytotoxic products like aldehydes. Aldehydes have mutagenic effects and can cause protein crosslinks. Carbohydrates are also prone to oxidation. Glucose can scavenge •OH thus becoming autooxidized itself. Some carbohydrates can form ketoaldehydes in the presence of metal ions. Monosaccharides can autooxidize, thus, forming dicarbonyls and hydrogen peroxide. Free radicals act as mutagens as they can damage DNA. Hydroxyl radicals were reported to cause strand breaks and base alterations. Thymine and cytosine seem to be more susceptible to oxidative damage than adenine, guanine and the deoxyribose sugar moiety. Mitochondrial DNA was investigated with special intention as mitochondria are the major source of ROS and mitochondria possess less DNA repair processes than nuclei [109]. The mtDNA has a mutation rate that is about 10 to 20 times higher than the one of the nuclear DNA [116].

2.3 The antioxidants MitoQ, Resveratrol and Curcumin

2.3.1 MitoQ

MitoQ and MitoVit E were developed by Michael Murphy and colleagues with the intent to create antioxidants which selectively target mitochondria [117, 118]. As mitochondria are commonly considered as the major source of ROS, mitochondria targeted antioxidants would neutralize ROS at the site where they are formed and prevent cellular damage. MitoVit E consists of a vitamin E moiety coupled to a triphenylphosphonium cation (TPP). $MitoQ_{10}$ is a CoQ analogue which is coupled to a TPP via a C_{10}-alkyl chain [119, 120]. Due to their positive charge TPPs easily pass lipid bilayers. [117, 118].

Herein after, $MitoQ_{10}$ and its carrier, a TPP linked to a C_{10} chain, are referred to as MitoQ and decylTPP.

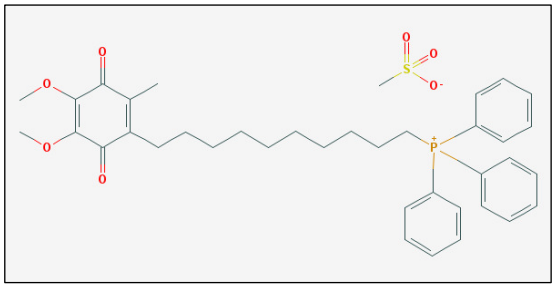

Fig. 10. Mitoquinone

2.3.1.1 MitoQ and the respiratory chain

Triphenylphosphonium cations accumulate within cells due to the plasma membrane potential and further concentrate within mitochondria [121] several hundred folds [117, 118] . More than 90% of intracellular TPPs appear within mitochondria [121]. These properties make TPPs interesting compounds for targeting substances selectively to mitochondria. Like other TPPs, MitoQ is accumulated within mitochondria and accumulation can be abrogated by uncoupling mitochondria with FCCP (Carbonyl cyanide 4-(trifluoromethoxy)phenylhydrazone), thus, abolishing the mitochondrial membrane potential. MitoQ is a mixture of the reduced form mitoquinol

which exerts antioxidant effects and the inactive oxidized form mitoquinone [120]. Kelso *et al.* [120] showed that MitoQ can be reduced by complex I and complex II of the respiratory chain in rat liver mitochondria. MitoQ could not restore respiration in ubiquinone depleted cells indicating that it cannot be oxidized by complex III. Experiments using radiolabeled MitoQ showed that it binds to the membrane part of cell fractions. Thus, it was suggested that it integrates into the inner mitochondrial membrane with the TPP part to the matrix side [120].

The same group further investigated the interactions of MitoQ with the respiratory chain. They showed that un-targeted exogenous CoQ could restore growth in CoQ-deficient yeast dependent on the length of the isoprenoid chain. MitoQ and non-targeted ubiquinones carrying an alkyl instead of an isoprenoid chain failed to save the phenotype. MitoQ could not restore respiration in mitochondria isolated from this yeast strain. In bovine heart mitochondria MitoQ was not oxidized by complex III. It was reduced by complex II but not by complex I in contrast to the publication cited above. Reduction by complex II was most efficient with $MitoQ_{10}$ while the analogues with C_3, C_5 and C_{15} alkyl chains were reduced less efficiently [122].

2.3.1.2 MitoQ *in vitro*

MitoQ was used in many *in vitro* studies. It has been shown to decrease lipid peroxidation [120, 122-125], ROS production [126-130] and apoptosis [120, 125, 127, 130-138]. Some of these studies are summarized in the following section.

In isolated mitochondria, the membrane potential and respiration were not impaired up to a concentration of 10 µM. MitoQ dose-dependently inhibited lipid peroxidation induced by cis-parinaric acid in isolated mitochondria and highly decreased hydrogen peroxide induced apoptosis in Jurkat cells [120].

Jauslin *et al*. [134] examined whether MitoQ and MitoVit E could prevent cell death in fibroblasts from Friedreich Ataxia (FRDA) patients. Friedreich Ataxia is a neurodegenerative disorder leading to dysfunction of the musculoskeletal system, cardiomyopathy and other symptoms. The disorder is caused by a mutation in the gene coding for frataxin which is located in mitochondria. It is important for repairing iron-sulfur clusters and for biosynthesis of heme. Mitochondrial oxidative damage is

increased in this condition, thus, antioxidants may have a beneficial effect. Fibroblasts from FRDA patients were treated with L-buthionine-(S,R)-sulfoximine, an inhibitor of glutathione synthesis which leads to apoptosis of FRDA cells while healthy cells are not affected. MitoQ prevented apoptosis at an EC_{50} of 0.5 nM and was about 50 fold more efficient than decylubiquinone. MitoVit E prevented 50% of cell death at a concentration of 23.6 nM and was about 20-fold more potent than vitamin E. In contrast to MitoQ, the EC_{50} of MitoVit E did not increase when FCCP was added to the cells [134].

Saretzki *et al.* [128] examined the effect of MitoQ on population doubling and telomere shortening under hyperoxia. They pretreated MRC-5 fibroblasts with 10-20 nM MitoQ for one week, afterwards the cells were challenged with partial oxygen pressure of 40% under maintenance of MitoQ treatment. After one week of hyperoxia they detected a decrease in ROS levels in MitoQ treated cells. Replicative lifespan significantly increased and telomere shortening decreased. These results suggest that MitoQ can slow the process of cell senescence [128].

In contrast to many other publications, Fink *et al*. [139] reported a pro-oxidant effect of MitoQ in mitochondria isolated from beef aortic epithelial (BAE) cells. Mitoquinone and mitoquinol highly increased H_2O_2 production when mitochondria were respiring on complex I substrates. They also showed an increase in oxygen consumption of isolated mitochondria respiring on glutamate and malate in state 4 and uncoupled state 4 in response to treatment with mitoquinone. However, the ADP:O ratio was not affected as state 3 respiration also raised, indicating an uncoupling effect. Mitoquinone changed fuel selectivity. It increased glucose oxidation and decreased oleate oxidation in BAE cells [139].

2.3.1.3 MitoQ *in vivo*

MitoQ has also been tested in some animal models *in vivo* and few clinical trials were performed.

The first *in vivo* study was done by Smith *et al.* in 2003 [119]. They performed experiments with radiolabelled methyltriphenylphosphonium cation (TPMP). TPMP was taken up by the liver, kidney and heart but not by the brain when injected intraperitoneally. When the substance was injected intravenously, uptake was much

more efficient and also happened in the brain. Accumulation of MitoVit E and MitoQ after feeding in drinking water during 4 and 10 days respectively was detected in heart, brain, liver, kidney and muscle. Thus, this study suggested that MitoVit E and MitoQ may be beneficial in conditions associated with increased oxidative stress.
MitoQ has been tested in several rodent models for heart diseases. Feeding rats for 14 days with MitoQ in their drinking water ameliorated cardiac function in an *ex vivo* model of ischaemia-reperfusion injury. MitoQ significantly lowered lactate dehydrogenase release and electron microscopy showed less pronounced damage to the heart muscle compared to tissue from untreated animals. Cytochrome *c* release and up-regulation of caspase 3 were inhibited. MitoQ protected mitochondrial function as respiration was less impaired in isolated mitochondria from treated animals [140].Graham *et al.* [141] fed spontaneously hypertensive rats during eight weeks with 500 µM MitoQ in their drinking water. After this period systolic blood pressure was significantly decreased and cardiac hypertrophy was reduced [141]. MitoQ was also tested in a rat model of sepsis. It protected heart mitochondria from endotoxin induced decrease in state 3 respiration and impairment of respiratory control ratio. MitoQ also abolished the increase in caspase 3 and caspase 9 activity. It normalized left ventricular pressure and systolic blood pressure. Thus, MitoQ could prevent sepsis induced cardiac dysfunction [142].

Hobbs *et al.* [143] examined whether mitoquinone has a neuroprotective effect in a rat model of stroke. During three days mitoquinone was infused continuously into the right striatum. Afterwards they ligated the right carotid artery during 2.5 h under anesthesia. Then the animals were exposed to 8% oxygen to mimic hypoxic conditions. In this model no protective effect of mitoquinone regarding the number of medium-spiny neurons was detected [143]. This study suggests that mitoquinone has no protective effect against hypoxia induced brain injury. However, mitoquinol and not mitoquinone is considered to act as an antioxidant but one would expect that mitoquinone gets reduced by the respiratory chain to the active form mitoquinol.

In another study the consequences of a long-term administration of MitoQ to mice was elucidated. Rodriguez-Cuenca *et al.* [144] administered MitoQ to mice in their drinking water during 24 to 28 weeks. MitoQ accumulated in the heart, to a lower extent in the liver and in the brain. The amount in the brain was almost 50 times lower than the one in the heart. Oxygen consumption and physical activity were not

affected by MitoQ treatment while the respiratory quotient (RQ) decreased in the dark period when mice were fed with 500 µM MitoQ. Treated mice performed better on the rotarod test indicating improved coordination. Overall bodyweight was not changed but MitoQ treated mice had less fat mass per body weight, less triglyceride content in the liver and average adipocytes size was decreased. Glucose and insulin tolerance were not altered but triglyceride concentration in the blood was diminished [144]. This study indicates that MitoQ can safely be administered for a long time in mice.

1.1.1.1 Clinical trials

Two clinical studies were performed so far. In the PROTECT study the effect of MitoQ on progression of Parkinson's disease was assessed in a double-blind 13-center study in New Zealand and Australia. 128 newly diagnosed patients were treated with either 40 mg or 80 mg MitoQ or placebo for 12 months. There was no effect on disease progression by MitoQ [145]. One explanation is that at the time of diagnosis approximately 50% of dopaminergic neurons are already lost [146]. Another possibility is that MitoQ does not penetrate the blood brain barrier efficiently enough to exert a clinical effect. However this study showed that it can safely be administered to humans for a long time.

The second clinical study was the CLEAR trial with 30 patients suffering from chronic hepatitis C. The effect of mitoquinone on serum amino-transferases and levels of viral RNA was assessed. Thirty patients were randomized for placebo or treatment with 40 mg or 80 mg mitoquinone per day. After 28 days, serum level of alanine-transaminase was significantly lowered compared to baseline but viral load did not change. Thus, this study suggests that MitoQ can reduce liver pathology in hepatitis C [147]. Both trials were performed by Antipodean Pharmaceuticals Inc. This company recently announced that a phase 2b trial with MitoQ on liver disease will be completed this year and that a serum and a cream containing MitoQ are ready to be launched. These two cosmetic products should protect skin keratinocytes and fibroblasts from oxidative damage.

2.3.2 Resveratrol

Resveratrol is a naturally occurring antioxidant mainly found in grapes but also in other plants. It is found in red wine, some berries and purple grape juice. The most abundant form in plants is *trans*-resveratrol-3-O-β-D-glucoside, usually called piceid. Lancon *et al.* showed that cellular uptake involves both diffusion and a carrier-mediated process [148].

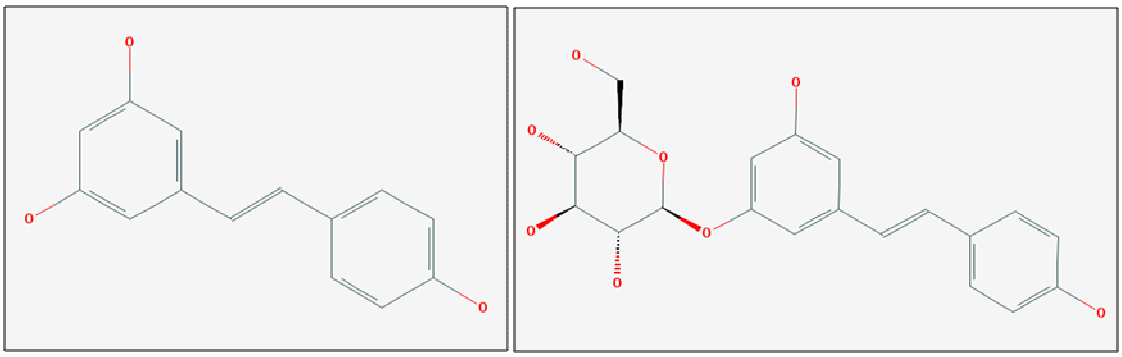

Fig. 11. ***trans*-Resveratrol** **Piceid**

The effets of resveratrol on adipocyte differentiation, oxidative stress, obesity and diabetes, cardiac function and cancer was extensively investigated *in vitro* and *in vivo*. In addition, some clinical studies were performed.

2.3.2.1 Resveratrol and adipocyte differentiation

In human SGBS pre-adipocytes, resveratrol inhibits proliferation and differentiation to adipocytes in a SIRT-1 (NAD-dependent deacetylase sirtuin-1) dependent manner. Resveratrol increased glucose uptake, inhibited lipid accumulation and expression of lipogenic genes [149]. Resveratrol has been shown to dose-dependently reduce lipid accumulation and viability of 3T3-L1 cells during differentiation into adipocytes [150].

Resveratrol down-regulates the expression of several genes involved in adipogenesis including PPARγ and C/EBPα [150] and increases the expression of SIRT-3, UCP1 and Mfn2. [151]. The activity of sirtuins, a family of histone deacetylases, is increased by resveratrol. When SIRT-1 is activated, it de-acetylates PGC-1α and represses PPARγ. PGC-1α induces the expression of genes involved in fatty acid oxidation and

mitochondrial biogenesis while PPARγ is involved in adipocytes differentiation [152]. Expression of SIRT-3, a mitochondrial sirtuin, enhances UCP1 expression via PGC-1α [152]. Beside its function in mitiochonrial fusion, Mfn2 plays an important role in glucose oxidation [151].

Furthermore, resveratrol regulates fat cell number by inhibiting differentiation and by inducing apoptosis. Also in other cell lines cell cycle arrest, inhibition of proliferation and induction of apoptosis was shown under resveratrol treatment [153, 154].

2.3.2.2 Resveratrol and oxidative stress

The mechanism of the antioxidant effect of resveratrol has been characterized *in vitro* and *in vivo*.

Mainly in culture media resveratrol can undergo auto-oxidation, thus, producing the cytotoxic ROS superoxide and hydrogen peroxide. This reaction may influence *in vitro* results. However, there is also a report that degradation can happen without production of hydrogen peroxide [155]. About 80% of resveratrol is degraded after 24 h at 37°C while the sulfate metabolites are stable [156].

Resveratrol has been shown to increase MnSOD levels *in vitro* and *in vivo*. Robb *et al.* [157] treated the human fibroblast-like cell line MRC-5 with resveratrol for two weeks. They showed an increase in the activity of catalase, GSH-PX and MnSOD [157].

Mokni *et al.* [158] injected rats with resveratrol for seven days and measured the activity of several antioxidant enzymes and protein peroxidation in the brain. They measured an increase in activity of SODs, catalase and peroxidases as well as a dose-dependent decrease in malondialdehyde levels, a marker of protein peroxidation [158]. In another study Robb *et al.* [159] administered resveratrol in a normal or high fat diet to mice during four weeks. In brain tissue they observed an increase in MnSOD protein levels and activity in mice on high fat diet in response to resveratrol. In the liver no changes were seen in MnSOD levels while in the heart MnSOD even decreased in mice on high fat diet after resveratrol treatment. Resveratrol had no effects on tissues of mice on normal diet in this study [159]. Thus,

the antioxidant effect of resveratrol seems to be at least in part due to the up-regulation of antioxidant enzymes and is tissue specific.

2.3.2.3 Resveratrol in obesity, diabetes and inflammation

As obesity is known to be accompanied by increased oxidative stress, antioxidants are interesting compounds in this context.

Szkudelska *et al.* treated freshly isolated rat adipocytes with different resveratrol concentrations; they reported that resveratrol reduced glucose conversion to lipids and increased lipolysis after stimulation with epinephrine [160].

Kozawa *et al.* [161] administered a corn-oil mixture and resveratrol or its metabolite piceid either orally or intraperitoneally to rats during three days. Then they injected ^{14}C-palmitate, sacrificed the animals and estimated lipogenesis from ^{14}C-activity. They reported that resveratrol and piceid reduced triglyceride synthesis from ^{14}C-palmitate in the liver. Serum triglyceride and LDL-cholesterol was reduced by piceid after seven days of treatment with piceid [161].

An anti-hyperglycemic effect of resveratrol in obese rodents with experimentally-induced diabetes has been reported in several studies. Baur *et al.* [162] fed mice with either standard (SD), high calorie diet (HC) or high calorie diet supplemented with resveratrol (HCR) and collected data during 24 months. The addition of resveratrol reversed the shortening of lifespan seen in mice on HC. Mice fed HC and HCR showed a significantly impaired performance on the rotarod test compared to mice on SD. Resveratrol treated mice improved during the whole experimental period and they reached equal performance as the SD fed animals at the end of the study. Insulin and glucose levels of HCR mice significantly decreased compared to HC animals. Resveratrol reversed liver and heart pathology as well as the decrease in mitochondrial number seen in HC fed mice [162]. Su *et al.* [163] treated streptozotocin-induced diabetic rats with resveratrol and measured the effects on glucose and insulin metabolism. Resveratrol lowered plasma insulin and glucose concentrations as well as plasma triglyceride content. Importantly, resveratrol prevented weight loss and decreased food and water consumption. Body weight loss and an increase in water and food intake are typical symptoms of untreated diabetes.

Resveratrol also dose-dependently increased glucose uptake of muscle, liver and adipocytes of diabetic rats as well as glycogen synthesis of isolated rat hepatocytes [163]. However, in some publications on streptozotocin-induced diabetic rats resveratrol failed to decrease blood glucose levels [164].

Other studies on rats with experimentally induced diabetes showed an increased expression of the insulin-dependent glucose transporter GLUT4 in resveratrol treated animals [165, 166]. Penumathsa *et al.* reported this effect to be insulin-independent [165] while Chi *et al.* suggested both an insulin-dependent and an insulin-independent pathway [166].

2.3.2.4 Resveratrol in cardiac function and arthersclerosis

In 1992, the observation that daily drinking wine in moderate amounts has beneficial health effects has been published as the “French Paradox”. Scientists believed that not the alcohol itself may cause this effect but one of the polyphenols present in red wine. The one which gained most attention was resveratrol and now it becomes more and more evident that resveratrol is indeed the major factor responsible for cardioprotection of red wine [167].

Beside other beneficial effects, resveratrol blocks peroxidation of LDL in the heart, increases HDL levels and reduces ROS load in the heart [167]. Liu *et al.* [168] treated rats with experimentally-induced hypertension and cardiac hyperthrophy with resveratrol for four weeks. After this treatment period they measured reduced blood pressure, lower heart weight and a decrease in the vasoconstrictors endothelin-1 and angiotensin II while the level of the vasodilatator NO was increased [168]. In another study, spontaneously hypertensive rats were treated with resveratrol for ten weeks. The untreated control group showed cardiac hypertrophy what could be prevented by resveratrol. However, in contrast to other reports, resveratrol did not lower blood pressure [169]. Resveratrol was also reported to inhibit platelet aggregation, thus, exerting a cardioprotective effect similar to aspirin [170].

Other studies suggested that resveratrol may facilitate regeneration of the myocardium after infarction. Rats were pre-treated with resveratrol for two weeks before inducing myocardial infarction by occlusion of the left anterior descending

coronary artery. Following infarction, fluorescence labeled adult cardiac stem cells were injected on the border zone of the myocardium. Twenty-eight days later the resveratrol treated animals showed improved cardiac function and increased survival, proliferation and differentiation of the injected cells. In addition, adult cardiac stem cells expressing GFP (green fluorescent protein) were treated with resveratrol for 60 min. Myocardial infarction was induced in rats as described above and the pre-treated cells were injected after occlusion. One, two and four months after infarction the rats injected with resveratrol treated cells showed better cardiac function and the survival and proliferation of the pre-treated stem cells was increased compared to the untreated control [171].

As resveratrol has anti-inflammatory effects it is also suggested to be beneficial in artherosclerosis. *In vitro* resveratrol showed anti-inflammatory properties. It inhibited secretion of the inflammatory mediators IL-6, IL-8 and granulocyte-macrophage colony stimulating factor (GM-CSF) in macrophages and the expression of COX-2, which catalyses the synthesis of prostaglandin E_2 (PGE_2), a major player in inflammatory reactions [167]. In the epithelial cell line CHO-K1 resveratrol decreased the oxidation and uptake of LDL which is the main cause of artherosclerosis [172].

2.3.2.5 Resveratrol and cancer

The anti-cancer potential of resveratrol was published for the first time by Jang *et al.* in 1997 [173]. Since then, the anti-cancer effects of resveratrol have extensively been investigated. A major problem in chemotherapy is the development of chemo-resistance by the tumor, thus, making chemotherapy ineffective. Therefore, sensitizing the tumor to anti-cancer drugs is an important strategy to overcome chemoresistance [174]. Chemoresistance can have several reasons like increased efflux or inactivation of the drug, alterations of the target molecule and changes in intracellular signaling pathways.

Most reports show that the chemo-sensitizing effect of resveratrol is due to modulation of cell survival proteins. For example Fulda *et al.* [175, 176] and Zhao *et al.* [175, 176] showed that resveratrol decreased the expression of the caspase inhibitor survivin and increased apoptosis in a variety of cancer cell lines. In other

studies resveratrol modulated the tumor suppressor p53 [174]. For example resveratrol up-regulated p53 in chemoresistant B16 melanoma cells [177].

In few studies, down-regulation of NFκB (Nuclear factor NF-kappa-B) and STAT3 (Signal transducer and activator of transcription 3) pathways were reported. Amongst other functions, NFκB is involved in growth regulation, carcinogenesis, apoptosis and inflammation. NFκB has been shown to inhibit drug-induced apoptosis when it is constitutively active [174]. Aberrant STAT3 signaling is involved in uncontrolled cell growth, invasion, angiogenesis, metastasis and resistance to apoptosis [178]. In multiple melanoma cells resveratrol enhanced the apoptotic and anti-proliferative effect of two anti-cancer drugs. This enhancement was accompanied by inhibition of NFκB and STAT3 activation and also observed in melanoma patients [174].

Zhao *et al.* [176] injected multidrug-resistant human non-small-cell lung cancer cells (NSCLC) into nude mice and treated them with a resveratrol containing diet. Resveratrol exerted an anti-tumor effect without showing any toxicity. It decreased proliferation and survivin expression and increased apoptosis. In addition, resveratrol decreased the IC_{50} of various anti-cancer agents [176]. However, there are also reports that resveratrol counteracts chemotherapeutic agents in some tumor cells [174].

2.3.2.6 Pharmacological properties of resveratrol

Resveratrol has rather unfavorable pharmacological properties. It is efficiently absorbed but its bioavailabilty is low and it is rapidly cleared from the circulation [179]. It is metabolized into different derivates, mainly glucuronide and sulfate conjugates [155]. The major metabolite in humans is picetannol (3,5,3',4'-tetrahydroxystilbene) which has an additional hydroxyl group [155]. Different strategies were used to increase its bioavailability without losing activity. Acetylation increases absorption and cellular uptake, binding to hexanoic acid enhances the affinity to human serum albumin and nanoparticles which should improve stability and bioavailability are in development [155].

At high concentrations resveratrol binds to human serum albumin (HSA) and hemoglobin. The affinity to hemoglobin (Hb) is lower [180], but Hb has a higher

concentration in the serum than HSA. Thus, both proteins are supposed to play an important role in resveratrol distribution [155]. Fatty acids facilitate the binding of resveratrol to bovine serum albumin (BSA).

2.3.2.7 Human *ex vivo* studies and clinical trials with resveratrol

To date about 30 clinical trials and human *ex vivo* studies with resveratrol are published. Many of them investigated the pharmacokinetics of resveratrol or its effects on different parameters important in heart disease. In few studies the influence of resveratrol on insulin sensitivity and oxidative stress was examined. However, all trials were performed with a small number of probands and in many of them either red wine or plant extracts instead of pure resveratrol was used.

In *ex vivo* experiments using vascular rings from different arteries and veins, resveratrol caused relaxation of the blood vessel. This was seen in blood vessels from healthy probands as wells as in the ones from patients with heart diseases. This effect was observed at concentrations which can be achieved by ingestion of resveratrol-rich food [181, 182]. Brasnyó *et al.* [183] treated T2DM patients with either resveratrol or placebo for four weeks in a double blind study with nine or ten probands in each group. Resveratrol improved insulin sensitivity, decreased oxidative stress but had no effect on parameters related to β-cell function [183].

2.3.3 Curcumin

Curcumin is an ingredient of turmeric, a spice prepared from the root of *Curcuma longa*. Turmeric is a condiment of curry powder and mainly used in the Asian kitchen. Curcuminoid isolated from plants consists of 3 major natural analogues: curcumin is the most abundant one at ca. 77%, demethoxycurcumin and bis-demethoxycurcumin account for 17% and 3%, respectively. Efficacy of the different analogues varies between cell types, function, models of disease and among species. Curcumin is commercially available as a pure substance of only one individual analogue which was synthesized chemically or as a mixture of all 3 natural curcuminoids isolated from plants [178].

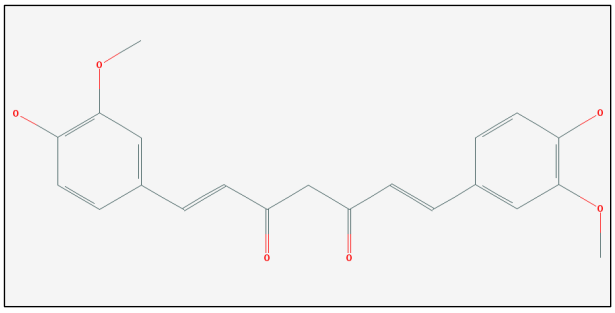

Fig. 12. Curcumin

Curcumin shows anti-inflammatory, antioxidant, pro-apoptotic and anti-cancer effects *in vitro* and *in vivo*.

2.3.3.1 The impacts of curcumin on proliferation, apoptosis and cancer

Curcumin interacts with the transcription factors NFκB and STAT3 [178]. Shishodia *et al.* reported that curcumin induced cell cycle arrest, apoptosis and suppression of proliferation in four different human lymphoma cell lines by down-regulation of NFκB [184]. Curcumin suppresses cell proliferation induced by IL-6 production by inhibiting STAT3 signaling in human multiple melanoma cells [185] and also inhibits STAT3 activation in different human lymphoma cell lines [186].

It was also reported that curcumin altered the expression of the tumor suppressor p53 which plays an important role in many cancer types [187]. Several reports showed that curcumin induced apoptosis by up-regulation of p53 [187]. For example, Choudhuri e*t al.* reported that curcumin induced apoptosis in human epithelial breast cancer, prostate cancer and B cell lymphoma cell lines [188]. Han *et al.* [189] saw a

decrease in proliferation in two murine immature B cell lymphoma cell lines while this effect was much weaker in normal B cells. Surprisingly, they demonstrated a down-regulation of expression of p53. Another report demonstrated reduced activity of p53 in the RKO colon cancer cell line where curcumin impaired the correct folding of the p53 protein [190] and it also enhanced degradation of p53 in myeloid leukaemia cells [191].

In the context of cancer, the effects of curcumin on matrix metalloproteases (MMPs) were also investigated. MMPs are endopeptidases and are over-expressed in inflammation and cancer [178]. Over-expression of MMPs leads to fibrosis, tissue destruction and inflammation [192]. MMPs also play an important role in invasion, metastasis and angiogenesis of cancer as they cause matrix dissolution [193]. It has been shown that curcumin decreases MMP-9 expression via inhibiting NFκB expression in human astroglioma cells [194]. Curcumin down-regulates MMP-2 and MMP-9 and decreases invasion and migration in human fibrosarcoma cells. Curcumin was also reported to decrease MMP-9 production of human and rabbit peripheral blood mononuclear cells [178].

2.3.3.2 Curcumin in obesity, diabetes and inflammation

Curcumin was extensively described as a modulator of inflammation and metabolic disorders in obesity. It was suggested that curcumin has beneficial effects in obesity, diabetes, artherosclerosis and metabolic syndrome [22].

Lee and colleagues showed that curcumin down-regulates PPARγ in 3T3-L1 adipocytes, thus, inhibiting differentiation [195]. However, in contrast to the publication above Kuroda *et al.* [196] reported that ethanol extracts of turmeric dose-dependently stimulated differentiation of human pre-adipocytes into adipocytes and increased PPARγ activity.

In KK-A(γ) mice, a modelT2DM, the turmeric extract lowered blood glucose [196]. In addition, curcumin enhanced the expression of adiponectin in obese *ob/ob* mice [197]. Ejaz *et al*. treated mice fed with a high fat diet with dietary curcumin for 12 weeks: Curcumin supplementation reduced weight gain, adiposity and micro-vessel density in fat tissue but did not affect food consumption [198].

Another group used the same animal model and examined erythrocytes, heart, liver, kidney and pancreas for oxidative stress and activity of the antioxidant enzymes SOD, catalase and GSH-PX. They showed lower lipid peroxidation in all tissues examined in diabetic rats treated with curcumin compared to the untreated animals. In addition, they observed higher SOD activity in pancreas but not in the other tissues and GSH-PX was more active in erythrocytes and pancreas while catalase activity was higher in all five tissues [199].

Curcumin also acts as an anti-inflammatory agent. It was shown to decrease expression of TNFα in various tissues [200]. Other groups reported that curcumin decreased various inflammatory cytokines expressed by adipocytes such as IL-1, IL-6 and several chemokines [201, 202]. Jain and colleagues [203] cultured U937 macrophages in high or low glucose medium and treated the cells with curcumin. They observed a decrease in lipid peroxidation and secretion of IL-6, IL-8 TNFα and monocyte chemoattractant protein 1(MCP-1) in the cells cultured in high glucose in response to curcumin. Furthermore, they elucidated the effects of curcumin on inflammatory cytokines in rats with experimentally-induced diabetes. After seven weeks of oral administration of curcumin, diabetic rats showed significantly lower concentrations of IL-6, TNFα and MCP-1, lower blood glucose and higher plasma insulin as well as decreased oxidative stress compared to untreated animals [203]. It was also shown that curcumin reduced MMP-9 in human intestinal epithelial cells and dose-dependently inhibited MMP-3 production in primary human colonic myofibroblasts from subjects with inflammatory bowel disease [178].
Thus, curcumin not only acts on adipose tissue but also directly on cells which mediate inflammation.

2.3.3.3 Curcumin and cardiac dysfunction

Morimoto *et al.* [204] could show that curcumin prevents cardiac hypertrophy in rats by inhibiting the histone acetyltransferase p300. It also prevented heart-failure induced increase in cardiac wall thickness and diameter in two rat models.

2.3.3.4 Clinical trials with curcumin

About 60 clinical trials using curcumin are published so far. Amongst others curcumin was tested in the field of cancer, Alzheimer's disease, heart diseases and blood lipid profile. All these studies included only a small number of patients. Some of these trials are shortly summarized below.

Carroll *et al.* [205] investigated the effect of curcumin on colorectal neoplasia in smokers treated with 2 g or 4 g curcumin daily for 30 days. The group treated with 4 g curcumin showed a reduction of 40% in the number of aberrant crypt foci, a preneoplastic lesion [205]. In another phase II trial patients with advanced pancreatic cancer were treated with 8 g curcumin daily until disease progression. Two out of 21 patients showed a clinical response. In one patient the disease was stable for more than 18 months and the other responder had a brief tumor regression of 73% accompanied by significant increases in serum levels of IL-6, IL-8, IL-10 and IL-1 receptor antagonists. Curcumin showed low steady-state levels indicating poor bioavailability and was detected as glucuronide and sulfate conjugates [206]. Usharani *et al.* [207] treated patients suffering from T2DM with 150 mg curcumin or placebo twice daily for eight weeks. They observed improved endothelial function and a decrease in serum levels of TNFα, IL-6 and malondialdehyde, a marker for oxidative stress [207]. Another group investigated the effects of curcumin on blood lipid profile in a randomized double-blind trial. They treated elderly people with either 4 g or 1 g curcumin daily or with placebo during six months. No changes in total cholesterol, HDL cholesterol, LDL cholesterol or triaglycerols were detected. Almost no side effects appeared, thus, curcumin is well tolerated during a long-term treatment [208].

3 Aims of the thesis

As argued above, good *in vitro* models are needed for research into the elucidation of the mechanisms of fat accumulation in overweight-associated diseases. So far, most *in vitro* studies have been performed in murine cell lines, although a primary human model would be much closer to the needs for preclinical research. Therefore, the first aim was to characterize hBM-MSCs as a model for adipocytes and adipogenesis. Several important parameters such as fat accumulation, ROS production, mitochondrial mass and morphology and cellular oxygen consumption should be analyzed during the whole differentiation process from the stem cell to the adipocyte. The study was also intended to show analogies and differences between primary human cells and the commonly used murine adipocytes-like cell lines.

The second aim of this thesis was to investigate the effect of antioxidants to reduce oxidative stress in the hBM-MSC adipocyte cell model. As explained above, oxidative stress is increased in obesity and is supposed to lead to insulin resistance. Obese people often have mutations in mtDNA of β-cells which lead to defective insulin secretion and apoptosis. In addition, mitochondrial mass of white adipocytes is significantly decreased in genetically obese and diabetic *ob/ob* mice compared to wild-type animals. As mitochondria are the main source of intracellular ROS themselves, they are especially vulnerable to oxidative stress. Therefore, an antioxidant treatment may have beneficial effects on insulin sensitivity and mitochondrial function. The aim was to investigate the effects of three antioxidant compounds on hBM-MSC derived adipocytes, namely the synthetic mitochondrial-targeted coenzymeQ analogue MitoQ and the natural compounds resveratrol and curcumin. The impact on different mitochondrial functions of these substances should be assessed. In particular their influence on ROS production, respiration and intracellular ATP content should be investigated. These experiments should give a clue whether MitoQ, resveratrol and curcumin may be interesting candidates for preventing mitochondrial dysfunction in obese patients.

4 Description of human bone marrow stem cells as a model for adipogenesis and adipocytes

E. Hirzel[1,2], P. Lindinger[1,2], M. Hoch[1,3], S. Krähenbühl[2], A.N. Eberle[1]

[1] Laboratory Endocrinology, Department of Biomedicine, University of Basel, Basel, Switzerland

[2] Laboratory of Clinical Pharmacology and Toxicology, Department of Biomedicine, University of Basel, Basel, Switzerland

[3] Actelion Pharmaceuticals Ltd., Allschwil, Switzerland

Abstract

Overweight represents a major threat to public health in many countries. We describe primary human bone marrow stem cells (hBM-MSCs) as a model for adipogenesis and adipocytes. During adipogenesis the following cellular and mitochondrial functions were assessed: fat accumulation, reactive oxygen species (ROS) production, cellular protein content, oxygen consumption and mitochondrial mass per cytoplamic volume. All these measures increased during differentiation except the cell number remained uneffected. During adipogenesis, the density and interconnectivity of the mitochondrial networks increased. mitochondria while cristae structure was not altered. Here, we present data about respiration and ROS production during the differentiation process of the hBM-MSC based adipogenesis model for the first time.

Introduction

Overweight and obesity represent a main threat to public health in many countries worldwide. In the United States 68% of men were overweight and 32.2% were obese in 2008. In the same period 64.1% of women were overweight and 35.5% were obese [1]. Obesity can lead to severe co-morbidities such as metabolic syndrome, hypertension, type II diabetes mellitus (T2DM), coronary heart disease and stroke. Obesity is accompanied by elevated plasma concentrations of free fatty acids (FFA), a chronic low level inflammation and an increase of reactive oxygen species (ROS) production, both at a systemic level [19]. High levels of FFA are likely to contribute to insulin resistance (IRe) [209]. Fatty acids can either be oxidized in mitochondria or stored as triglycerides. Lipid overload leads to an accumulation of fatty acid intermediates which can activate inflammatory pathways, thus, leading to an inhibition of insulin function [209]. In animal and human models of genetic and diet induced obesity, macrophages infiltrate adipose tissue and secrete inflammatory mediators which could promote obesity-induced insulin resistance [210, 211]. It has been shown that elevated concentrations of glucose or FFA induce the formation of ROS in muscle, pancreatic β-cells, adipocytes and also other cell types [212-215]. Reactive nitrogen species (RNS) and ROS are unavoidably generated by oxidative phosphorylation [216-219]. Augmented levels of substrates lead to higher mitochondrial respiration causing increased oxidative stress to the cell. Antioxidant mechanisms include ROS converting enzymes such as mitochondrial manganese

superoxide dismutase (MnSOD) which converts superoxide to hydrogen peroxide within mitochondria. Glutathione peroxidase (GSH-PX) and catalase further catalyze the reaction from hydrogen peroxide to water. In addition, the inner mitochondrial membrane contains non-enzymatic antioxidants like vitamin E [217-219]. Cell damage can occur when the endogenous ROS defense mechanisms are overwhelmed. Increased levels of ROS load have been reported in reperfusion injury after myocardial infarction, cancer, Alzheimer's disease, amyotrophic lateral sclerosis, atherosclerosis, hypertension, diabetes and other disorders [220]. In mouse adipocytes ROS levels increased in response to high concentrations of glucose [215]. Primary rat adipocytes showed augmented generation of ROS when exposed to high glucose and insulin concentrations. This reaction could be prevented by pre-incubation with the antioxidant N-acetylcystein [221]. It has also been shown that exposure of 3T3-L1 adipocytes to hydrogen peroxide caused IRe [222]. Thus, IRe has been proposed to be a physiological mechanism to prevent oxidative stress [51].

The former view of adipocytes being only an inactive depot of triglycerides changed completely during the last years. Fat cells are now recognized as an important player in disease mechanisms. Due to the high prevalence of obesity in the western world these cells deserve even closer attention. Usually the murine 3T3-L1 fibroblast-like cell line is used as an adipocytes model for in vitro studies. The use of these murine cells has the disadvantage that the cells might behave distinct in comparison to human cells. Human adipocytes isolated directly from adipose tissue cannot be expanded and are difficult to handle as they are extremely fragile. In our hands human preadipocytes from adipose tissue did not differentiate efficiently and reproducible into adipocytes. Here we describe primary human bone marrow derived mesenchymal stem cells (hBM-MSC) as a model for human adipocytes and adipogenesis. These human cells can easily be grown and differentiated into fat cells and may be closer to the clinics than murine 3T3 cells, thus, providing a more relevant model for research.

Materials and Methods

Chemicals

All chemicals were purchased from Sigma-Aldrich (Buchs, Switzerland) if not mentioned otherwise.

Cell culture

Primary human bone marrow derived mesenchymal stem cells (hBM-MSC) were expanded until confluency was reached. Then the cells were differentiated for 22 days by applying differentiation medium containing insulin, rosiglitazone, 3-Isobutyl-1-methylxanthine (IBMX) and other substances. The exact media composition was performed as described in Hoch *et al* [223]. The cells were kindly provided by Prof. Ivan Martin (Department of Biomedicine, University of Basel, Switzerland).

ROS measurements

The cells (hBM-MSCs) were cultivated in 96-well cell culture plates and differentiated into adipocytes.

2', 7'-Dichlorodihydrofluorescein diacetate (DCFH-DA) assay

The cells were washed with PBS and per well 100 µl of 50 µM DCFH-DA in DCF buffer (hepes 1 M, glucose 1 M, 10 % BSA in PBS) were added. After incubation for 30 min at 37 °C and 5% CO_2, the cells were washed twice with ice cold PBS and permeabilised with 0.2 % triton-X-100 on ice for 10 min. The plates were centrifuged at 3000xg for 5 min and 100 µl of the supernatants were transferred into a white 96-well plate. Fluorescence was measured in a SpectraMAX Gemini XS (Molecular Devices; Ismaning, Germany) fluorometer at 490 nm (excitation) and 535 nm (emission).

Nitroblue tetrazolium (NBT) assay

The cells were washed with PBS and per well 100 µl of 0.1% NBT in PBS were added. After 2 h of incubation at 37 °C and 5% CO_2 the cultures were washed with PBS. To dissolve the precipitated formazan, 100 µl DMSO containing 2 M KOH were added and the plate was placed on a shaker for 10 min. Afterwards, the plate was centrifuged at 3000xg for 5 min and 60 µl of the supernatants were transferred into a

new plate. Absorbance was measured at 650 nm in a SpectraMAX 190 (Molecular Devices; Ismaning, Germany) reader.

Oil Red Orange (Red Oli O) staining

The cells were grown to confluency and differentiated into adipocytes in 96-well plates. At the indicated time points, the cultures were fixed with 4% methanol free paraformaldehyde (Thermo Scientific) in PBS for 20 min, washed with 60% 2-propanol and water. Per well 100 µl of a staining solution consisting of 4 parts Red Oil O stock solution (0.5 % Red Oil O in 60 % 2-propanol) and 6 parts MiliQ-water were added. After 30 min incubation the cultures were washed extensively with MiliQ-water. The samples were analyzed in an IX 50 microscope (Olympus; New York, USA) using a 20x objective (Olympus; New York, USA) and quantification was done by Analysis software (Olympus; New York, USA).

Determination of cell number

Cells were cultured and differentiated in 6-well plates. At the indicated time points the cells were washed with PBS, detached with trypsin-EDTA and counted using a Z1 Coulter Particle Counter (Beckman Coulter; Nyon, Switzerland).

Oxygen consumption and extracellular acidification measured with a Seahorse flux analyzer

To determine basal oxygen consumption and extracellular acidification of intact cells, a seahorse flux analyzer (Seahorse Bioscience; Copenhagen, Denmark) was used. The seahorse instument is a fluorophor-based open system and measures oxygen flux in special cell culture plates. The cells were grown and differentiated in 24-well V7 Seahorse microtiter cell culture plates. Four wells did not contain cells and were required for the calibration of the system. For the measurements the usual cell culture medium was replaced by unbuffered DMEM without bicarbonate. First, basal respiration was measured, afterwards oligomycin, Carbonyl cyanide 4-(trifluoromethoxy)phenylhydrazone (FCCP) and rotenone were added consecutively to a final concentration of 1 µM each. Oligomycin inhibits the ATP-synthase, thus, showing leak respiration. FCCP is an ionophore used to display the maximal capacity of the electron transport chain (ETC). Rotenone is a complex I inhibitor and was used

as a control. Oligomycin and FCCP were titrated in preliminary experiments to determine optimal concentrations.

The extracellular acidification rate (ECAR) is an indicator for glycolysis and was measured simultaneously. The measurement o fECAR is also based on fluorescence.

Determination of protein content

Protein content of the cell cultures during differentiation was determined using the seahorse cell culture plates after performing the seahorse experiments. Per well, trichloroacetic acid at a final concentration of 10% was added. The cells were fixed for 1 h at 4 °C, washed with tap water and air dried. Afterwards, 150 µl of the staining solution containing sulforhodamine B 0.4% in acetic acid 1% were added to each well and the plates were incubated for 30 min. Then, the plates were rinsed 4 times with acetic acid 1 %, air dried and the stain was solubilized in 120 µl Tris-base (Fluka) 10 mM pH 10.5. Afterwards, 100 µl were transferred from each well into a 96-well plate and absorbance was measured at 530 nm in a SpectraMAX 190 (Molecular Devices; Ismaning, Germany) reader.

Confocal laser scanning microscopy

To examine the mitochondrial structure during differentiation, confocal microscopy was performed. First, the cells were cultured and differentiated on conventional cover glasses placed in 24-well cell culture plates. Second, the cells were fixed with 4% methanol free paraformaldehyde in PBS for 20 min and permeabilized with 0.15% Triton-X-100 in PBS for 15 min. Afterwards, the specimens were blocked with 10% BSA in PBS for 30 min, incubated with a mouse-anti-human cytochrome *c* antibody (BD Pharmingen; San Diego, USA) diluted 1:1000 in 10% BSA at 4 °C overnight and then washed with PBS. The secondary goat-anti-mouse antibody labeled with AlexaFluor 488 (Invitrogen Ltd.; Paisley, United Kingdom) was applied at a dilution of 1:500 in PBS containing 5% BSA. After incubation at room temperature for 1 h, the cells were washed with PBS and the nuclei were stained with DAPI 1 µg/ml for 5 min. The coverglasses were mounted onto glass slides with VectaShield (Vector Laboratories LTD.; Peterborough, United Kingdom). A Zeiss LSM710 confocal laser scanning microscope with 63x/1.4 oil objective and ZEN software (Carl Zeiss

Microimaging GmbH; Jena, Germany) were used for examination. Z-stacks with 0.8 µm thickness at a 0.4 µm interval were performed. Two layers were used for generating a cuboid, one in the middle of the cell and the next but one (n+2). To quantify mitochondrial volume per cytoplasmic volume, 3 equal cuboids of 69.47 μm^3 each were analyzed per cell. All pictures were taken with the same detector adjustments.

Transmission electron microscopy

Cells were cultured in 60 cm^2 petri dishes. At the indicated time points, the cells were washed with PBS and fixed with a PBS solution containing 3% paraformaldehyde and 0.5% glutaraldehyde for 1 h. Then, the cells were scraped, transferred into an eppendorf tube and centrifuged at 10'000 rpm using a table centrifuge (Eppendorf; Hamburg, Germany) for 4 min. After resuspension in PBS, the cells were centrifuged again at 6'000 rpm for 4 min. The following steps of sample preparation and picture acquisition were done in the microscopy centre at the Biocenter, University of Basel, Switzerland. Briefly, the samples were washed with PBS and osmiumtetroxid 1% was added for 1 h. After a washing step with water, the samples were dehydrated with ascending concentrations of ethanol. Finally, ethanol 100% was replaced by aceton, aceton:epon 1:1 and pure epon consecutively. The specimens were imbedded in epon at 60°C for 24-48 h, cut in 60-70 nm slices with an ULTRACUT microtome (Reichert-Jung) and analyzed with a FEI Morgagni268D (FEI; Eindhoven, Netherlands) transmission electron microscope.

Statistical analyses

Statistical analyses were performed using Prism 5 software (Graphpad Software Inc.; La Jolla, USA). ANOVA and Tuckey's post test were applied and a p-value < 0.05 was regarded as significant. Data are shown as mean plus SD.

Results

To follow the differentiation process of stem cells into adipocytes, various parameters relevant for fat tissue were monitored during 22 days. Differentiation was induced after the cells reached confluence by exchanging growth medium with differentiation medium.

Fat accumulation was visualized by bright field microscopy. Lipid droplets were stained with Red Oil Orange and quantified. First signs of fat accumulation were seen at day 6 after starting differentiation. Lipid content per cellular surface highly increased between day 6 and day 10 from 3% to 22%. The maximum was reached at day 18 when 34% of the growth area was covered by fat. At day 22, lipid content slightly decreased to 29% (Fig. 1A + B).

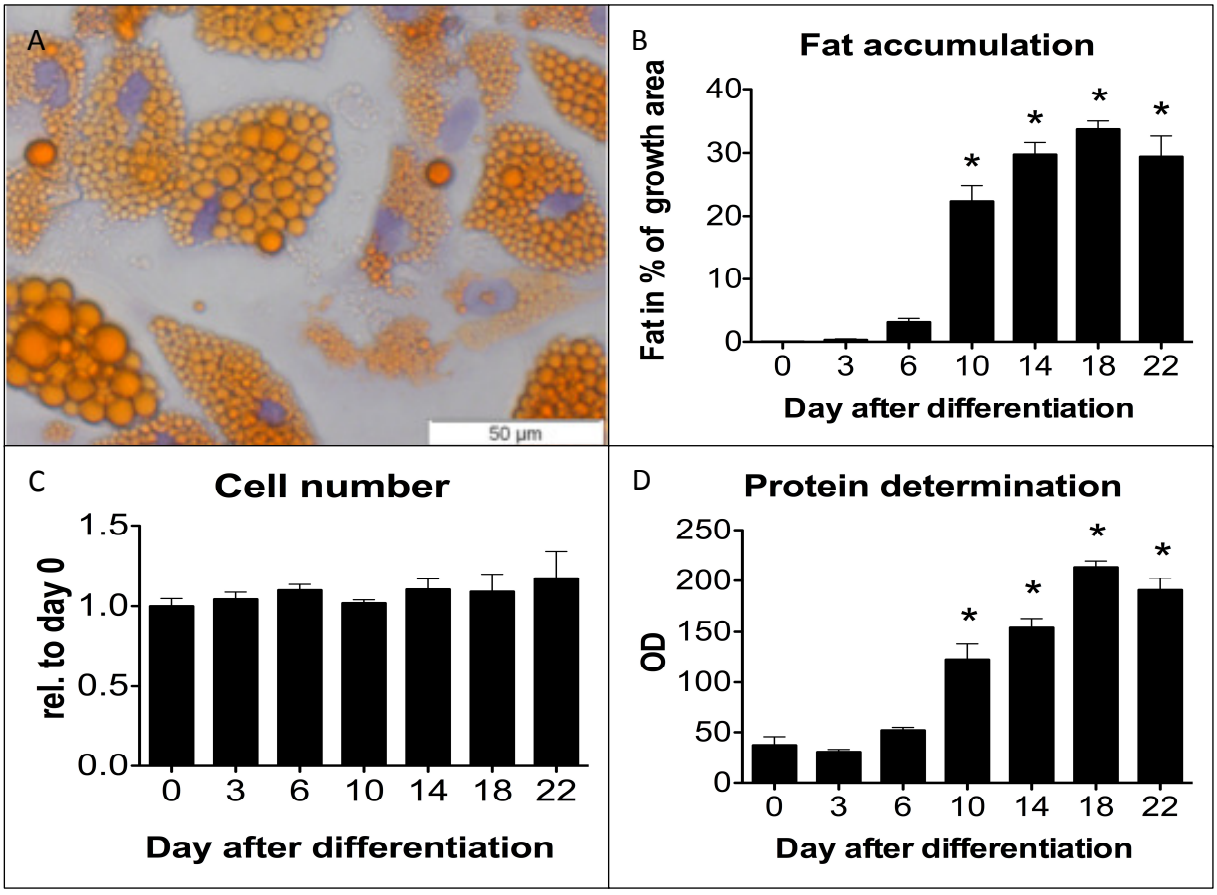

Fig. 1. Cellular characteristics during differentiation.
A) Red Oil O staining of adipocytes at day 14 of differentiation, counterstaining with Mayer's Haemalaun; bar 50 µm. B) Quantification of growth area covered by fat. C) Cell number during differentiation. D) Protein content during differentiation.
★ $p \leq 0.05$ compared to day 0.

To investigate whether cells continue to proliferate or may supersede each other, the cells were counted during adipogenesis. No change in cell number appeared during the differentiation process (Fig. 1C).

Protein content was investigated using sulforhodamine beta staining in the seahorse cell culture plates after measuring oxygen consumption (as described below). Protein content increased over time and reached a plateau at day 14 (Fig. 1D).

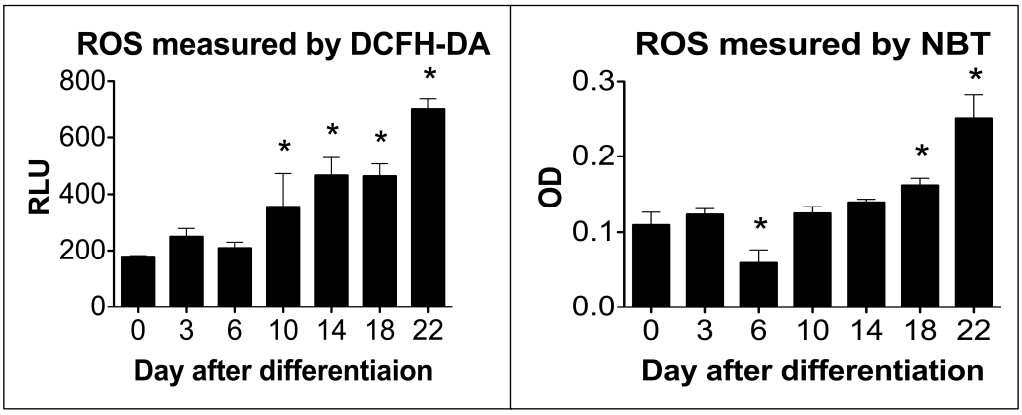

Fig. 2. Measurement of ROS production during differentiation.
★ $p \leq 0.05$ compared to day 0

Production of reactive oxygen species (ROS) was examined using two different 96-well plate based assays. The DCFH-DA fluorescence assay showed a clear increase of ROS production at day 10, thereafter a plateau until day 18 was observed, followed by a strong augmentation at day 22. Production of ROS increased 390% during this time period (Fig. 2A). The NBT absorbance assay indicated the same tendency (Fig. 2B). However, the effect was less pronounced.

To analyze oxygen consumption during differentiation a seahorse flux analyzer was used. Respiration was highly increased from day 10 on and reached the maximum at day 18, when it was 570% higher than at day 0. However, oxygen consumption not only augmented under basal conditions, but also after the addition of oligomycin, an ATP-synthase inhibitor. Respiration after FCCP addition highly increased during the adipogenesis showing that the maximal capacity of the electron transport chain also raised (Fig. 3A). Oxygen consumption rates normalized on the cellular protein content were approximately constant over time but increased relative to cell number.

The extracellular acidification rate, an indicator of glycolysis, increased over time under basal conditions and after addition of oligomycin (Fig. 3B).

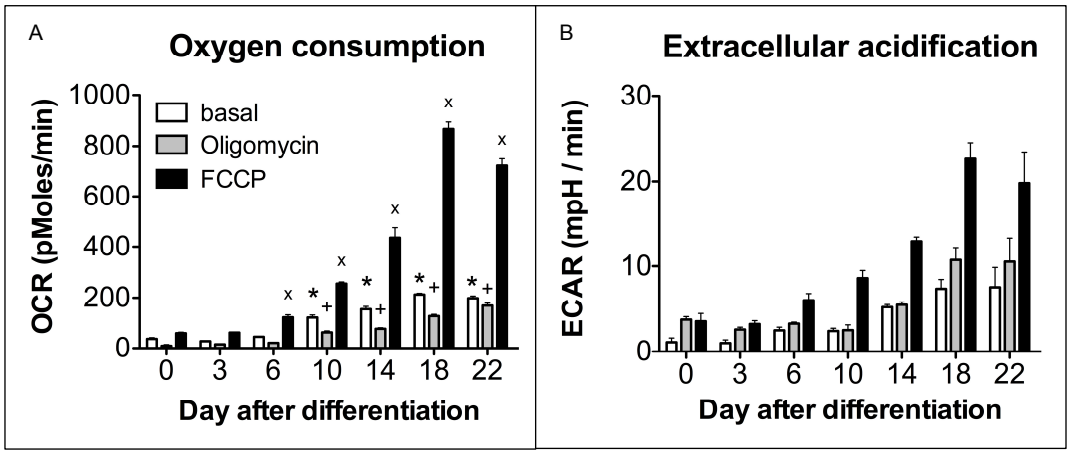

Fig. 3. Oxygen consumption rate and extracellular acidification rate.
★ $p \leq 0.05$ compared to basal at day 0.
+ $p \leq 0.05$ compared to oligomycin at day 0.
x $p \leq 0.05$ compared to FCCP at day 0.

However, the absolute values were very low and hardly exceeded the detection limit. Uncoupling with FCCP resulted in an augmentation of ECAR compared to the two foregoing measurements as the cells were forced to change their metabolism to glycolysis.

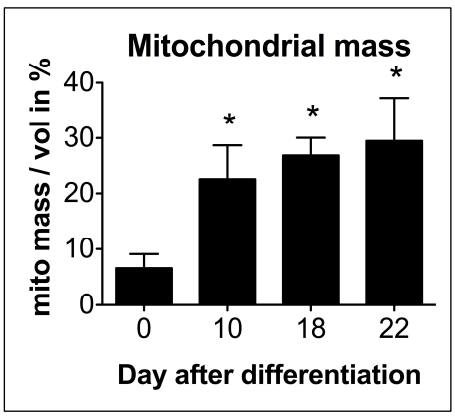

Fig. 4. Mitochondrial volume per cytoplasmic volume during differentiation.
★ $p \leq 0.05$ compared to day 0

Mitochondrial volume and morphology were investigated by confocal laser scanning microscopy. An anti-cytochrome *c* antibody was used to visualize mitochondria. Using computed three dimensional pictures mitochondria appeared as a network which became tighter during differentiation. Mitochondrial mass per volume increased from 6.5% to 28.5% during adipogenesis. The augmentation mainly happened between day 0 and day 10 (Fig. 4 + 5).

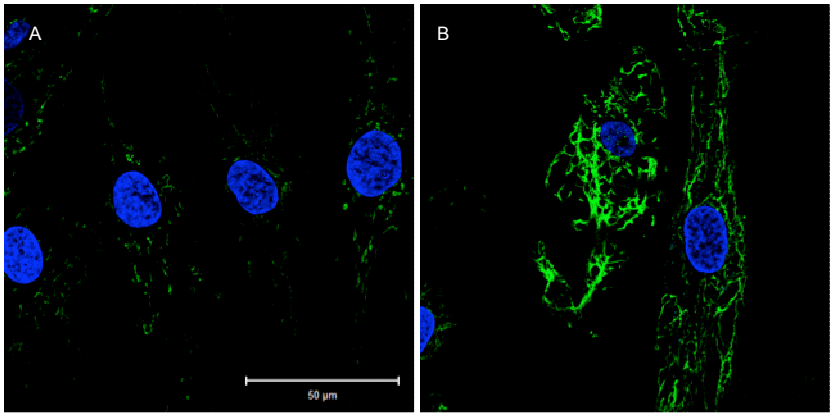

Fig. 5. CLSM pictures of mitochondria. A) day 0. B) day 22.
green: mitochondria; blue: nuclei. bar: 50 µM

Transmission electron microscopy was performed to visualize mitochondrial morphology during differentiation. Mitochondria could nicely be displayed and showed no change in cristae structure during differentiation (Fig. 6).

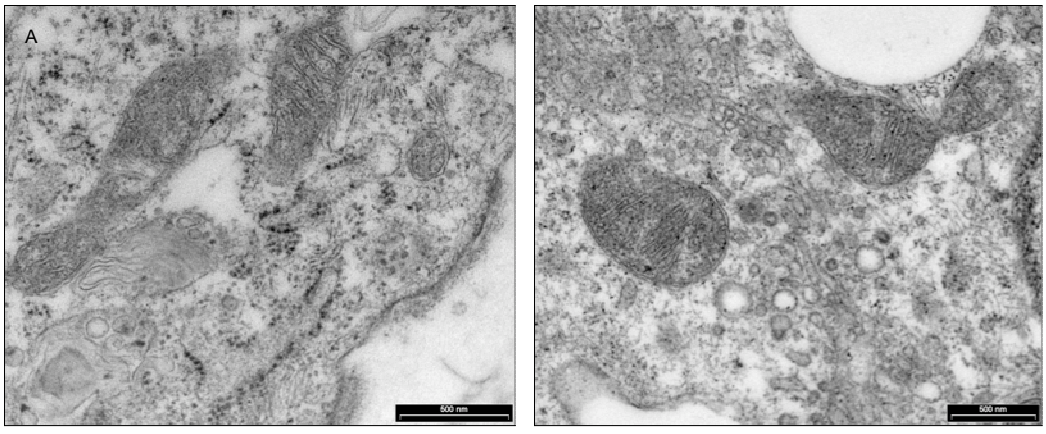

Fig. 6. Transmission electron microscopy showing mitochondria.
A) day 0. B) day 22. bar: 500 nm.

Discussion

The increase in fat content over time showed, that hBM-MSC efficiently differentiate into adipocytes. As expected for differentiating cells, no proliferation was detectable during adipogenesis. It was reported previously that growth arrest is mandatory for the differentiation process in many cell types including adipocytes [224]. The protein content assessed in the Seahorse cell culture plates increased over time, indicating that cell volume raised, what was also observed under the microscope.

Production of ROS has been reported to increase during adipogenesis *in vitro* [225]. Lee e*t al.* even reported that ROS facilitate fat accumulation in 3T3-L1 cells [226]. We could show a strong increase in ROS levels in differentiating hBM-MSCs. Both assays applied showed the same trend, thus, providing good evidence for an increase in ROS levels during differentiation. The reason why this effect was much weaker in the NBT assay compared to the DCFH-DA experiments may be that these dyes react with different radicals. DCFH-DA is de-esterified by intracellular esterases and becomes highly fluorescent upon oxidation while NBT forms blue insoluble formazan when it gets reduced. Therefore, the oxidative ROS H_2O_2 and HO_2• can react with the de-esterified derivative DCFH whereas the NBT assay mainly shows production of the reducing radical O_2^-•.

To elucidate whether this augmentation of oxidative stress may be due to enhanced respiration, we focused on mitochondria, the major source of ROS production in cells. Respiration under basal conditions increased over time and the same progression was seen in oligomycin inhibited oxygen consumption. These findings indicate that the elevated basal respiration may be due to partial uncoupling. Ducluzeau *et al.* recently reported an increase in oxygen consumption during differentiation of 3T3-L1 fibroblasts into adipocytes which they also ascribed to an augmentation of uncoupling [227]. Thus, our finding goes along this report. Furthermore, the striking augmentation of oxygen consumption after addition of FCCP suggests that elevated uncoupling may not be the exclusive reason for the increase in respiration. Extracellular acidification rate, a measurement for glycolysis, showed very low values indicating that glycolysis may only play a minor role in ATP production.

To further investigate the reason for the observed increase in oxygen consumption, we estimated the mitochondrial mass per cytoplasmic volume using confocal microscopy. We detected a strong increase in mitochondrial mass per volume

suggesting mitochondrial biogenesis may contribute to increased respiration. This result is in agreement with Lu *et. al.* who reported an increase during differentiation of rat adipocytes *in vitro* [228]. As Sarsour *et al.* showed age associated loss of cristae in quiescent fibroblasts which could be prevented with overexpression of mitochondrial manganese superoxide dismutase [229], we questioned whether mitochondrial morphology may change during differentiation as ROS levels increase in adipocytes. To visualize mitochondria we performed electron microscopy during the differentiation process. In our cellular model we did not detect any alterations in mitochondria and cristae structure during the 22 days of differentiation. In a previous study in our lab the production of inflammatory cytokines in human adipose tissue and hBM-MSC derived adipocytes in response to lipopolysacharide was investigated. [230]. It has been published that TNFα, IL-6 and IL-8 [20] are produced in white adipose tissue (WAT). TNFα and IL-6 are increased in obesity and TNFα was reported to induce insulin resistance [20]. IL-10 is also produced in adipose tissue [231] but to a lower extent. In our former study mentioned above, an increase in IL-6 and IL-8 secretion in both adipose tissue explants and hBM-MSC derived adipocytes was observed. In contrast to the tissue, hBM-MSC did not produce IL-10 and TNFα [230]. This correlates with the findings that adipose tissue derived TNFα and IL-10 is mainly produced by macrophages and not by adipocytes [232].

Here we describe fat accumulation, ROS production, oxygen consumption, mitochondrial mass and morphology during differentiation of hBM-MSC into adipocytes. The data presented are in agreement with previous reports from 3T3-L1 cells. In summary, our results show that hBM-MSC derived adipocytes are a good model for adipocytes and adipogenesis. Compared to 3T3-L1 our model has the advantage to be closer to the clinics as these cells are of primary human origin.

Acknowledgements

We thank Prof. Ivan Martin (Department of Biomedicine, University of Basel, Switzerland) for kindly providing the hBM-MSCs. We also thank Beat Erne (Department of Biomedicine, University of Basel, Switzerland) for teaching at the CLSM, Ursula Sauder and Vesna Olivieri (Microscopy Center, Pharmazentrum, University of Basel, Switzerland) for performing electron microscopy and Jean

Grisouard (Department of Biomedicine, University Hospital of Basel, Switzerland) for helpful discussions.

Conflicts of interest

The authors declare no conflicts of interest.

5 Differential modulation of ROS signals and other mitochondrial parameters by the antioxidants MitoQ, resveratrol and curcumin in human adipocytes ⋆

Estelle Hirzel[1], Peter W. Lindinger[1,2], Swarna Maseneni[2], Maria Giese[3], Véronique Virginie Rhein[3,4], Anne Eckert[3], Matthias Hoch[1,5], Stephan Krähenbühl[2] and Alex N. Eberle[1,6]

[1]Laboratory of Endocrinology, Department of Biomedicine, University Hospital and University Children's Hospital, University of Basel, Basel, Switzerland

[2]Division of Clinical Pharmacology and Toxicology, Department of Biomedicine and University Hospital, University of Basel, Basel, Switzerland

[3]Neurobiology Laboratory for Brain Aging and Mental Health, Psychiatric University Clinics, University of Basel, Basel, Switzerland

[4]Proteomics Laboratory, MRC Mitochondrial Biology Unit, Cambridge, United Kingdom

[5]Actelion Pharmaceuticals Ltd, Allschwil, Switzerland

[6]Collegium Helveticum, ETH Zürich, Zürich, Switzerland

Keywords: Reactive oxygen species (ROS), human mesenchymal stem cell, adipocyte, antioxidant, MitoQ, resveratrol, curcumin

Correspondence: Alex-N.Eberle@unibas.ch

⋆ Hirzel, E., et al., *Differential modulation of ROS signals and other mitochondrial parameters by the antioxidants MitoQ, resveratrol and curcumin in human adipocytes*. J Recept Signal Transduct Res, 2013. **33**(5): p. 304-312.

Abstract

Mitochondrial reactive oxygen species (ROS) have been demonstrated to play an important role as signaling and regulating molecules in human adipocytes. In order to evaluate the differential modulating roles of antioxidants, we treated human adipocytes differentiated from bone marrow derived human mesenchymal stem cells with MitoQ, resveratrol and curcumin. The effects on ROS, viability, mitochondrial respiration and intracellular ATP levels were examined. MitoQ lowered both oxidizing and reducing ROS. Resveratrol decreased reducing and curcumin oxidizing radicals only. All three substances slightly decreased state III respiration immediately after addition. After 24 h of treatment, MitoQ inhibited both basal and uncoupled oxygen consumption while curcumin and resveratrol had no effect. Intracellular ATP levels were not altered. This demonstrates that MitoQ, resveratrol and curcumin exert potent modulating effects on ROS signaling in human adipocyte with marginal effects on metabolic parameters.

Introduction

In prokaryotic and eukaryotic cells, reactive oxidant species (ROS) have been recognized as signaling molecules that affect downstream signaling of receptor-mediated input signals (reviewed in [233-237]). Intracellular signaling triggered by various extracellular regulators, peptide hormones and growth factors such as insulin, PDGF, VEGF, TNF-α, IL-1β, integrin and others has been shown to be modulated by ROS [233][235]. The detailed mechanisms of ROS homeostasis and signaling are however only partly understood but it has become clear that ROS signaling affects many cellular processes in aging and inflammation [235, 237, 238]. ROS are also important signaling molecules in adipose tissues where they regulate adipocyte differentiation [239] and adipocyte function [240], relevant aspects also in disease, considering the close correlation between ROS and lipolysis in obesity. Lipolysis in isolated human adipocytes has indeed been shown to be regulated by ROS [241] whereas mouse 3T3-L1 adipocytes display resistance to insulin after exposure to hydrogen peroxide [221].

Elevated concentrations of free fatty acids and glucose have been reported to induce the formation of ROS in many cell types including muscle, pancreatic β-cells and adipocytes [19, 212-215]. In many diseases such as cancer, inflammation, myocardial infarction, atherosclerosis, diabetes, or Alzheimer's disease, the ROS load is increased, possibly as a result of rather than as the cause for the disease [242], explaining the modest or missing benefit of antioxidant treatments [243]. In adipocytes, however, modulation of ROS as signaling molecules by antioxidants may have a better chance to exert a positive effect on the physiological state of the cells.

For studies of human adipocytes, frequently bone marrow-derived mesenchymal stem cells (hMB-MSC) differentiated into adipocytes are used as model [244] although more recently also stem cells originating from adipose tissue have been examined [245]. We have recently standardized the generation of differentiated hMB-MSC and analyzed various parameters [246]. Using these cells we now describe the effect of antioxidants on the modulation of generation of ROS as well as on some metabolic effects such as oxygen consumption, intracellular ATP and viability. The antioxidants MitoQ, resveratrol and curcumin were used in this study; they all have the potential for future *in vivo* application and their biological characteristics are briefly outlined:

MitoQ

MitoQ was designed by Murphy and collaborators [120] as a mitochondria targeted antioxidant. It is a mixture of the oxidized mitoquinone and the reduced mitoquinol and consists of a positively charged triphenylphosphonium ion linked to coenzyme Q via a C_{10} linker. MitoQ uptake is driven by the mitochondrial membrane potential. Rotenone and malonate, a complex I and complex II inhibitor, respectively, were shown to inhibit reduction of MitoQ. Apoptosis induced by hydrogen peroxide in Jurkat cells is prevented by MitoQ [120]. Long-term administration of MitoQ to mice revealed a decrease in fat mass but no change in body weight [144]. MitoQ is protective against ischaemia-reperfusion injury in the heart of mice [140] and against sepsis-induced liver damage in the same species [247]. Furthermore, MitoQ increased blood pressure in spontaneously hypertensive rats [141]. It was also investigated in patients with Parkinson's disease but had no effect on disease progression. The study showed that long-term administration of MitoQ to patients is

save [248]. A phase II study in patients suffering from chronic hepatitis C provided evidence that MitoQ may inhibit hepatitis-induced liver damage [147].

Resveratrol

Resveratrol (3,5,4′-trihydroxystilbene), a diphenolic compound naturally occurring in grapes and other plants, exerts numerous effects both *in vitro* and *in vivo* [249]. Resveratrol scavenges superoxide, peroxynitrite, hydroxyl radicals as well as radicals induced by metals. It was shown to cross the blood-brain barrier and to reduce malone dialdehyde levels, an indicator for protein peroxidation, in rat brain. At the same time protein levels and enzymatic activities of superoxide dismutase, catalase and peroxidase were increased [249]. Resveratrol dose-dependently decreased glucose conversion to lipids in rat adipocytes [160]. Furthermore a dose-dependent decrease in CO_2 release and an increase in lactate release were observed. Thus it was suggested that resveratrol impaired oxidative phosphorylation and elevated glycolysis [160]. When mice on standard diet, high fat diet and high fat supplemented with resveratrol were compared, an increase in lifespan and performance in the rotarod test of mice treated with resveratrol were noted [162]. Resveratrol improved glucose tolerance and decreased insulin levels. In addition a decrease in liver size and liver fat content and an improvement of liver and heart pathology were observed [162].

Curcumin

Curcumin ([1*E*,6*E*]-1,7-bis-(4-hydroxy-3-methoxyphenyl)-hepta-1,6-dien-3,5-dion) is a diphenolic compound found in turmeric, a yellow colored spice derived from *curcuma longa* and used in Asian cooking. Curcumin was reported to have antiinflammatory, antioxidant and hypolipidemic effects [250]. Antioxidant properties of curcumin were shown in several *in vitro* and *in vivo* studies. Curcumin inhibited stress-induced activation of the transcription factor activator protein-1 (AP-1) [251] as well as phorbol ester-induced expression of cyclooxygenase-2 [252]. Also, curcumin dose-dependently decreased intracellular ROS in hepatic stellate cells from rats [253]. When added to hamsters fed with a high fat diet, curcumin decreased plasma leptin and insulin levels as well as free fatty acids and triglycerides, but increased hepatic β-oxidation [254]. In a small clinical study with 8 subjects with abnormally high levels of LDL, curcumin treatment decreased LDL and apolipoprotein B while HDL and Apo

A were increased [255]. In another study of the same group, 8 subjects with elevated fibrinogen in the plasma were treated with curcumin for 15 days. Curcumin caused a significant decrease in fibrinogen [256]. Curcumin also lowered blood sugar in diabetic patients [257]. These data suggest a beneficial effect of curcumin in artherosclerosis and diabetes.

Materials and Methods

Reagents

All reagents were purchased from Sigma-Aldrich (Buchs, Switzerland); exceptions are mentioned in the text. MitoQ and TPP (decyl-triphenylphosphonium) were a gift from Dr. Michael Murphy (MRC Mitochondrial Biology Unit, Cambridge, UK). TTP is a triphosphonium ion coupled to a C_{10} alkyl chain which mimics the structure of MitoQ but lacks the coenzyme Q moiety; it was used as control to exclude that any observed effects may have been caused by the phosphonium ion rather than by the coenzyme Q moiety.

Cell culture

Primary human bone marrow-derived mesenchymal stem cells (hBM-MSCs) were kindly provided by Prof. Ivan Martin (Department of Biomedicine, University of Basel, Switzerland). The cells were expanded in DMEM (Invitrogen, Life Technologies Corp., Zug, Switzerland), supplemented with 10% fetal calf serum (FCS; Invitrogen) and 5 ng/mL basal fibroblast growth factor (Invitrogen) until confluency was reached. The cells were then differentiated for 22 days by exchanging the growth medium by differentiation medium [223]: DMEM/Nutrient Mix F12 (Invitrogen) containing 3% FCS, 100 nM insulin (Actrapid; Novo Nordisk, Küsnacht, Switzerland), 1 µM dexamethasone, 0.1 mM L-ascorbic acid, 250 µM 3-isobutyl-1-methylxanthine, 5 µM transferrin (Calbiochem, La Jolla, USA), 0.2 nM 3,3,5-triiodo-L-thyronine and 1 µM rosiglitazone (GlaxoSmithKline, Worthing, UK). The medium was changed every 3 days until at least 70% of the cells were differentiated into adipocytes. Before the experiments were conducted, the cells were incubated for 24–48 h in DMEM/F12 supplemented with 3% FCS.

ROS measurements

Differentiated hBM-MSCs, cultivated in 96-well plates, were treated with the three antioxidants at different concentrations for 24 h. ROS were determined using the following assays:

2',7'-Dichlorohydrofluorescin diacetate (DCFH-DA) assay

The cells were washed with PBS and per well 100 µl of 50 µM 2',7'-dichlorohydrofluorescin diacetate (DCFH-DA) in DCF buffer (1 M Hepes, 1 M glucose, 10% BSA in PBS) were added and the cells incubated at 37°C and 5% CO_2 for 30 min. The cells were washed twice with ice-cold PBS and permeabilized with 0.2% Triton-X-100 on ice for 10 min. The plates were centrifuged for 5 min at 3000x*g* and 100 µl of the supernatants were transferred to white 96-well plates. Fluorescence was measured in a SpectraMAX Gemini XS (Molecular Devices, Ismaning, Germany) microplate reader at 490 nm (excitation) and 535 nm (emission).

Nitroblue tetrazolium (NTB) assay

The cells were washed with PBS and per well 100 µl of 0.1% nitroblue tetrazolium (NBT) in PBS were added. After 2 h of incubation at 37°C and 5% CO_2, the cultures were washed with PBS. To dissolve the precipitated formazan, 100 µl DMSO containing 2 M KOH were added to the cells and the plate was placed onto a shaker for 10 min. The debris was centrifuged at 3000x*g* for 5 min and 60 µl of the supernatants were transferred to a new plate. Absorbance was measured at 650 nm in a SpectraMAX 190 (Molecular Devices) microplate reader.

Toxicity assays

Flow cytometry

The cells were cultured and differentiated in 25 cm^2 cell culture flasks; they were harvested by trypsinization, centrifuged at 240x*g* and then resuspended in 0.5 ml PBS. In order to detect apoptotic cells, 2 µl of propidium iodide and 2 µl of anti-annexin V antibody conjugated to Alexa 488 (Vybrant Apoptosis Assay Kit 2; Molecular Probes, Paisley, UK) were added. Measurement was carried out in a

FACSCalibur flow cytometry instrument (Becton Dickinson, Allschwil, Switzerland) and the data were analyzed with FlowJo 9.2 software (TreeStar Inc., Ashland, OR, USA).

ToxiLight assay

The ToxiLight assay (Lonza, Basel, Switzerland) is based on a luciferin-luciferase reaction and measures ATP produced by adenylate kinase which is released when the cells are leaky. The assay was performed according to the manufacturer's instruction. Briefly, differentiated adipocytes were treated with antioxidants in 96-well plates for 24 h. Then, 20 µl of the culture supernatants were transferred to a white 96-well plate and 100 µl of ToxiLight solution were added. Luminescence was measured in a HTS 7000 Plus Bioassay Reader (Perkin Elmer, Schwerzenbach, Switzerland).

High resolution respirometry

Immediate effects of antioxidants on oxygen consumption were measured with an Oxygraph O2-k instrument (Oroboros Instruments GmbH, Innsbruck, Austria). Cell cultures were grown and differentiated in 300 cm^2 cell culture flasks. Adipocytes were detached with EDTA, centrifuged at 240x*g* and resuspended in Mir05 respiration medium (0.5 mM EGTA, 3 mM $MgCl_2$, 60 mM K-lactobionate, 20 mM taurine, 10 mM KH_2PO_4, 110 mM sucrose, 1g/l BSA, pH 7.1; developed by Oroboros Instruments). Per chamber 10^6 cells were added in a final volume of 2 ml Mir05. After basal respiration reached steady state, the following substances were added consecutively (final concentration): 5 mM pyruvate together with 2 mM malate, 15 µg/ml digitonin, 2 mM ADP, 10 mM glutamate, 10 mM succinate, 10 µM cytochrome *c*, 0.4 µM carbonylcyanide-*p*-trifluoromethoxyphenylhydrazone (FCCP), 0.5 µM rotenone and 2.5 µM antimycin A (40). After each addition, oxygen consumption was measured when steady state was reached. Rotenone and antimycin A were used as a control.

Oxygen consumption

Basal oxygen consumption of intact cells treated with the different antioxidants was measured using a Seahorse XF24 Extracellular Flux Analyzer (Seahorse Bioscience, Copenhagen, Denmark). The Seahorse is an open oxygen sensor system and

measures oxygen flux with a specific fluorophor. The cells were grown and differentiated in XF24 V7 cell culture microplates (Seahorse Bioscience). Per plate four wells were kept without cells as required for calibration of the instrument. First, basal respiration was measured, followed by the consecutive addition of oligomycin, FCCP and rotenone to a final concentration of 1 μM each. The ATP-synthase inhibitor oligomycin was used to test for the degree of uncoupling. With the ionophore FCCP the maximal capacity of the electron transport chain (ETC) was determined. Rotenone is a complex I inhibitor and was used as a control. Oligomycin and FCCP were titrated in preliminary experiments to determine optimal concentrations. The results of these experiments are indicated as oxygen consumption rate (OCR) which is specified as oxygen consumption over time in picomoles per minute. In parallel to OCR, the instrument also recorded simultaneously the extracellular acidification rate (ECAR). ECAR is an indicator for glycolysis since lactate, the end product of glycolysis, is secreted into the medium, thus resulting in acidification. ECAR is defined as $-\Delta$pH over time using the units milli-pH and minute.

Intracellular ATP determination

Differentiated adipocytes were pretreated with different antioxidants for 24 h and then washed with buffer A (25 mM Tris-HCl, 10 mM KH_2PO_4, 150 mM KCl, 5 mM MgCl, 0.1% BSA, pH 7.8). For permeabilization the cells were covered with 200 µl 1x ATP-releasing reagent in buffer A per well for 2 min. Then 20 µl of each supernatant were transferred to a white plate. Per well 80 µl mastermix consisting of 0.3 mM beetle luciferin potassium salt (Promega, Dübendorf, Switzerland) and 4110 units/ml luciferase from Photinus pyralis in buffer A were added and the measurement in a Microlumat Plus luminescence reader (Berthold Technologies, Regensdorf, Switzerland) was started immediately.

Statistical analysis

Prism 5.0 software (GraphPad Software Inc., La Jolla, CA, USA) was used to perform statistical analyses. All data were analyzed using ANOVA and Tuckey's post test and are presented as mean ± SD. All experiments were performed at least three times.

Results

Modulation of ROS signals

The effective concentrations of MitoQ, resveratrol and curcumin for the modulation of ROS production were assessed by determining the ROS signals with the DCFH-DA and the NBT assay.

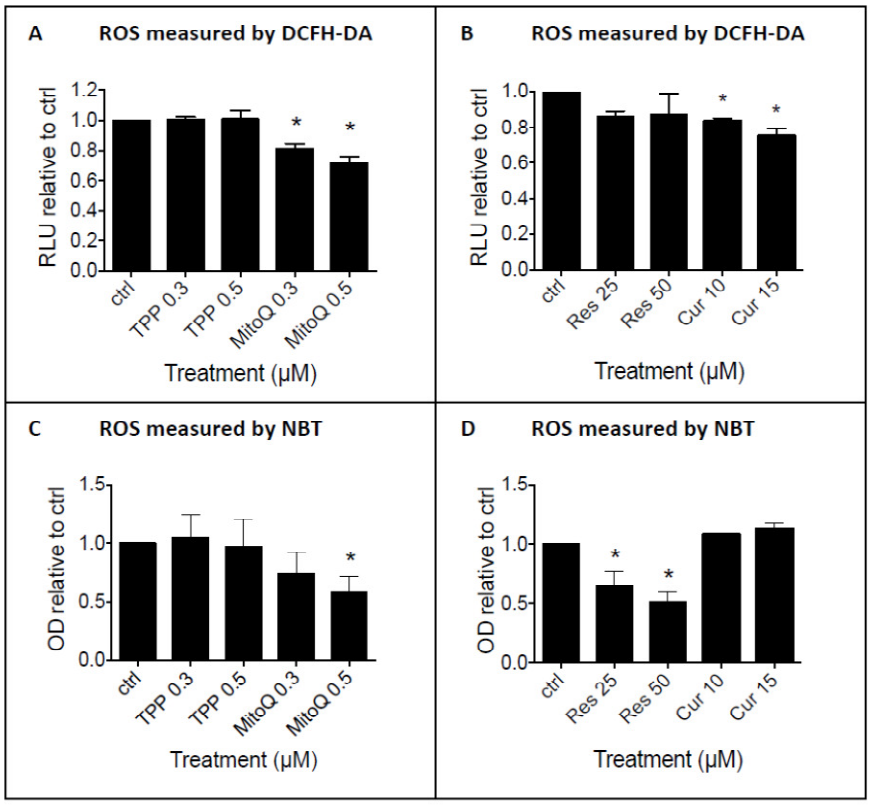

Fig. 1. ROS production after 24 h of treatment.
A, B: *2',7'*-Dichlorohydrofluorescin diacetate assay.
C, D: Nitroblue tetrazolium assay.
Ctrl: controls (untreated).
TPP: triphenylphosphonium;
Res: resveratrol;
Cur: curcumin.
Mean of 3 determinations ± SD;
★ $p \leq 0.05$

Toxicity assays were carried out to exclude toxic effects that may possibly interfere with the antioxidant activity of these compounds. The cells were exposed to the antioxidants for 24 h in both types of assay.

MitoQ decreased ROS concentration as measured with the DCFH-DA and the NBT assay. The NBT assay displayed a significant decrease in ROS only at a concentration of 0.5 µM MitoQ while the DCFH-DA assay revealed a significant effect also at a concentration of 0.3 µM (Fig. 1). Resveratrol decreased the oxidative stress signal at concentrations of 25 µM and 50 µM using the NBT assay while no effect was detected with the DCFH-DA assay. Interestingly, curcumin showed opposite

characteristics: it decreased ROS production at 10 µM and at 15 µM when measured in the DCFH-DA experiments only.

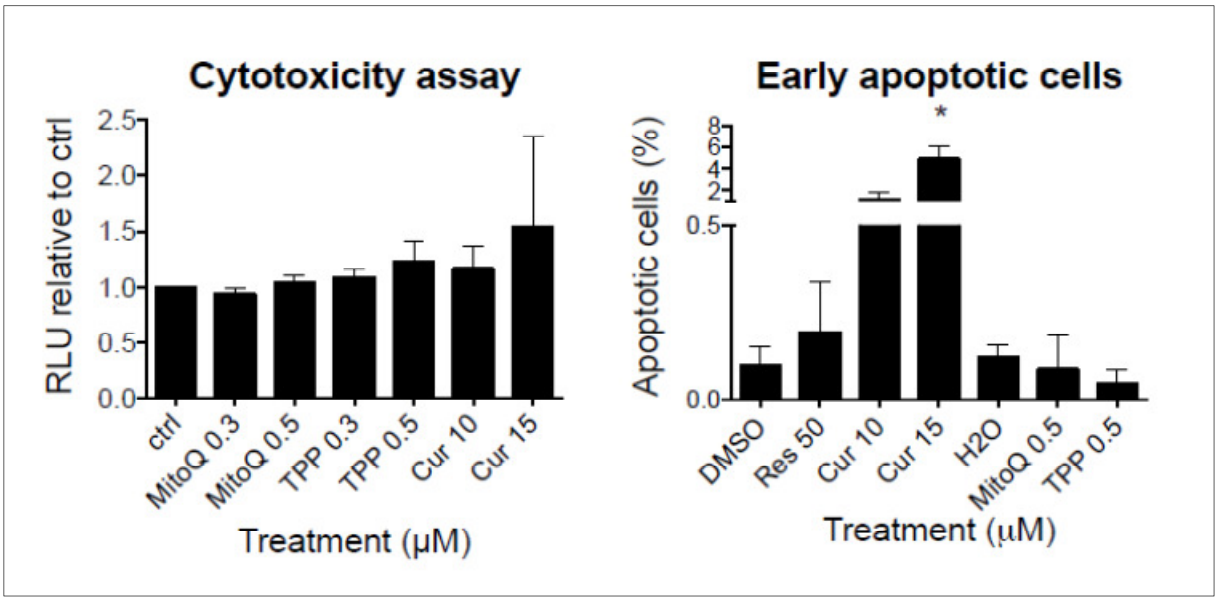

Fig. 2. Cytotoxicity assays after 24 h of treatment with antioxidants. ***Left:*** **Toxilight cytotoxicity assay.** *Right:* Early apoptotic cells, determined by FACS (staining for annexin V and propidium iodide). Cells positive for annexin V only and double positive ones are shown.
Antioxidants: MitoQ (0.3 and 0.5 mM); TPP (0.3 and 0.5 mM); resveratrol (Res; 50 mM); curcumin (Cur; 10 and 15 mM); ctrl (H_2O): control for MitoQ and TPP; DMSO: control for Res and Cur. Mean of 3 determinations ± SD; ★ $p \leq 0.05$ vs. DMSO.

The evaluation of cytotoxicity of the antioxidant compounds was carried out by flow cytometry using annexin V with PI staining and by the ToxiLight assay (Fig. 2). Whereas with the ToxiLight assay neither MitoQ nor curcumin had an effect on cell death at any treatment, resveratrol as compound interfered with this assay, i.e. the data had to be excluded. On the other hand, flow cytometry experiments demonstrated no toxicity for resveratrol and MitoQ (or TPP) at 50 µM and 0.5 µM, respectively (Fig. 2). Curcumin induced a slight increase of apoptosis of the cells (6% of the cells at 15 µM and 2% at 10 µM) but the effect was very small and most likely did not contribute significantly to the antioxidant effect observed with curcumin.

Effects on respiration

As mitochondria are the main source of intracellular ROS, a decrease in oxidative stress could also be the result of an inhibition of respiration and not solely be caused

by the antioxidant effect of the compound. To examine this possibility, the immediate effect of treatment with MitoQ, resveratrol and curcumin on oxygen consumption was measured with the Oxygraph instrument and the influence of a 24-h treatment with the Seahorse flux analyzer. None of the compounds influenced basal respiration immediately after application of antioxidants (Fig. 3). When the two complex I substrates pyruvate and malate were added and the cells permeabilized with digitonin, and when in addition coupled (state III) respiration was enabled by adding ADP, all antioxidant compounds caused a slight decrease in state III respiration (Fig. 3). The addition of the complex II substrate succinate further stimulated oxygen consumption but could not compensate the difference between treated and control cells. The subsequent addition of cytochrome *c* did not change respiration, i.e. the mitochondria were intact. The addition of the ionophore FCCP (trifluorocarbonylcyanide phenylhydrazone) highly increased oxygen consumption but a slight impairment of the cells challenged with the antioxidants still remained (Fig. 3).

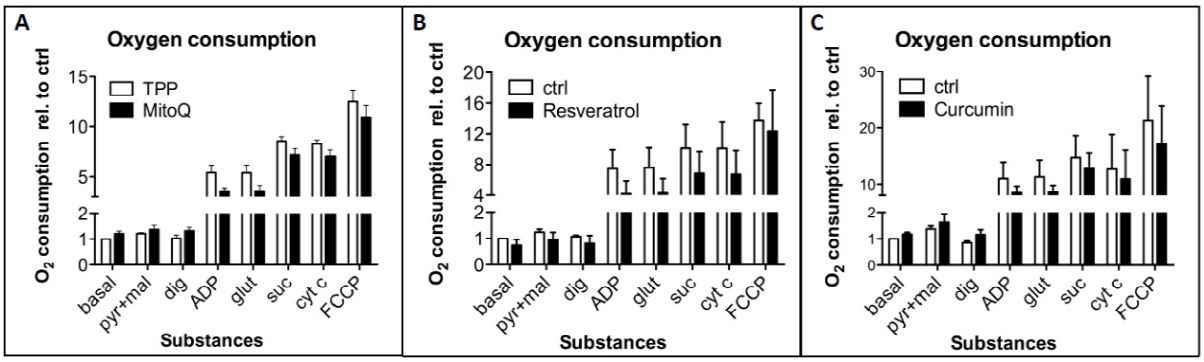

Fig. 3. Oxygen consumption measured in the Oxygraph instrument upon immediate treatment with antioxidants. *A:* MitoQ and TPP (50 µM each); *B:* Resveratrol (50 µM). *C:* Curcumin (15 µM). Mean of 3 determinations ± SD.

To examine whether the state of respiration measured immediately after addition of antioxidants persisted also after a longer incubation time, cell cultures were treated with antioxidants for 24 h and analyzed in the Seahorse flux analyzer (which provides a clearly higher throughput than the Oxygraph). First, oxygen consumption under basal conditions was measured, followed by leak respiration as determined by adding the ATP-synthase inhibitor oligomycin, and finally uncoupled respiration was measured by adding FCCP. Treatment with MitoQ at concentrations of 0.3 µM and

0.5 µM significantly reduced basal oxygen consumption as well as uncoupled respiration while oligomycin-inhibited respiration was not affected (Fig. 4). The carrier TPP inhibited oxygen consumption under basal conditions at a concentration of 0.5 µM (Fig. 4). Extracellular acidification did not provide a clearcut result as the ECAR values hardly exceeded the detection limit and were therefore difficult to interpret (Fig. 4).

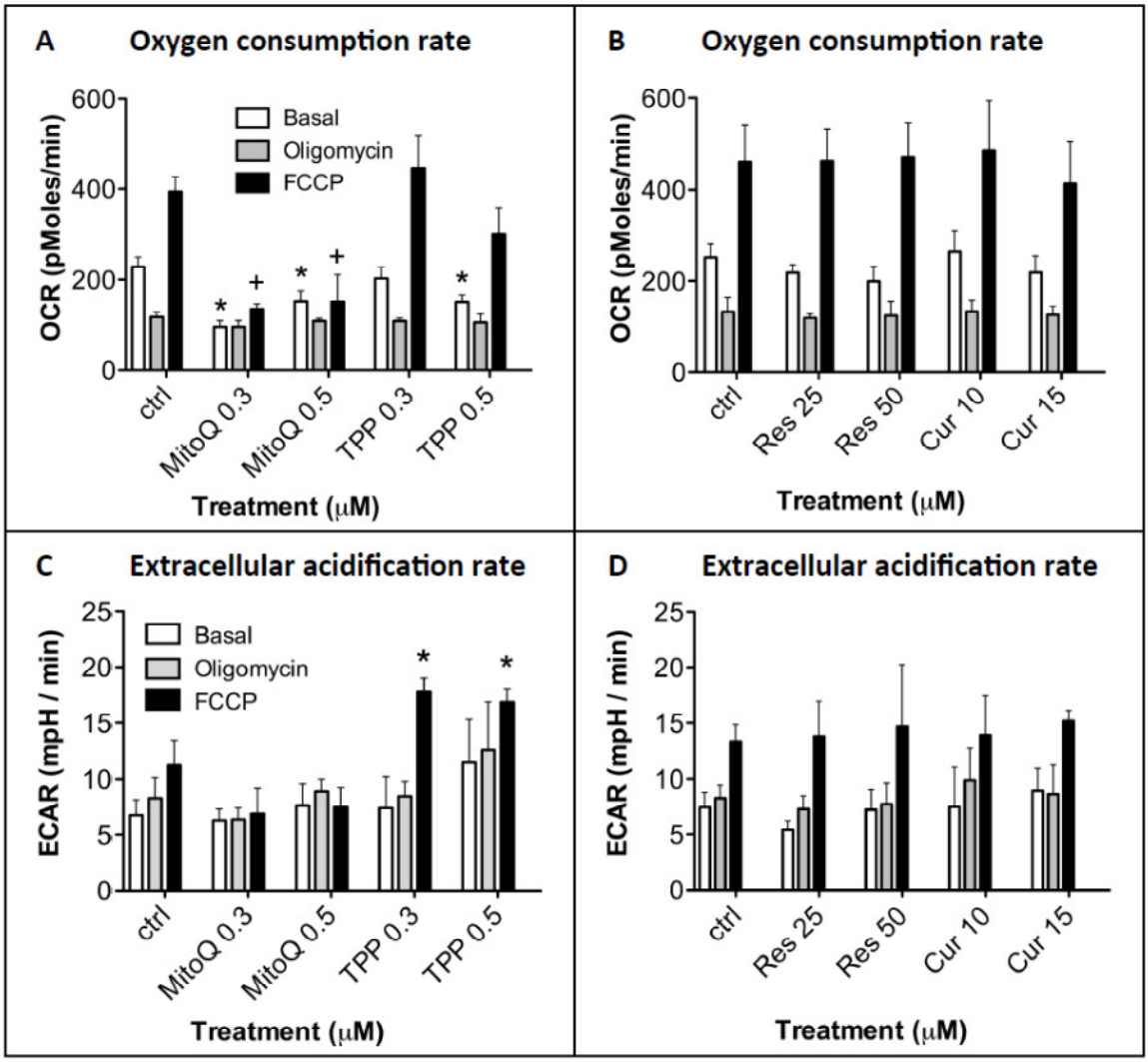

Fig. 4. Oxygen consumption *(A, B)* and extracellular acidification *(C, D)* as measured in the Seahorse instrument after 24 h of treatment with antioxidants. *A, C:* MitoQ (0.3 and 0.5 mM); TPP (0.3 and 0.5 mM). *B, D:* resveratrol (Res; 25 and 50 mM); curcumin (Cur; 10 and 15 mM); ctrl: control. Mean of 3 determinations ± SD.
A: ★ $p \leq 0.05$ vs. basal of untreated controls; **+** $p \leq 0.05$ vs. FCCP of controls. *C:* ★ $p \leq 0.05$ vs. FCCP of controls.

In order to assess whether respiration under MitoQ treatment had an influence on intracellular ATP content, the cells were permeabilized and ATP was measured by a luciferin-luciferase reaction. After treatment with either MitoQ, TPP, resveratrol or curcumin for 24 h, no differences in intracellular ATP content were detected (Fig. 5).

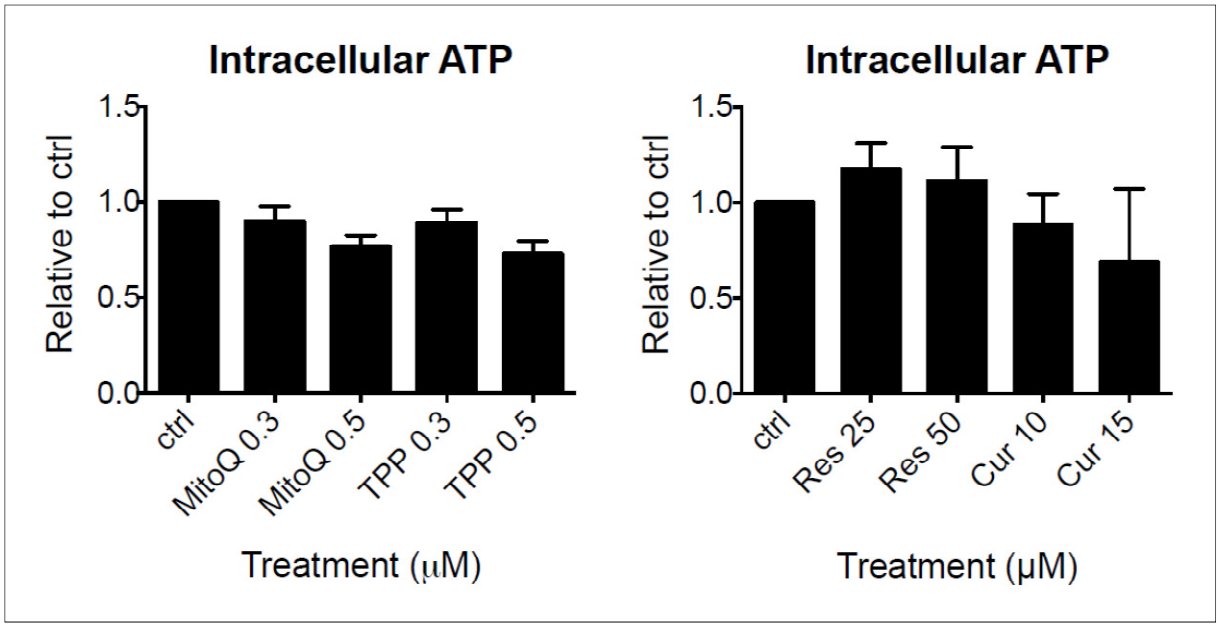

Fig. 5. Intracellular ATP content relative to control after 24 h of treatment with antioxidants. *Left:* MitoQ (0.3 and 0.5 mM); TPP (triphenylphosphonium; 0.3 and 0.5 mM). *Right:* Res (resveratrol; 25 and 50 mM); Cur (curcumin; 10 and 15 mM); ctrl: control. Mean of 3 determinations ± SD.

Discussion

Modulation of ROS signals

In this study, we demonstrated modulatory effects of three well established antioxidants, MitoQ, resveratrol and curcumin, on ROS production in bone marrow-derived human mesenchymal stem cells differentiated to functional adipocytes. In addition we examined effects of these antioxidants on cell viability, oxygen consumption and intracellular ATP levels. In order to differentiate between the different types of ROS signals, two assays were employed for their determination: the DCFH-DA assay showing oxidizing ROS (e.g. hydrogen peroxide and hydroxyl

radicals) and the NBT assay with which reducing ROS (e.g. superoxide) can be determined.

Compared to the control compound TTP, MitoQ significantly decreased ROS concentration in human adipocytes in both assays, i.e. MitoQ reacted with both oxidizing and reducing ROS at concentrations which did not display toxicity. This is in agreement with the report that mitoquinone is reduced by complex II of the respiratory chain to the active form mitoquinol which is recycled back by reaction with oxygen or nitrogen species [120, 124, 258, 259]. MitoQ has been shown to inhibit superoxide-induced uncoupling of mitochondria suggesting that MitoQ also reacts with reducing ROS [120].

The finding that resveratrol dose-dependently decreased reducing ROS as measured with the NBT assay while there was no change in the level of oxidizing radicals as seen with the DCFH-DA assay confirms the reported specificity of resveratrol also for human adipocytes: resveratrol is known to scavenge the primarily reducing radicals superoxide, hydroxyl, peroxinitrite and metal-induced radicals [249] as well as to upregulate superoxide dismutase. The observation time of 24 h may have been too short for the detection of an effect on oxidizing radicals in human adipocytes, since in some other systems, resveratrol – in addition – was found to upregulate peroxidase and catalase which react with hydrogen peroxide [249].

Opposite to resveratrol, curcumin reduced the ROS concentration of oxidative radicals as shown with DCFH-DA experiments but it did not display an effect in the NBT experiments, i.e. on reducing radicals. In contrast to our findings with human adipocytes, curcumin scavenged free superoxide and hydroxyl radicals in the human A549 alveolar epithelial cell line challenged with TNF-α to increase oxidative stress [260]. It is likely that this discrepancy of findings may be cell type-specific or due to the experimental induction of oxidative stress.

Effects on respiration

It was of interest to study whether the modulatory effects of the antioxidants on ROS production in human adipocytes were accompanied by changes of oxygen consumption. The two instruments used in this study, the Oxygraph and the

Seahorse, provide complementary information: the Seahorse only measures basal respiration of intact cells whereas with the Oxygraph the activity of individual complexes of the electron transport chain can be elucidated. In the Oxygraph basal (state I) respiration was measured first, followed by oxygen consumption under saturating concentrations of substrates for complex I, complex II (state II respiration) and ADP (state III respiration) after the cells had been permeabilized and substrates and ADP provided. In intact cells, ADP is usually limited and thus only basal (state I) respiration can be compared with the Seahorse experiments.

MitoQ did not show any difference in basal (state I) respiration in human adipocytes. Only a slight decrease in coupled (state III) and uncoupled (state IV) respiration upon short-term challenge with the antioxidant was detected but this was small enough and not further examined. By contrast, after 24 h of treatment with MitoQ, a significant reduction of basal oxygen consumption was noted. As TPP at the same concentration also inhibited respiration, the observed decrease in basal respiration of human adipocytes might have been due to depolarization. In general, oxygen consumption did not differ between treated and untreated cells after addition of oligomycin. Thus MitoQ did not have any impact on the coupling state of mitochondria. It has been shown that mitoquinol cannot restore respiration in cells lacking coenzyme Q as it is not oxidized by complex III [258]. Thus the competition of MitoQ with coenzyme Q for electrons can decrease respiration. This competition might be the reason for the decrease in oxygen consumption seen in our experiments with the Seahorse instrument. Intracellular ATP levels were not altered by the different treatments although there was no increase in glycolysis in response to MitoQ or TPP.

Resveratrol slightly inhibited state III respiration but not basal respiration when determined with the Oxygraph. When the cells were treated for 24 h and analyzed with the Seahorse, there was no change in basal and uncoupled respiration. On the other hand, exposition of primary rat renal tubules to resveratrol led to an increase in oxygen consumption [261]. High-fat fed mice treated with resveratrol induced an increase in mitochondrial copy number in muscle and brown adipose tissue, along with a differential expression of genes related to mitochondrial biogenesis [262]. By

contrast, in our experiments we did not observe any effect that suggests enhanced mitochondrial biogenesis.

Curcumin, similar to resveratrol, did not affect basal respiration but slightly decreased state III and uncoupled respiration when measured with the Oxygraph. After 24 h of incubation of human adipocytes with curcumin, basal oxygen consumption was not altered. By contrast, curcumin and curcumin derivatives dose-dependently decreased respiration and mitochondrial potential in isolated rat liver mitochondria [263]. At the concentrations used in our study, we did not observe such effects; higher concentrations of curcumin may however impair mitochondrial function also in human adipocytes.

With all three antioxidants, the ECAR values were very low, indicating that human adipocytes mainly generate ATP via oxidative phosphorylation and not via glycolysis. There was no change in intracellular ATP content after 24-h treatments with any of the antioxidants. By contrast, in a recent report using freshly isolated rat adipocytes, resveratrol was shown to lower the mitochondrial membrane potential and to decrease ATP content dose-dependently [264]. However, these experiments used shorter incubation times and higher concentrations of resveratrol.

Possible implications on health

The potential role of mitochondria-targeted antioxidants in disease prevention was already addressed in the Introduction; recent preclinical and clinical studies using resveratrol, MitoQ, curcumin and other antioxidants known to reduce oxidative stress *in vitro* and *in vivo* in different pathologies were shown to have clearly beneficial effects [265-269]. In the center stage is the control of ROS, i.e. of molecular species which are thought to function as second messengers activating numerous signaling molecules [270]. Although ROS are critical for healthy cell function [237], the control of excessive ROS is crucial for the treatment of cardiovascular disease [270] and cancer [271]. Although the molecular pattern of interactions of mitochondrial antioxidants is complex involving different signaling pathways, a possibly important aspect may be their involvement in modulating epigenetic processes [272, 273], e.g. by inhibiting histone deacetylase (resveratrol) or histone acetylase (curcumin). However, it will have to be demonstrated that histone modifications [274] can also be

evoked in human adipocytes using these antioxidants. At any case, resveratrol has been demonstrated to inhibit preadipocyte and adipogenic differentiation [149] and curcumin attenuates lipogenesis in liver and inflammatory processes in adipocytes, thus preventing high fat diet-induced insulin resistance and obesity [275]. The development of a water-soluble curcumin derivative may increase the availability of the compound in the circulation and hence improve the antidiabetic effect of curcumin [276]. The same will apply for resveratrol. On the other hand, MitoQ can be applied in pharmacologically safe doses that, e.g., protect pancreatic β-cells against oxidative stress [277] or prevent diabetic nephropathy [278] in experimental animals.

Conclusion

We have demonstrated that the three compounds MitoQ, resveratrol and curcumin display antioxidant activity in human adipocytes and that their modulating effect on ROS production is within a non-toxic concentration range. With the exception of MitoQ they did not impair oxygen consumption during the experimental period of 24 h. All three compounds had only minimal effects on cellular respiration. These findings are relevant in view of the potential role of MitoQ, reserveratrol and curcumin as pharmacological drugs. Yet, further studies with isolated human adipocytes and with experimental animals are required before these antioxidants can be considered as drugs for the management of obesity.

Acknowledgements

We thank Dr. M. Murphy (MRC Mitochondrial Biology Unit, Cambridge, UK) for the gift of MitoQ and Dr. J. Grisouard (Department of Biomedicine, University of Basel, Switzerland) for helpful discussions.

Conflict of interest

The authors declare no conflicts of interest.

6 General discussion

As adiposity is a common health problem in many countries [1], a primary human *in vitro* model for adipogenesis and adipocytes is important for research. Obesity is known to be associated with increased oxidative stress which is believed to favour insulin resistance [60]. Thus, substances which can reduce oxidative stress on adipocytes are an interesting approach to protect overweight people from insulin resistance and type II diabetes.

Here we described hBM-MSC as a model for adipocytes and adipogenesis *in vitro* and examined the effects of the antioxidants MitoQ, resveratrol and curcumin on several mitochondrial functions of these cells. We assessed the impact of these compounds on ROS production, oxygen consumption and intracellular ATP content at non-apoptotic concentrations. In the majority of the studies, the murine 3T3-L1 fibroblast-like cell line is used. Quian *et al.* recently showed that 3T3 cells and hBM-MSC behave differently regarding cell division after induction of differentiation [279]. It was also reported that there are differences in glucose metabolism, fatty acid synthesis from glucose and glucose metabolism in response to insulin between species [280]. Therefore, it would be desirable to have a human model for adipocytes and adipogenesis. First, we tried to isolate and cultivate pre-adipocytes from pieces of visceral fat tissue obtained from lean and obese patients undergoing surgery. However, these cell cultures were not predictable and reliable. The cultures from some donors died immediately after addition of the differentiation medium, while the cells derived from other donors differentiated into adipocytes. However, even in these cultures differentiation was not efficient and reproducible enough and only a rather small part of the cells showed fat accumulation. There was no gender-related pattern visible and no influence of diabetes was seen. Unfortunately, cell sorting was not possible, as only one specific cell marker for pre-adipocytes, pref 1, was known at that time and the only antibody available on the market did not recognize the protein during preliminary experiments performed to evaluate the antibody's specificity.

Cells derived from subcutaneous fat tissue differentiated more efficiently than cells from visceral adipose tissue. However, we could not but obtain pieces of fat tissue which were big enough to isolate a reasonable amount of cells. The reason was that cutting pieces of subcutaneous adipose tissue of a certain size will be visible and are also a risk to the patient.

Because of these problems we searched for a good alternative for fat tissue derived adipocytes. We decided to investigate of bone marrow derived mesenchymal stem cells. These cells differentiated efficiently and reproducibly into adipocytes and could be obtained in a quite high number from patients undergoing orthopedic surgery.

As mentioned above, oxidative stress is increased in obesity and it may be beneficial to lower ROS to a normal level. Therefore, we investigated ROS production during adipocyte differentiation and in response to antioxidant treatment. We detected a strong increase in ROS production and fat accumulation after induction of differentiation into adipocytes by the differentiation medium (manuscript 1: Fig. 1A & B; Fig. 2). Saitoh *et al.* [225] recently reported the same observation in the murine OP9 cell line. They compared fat accumulation and ROS production of OP9 cells cultivated in growth medium and adipogenic medium. Cells cultivated in adipogenic medium showed excessive fat accumulation during the investigated time period. The cells cultivated in growth medium also accumulated triglycerides, but in a much lower extent. ROS production measured by the NBT assay was also much higher in cells cultivated in adipogenic medium [225].
Imhoff *et al.* [281] showed that the natural intracellular antioxidants glutathione and thioredoxin-2 become oxidized during differentiation of 3T3-L1 cells into adipocytes. Fat accumulation and the expression of early genetic markers of adipogenesis were dependent on the extracellular redox environment. Adipocyte differentiation was enhanced under oxidizing and lowered under reducing conditions [281]. In another study, bone marrow stromal cells (BMSCs) of $SOD2^{-/-}$ and wild-type mice were used to investigate the correlation between ROS and adipocytes differentiation. The SOD knockout cells showed fat accumulation even under basal conditions, without induction of adipogenesis by differentiation medium, while the wild-type cells did not. Furthermore, addition of an antioxidant compound lowered fat accumulation in both the knockout and the wild-type cells after adipogenic induction [282]. Thus, the increase in ROS production during adipocyte differentiation may not only be a consequence of this process but also a prerequisite.

When we treated hBM-MSC derived adipocytes with MitoQ, resveratrol and curcumin, we identified a reduction in ROS production in response to all these three compounds. MitoQ decreased both oxidizing and reducing ROS while resveratrol and

curcumin were active only against reducing and oxidizing ROS, respectively (manuscript 2: Fig. 1). The antioxidant effect of these compounds may be the reason why resveratrol and curcumin have been reported to reduce adipocytes differentiation *in vitro* [156, 198].

We also examined whether cell number changes during differentiation of hBM-MSC into adipocytes. Therefore, the cells were counted during the whole differentiation process. No alterations in cell number were seen during differentiation (Fig. 1C). Thus, cells did neither proliferate nor undergo apoptosis during adipogenesis. There are some interesting reports regarding cessation of proliferation after induction of adipogenesis at the molecular level.

The transcription factors C/EBPα and PPARγ, which are required for adipocyte differentiation, were shown to be involved in growth arrest which is mandatory for adipocyte differentiation [283]. Timchenko *et al.* showed that C/EBPα increases mRNA and protein levels of the anti-mitotic protein cyclin-dependent kinase inhibitor 1 (p21/SDI-1) and that p21/SDI-1 anti-sense mRNA abolished C/EBPα-induced growth arrest [284]. Furthermore, Altiok *et al.* reported that activated PPARγ is sufficient to induce growth arrest in fibroblasts [285]. They proposed that PPARγ and C/EBPα both contribute to growth arrest. In studies on pre-adipocyte cell lines, it was shown that growth arrested cells undergo one or two rounds of cell division upon induction of adipogenesis. However, in primary human pre-adipocytes derived from adipose fat tissue, cell division after induction of adipogenic differentiation is not observed [283]. Recently, Qian *et al.* [279] directly compared the behavior of 3T3-L1 cells and hBM-MSCs during differentiation. They incubated the cell cultures with bromodeoxyuridine (BrdU) after the addition of differentiation medium for several hours, removed the stain and differentiated the cells into adipocytes. By confocal microscopy they could show that in contrast to 3T3-L1 cells, hBM-MSC did not did divide after induction of adipogenesis [279]. This report is in agreement with our results.

In addition to cell number, the protein content of the cultures was also assessed during the differentiation process. The protein content highly increased during adipogenesis which correlates with the increase of intracellular fat content (manuscript 1: Fig. 1D). Furthermore, we observed an increase in cell size under the microscope. Already in the 1970s it was reported that in humans cell size of

adipocytes increases with age [286]. This allows the conclusion that fat cells *in vivo* become bigger the older they get. Therefore, our *in vitro* model is in agreement with *in vivo* data of humans. Kubota *et al.* [287] produced a PPARγ$^{+/-}$ mouse and investigated the effects on adipose tissue. The adipocytes from the PPARγ$^{+/-}$ mice were smaller and the weight of adipose tissue was lower compared to wild-type animals [287]. Thus, activation of PPARγ during adipogenesis may be at least partially responsible for the increase in protein content and cell size during differentiation of hBM-MSC into adipocytes.

To assess the metabolic activity of hBM-MSCs during the differentiation process, we examined oxygen consumption and extracellular acidification which is an indicator for glycolysis. Respiration was measured under basal conditions, afterwards the ATP-synthase was blocked with oligomycin and mitochondria were uncoupled with FCCP. All of these values increased during differentiation. Extracellular acidification also raised (manuscript 1: Fig. 3). However the ECAR values were very low and hardly exceeded the detection limit. Therefore, we conclude that adipocytes use mainly oxidative phosphorylation and not glycolysis for ATP generation.

Only few data regarding oxygen consumption during adipogenesis are available so far. Ducluzeau *et al.* [288] examined respiration in 3T3-L1 cells during adipogenesis with the Seahorse instrument. They reported an increase in oxygen consumption under basal conditions and after inhibition of ATP-synthase by oligomycin. They did not see any alterations in uncoupled respiration but the respiration control ratio (RCR) decreased at the end of the differentiation process. As they also measured a lower mitochondrial membrane potential in adipocytes, they concluded that the extent of uncoupling increases during adipocyte differentiation. In contrast to us, they normalized their measurements to the protein content [288]. When we normalized oxygen consumption to protein content, almost no alterations during differentiation were seen. However, as we showed that cell size increases during adipogenesis and that the cell number did not change, we did not consider this normalization useful as it may reflect oxygen consumption of fewer cells at the end of differentiation compared to the beginning. Wilson-Fritch *et al*. [289] used a Clark-type electrode to compare respiration of 3T3-L1 cells which were either undifferentiated or differentiated into adipocytes. Adipocytes showed higher oxygen consumption under basal conditions. When mitochondria were uncoupled with FCCP, this difference was even much higher [289]. Therefore, mitochondria in adipocytes may run far below

their maximal capacity. Another group compared oxygen consumption of undifferentiated versus differentiated 3T3-L1 cells and primary human adipose tissue derived pre-adipocytes. 3T3-L1 cells differentiated into adipocytes showed an increase in oxygen consumption compared to undifferentiated cells. In adipocytes differentiated from pre-adipocytes the result was dependent on the serum concentration in the adipogenic medium. When pre-adipocytes were differentiated in medium containing 10% serum, no difference in respiration compared to undifferentiated cells was seen. When these cells were differentiated in medium without serum, respiration of adipocytes was clearly higher than the one of pre-adipocytes [290]. In our protocol, we used 3% serum in the differentiation medium. Thus, these reports are in agreement with our results.

To evaluate the mechanism of these antioxidants and their influence on mitochondrial function, we measured oxygen consumption of adipocytes after treatment with MitoQ, resveratrol or curcumin. As described in the second manuscript we used two different techniques. Respiration upon immediate addition of the antioxidants was measured in an Oxygraph (manuscript 2: Fig. 3 and 4 A&B) and the effects of a 24 h treatment were analyzed in a seahorse instrument. MitoQ, resveratrol and curcumin all slightly decreased state 3 respiration in the Oxygraph experiments. However, after 24 h incubation with resveratrol or curcumin, there was no impact on basal, oligomycin inhibited respiration and uncoupled oxygen consumption. Thus, resveratrol and curcumin did not impair mitochondrial coupling. MitoQ inhibited basal and uncoupled respiration at both concentrations applied and decylTPP reduced basal oxygen consumption at 0.5 µM. Thus, the inhibition of respiration by MitoQ at a concentration of 0.5 µM may be the beginning of mitochondrial toxicity. In contrast to our findings, Kelso *et al*. [120] reported an increase in state 2 respiration but a dose-dependent decrease in state 3 and uncoupled respiration as well as in mitochondrial membrane potential in isolated rat liver mitochondria. As lactate dehydrogenase (LDH) release increased, the effects on respiration may be due to mitochondrial toxicity. However, these effects were observed at 25 µM and 50 µM while we used clearly lower concentrations [120].

None of the antioxidants used showed an effect on intracellular ATP content (manuscript 2: Fig. 5) and glycolysis was very low (manuscript 2: Fig. 4C&D) under all conditions. Therefore, the remaining respiration under MitoQ treatment seems to

be sufficient to generate a mitochondrial membrane potential which is high enough to produce the amount of ATP required for the cells. Resveratrol was reported to enhance mitochondrial biogenesis [261, 262] and oxygen consumption [261]. We did not observe such effects but an incubation time of 24 h may not be enough to exert these changes in adipocytes. The antioxidant effect of resveratrol and curcumin after 24 h incubation is not due to an inhibition in respiration but for MitoQ this possibility cannot be excluded. In contrast to MitoQ, resveratrol and curcumin did not impair mitochondrial function. Respiration was strikingly decreased by MitoQ but this effect was not fatal. This is the first report about oxygen consumption in human adipocytes under MitoQ, resveratrol and curcumin treatment.

As respiration increased during differentiation but cell number did not, we questioned whether this observation may result rather from an increase in mitochondrial mass or mainly from uncoupling. Therefore, we assessed mitochondrial volume per cytoplasmic volume by confocal microscopy using an anti-cytochrome *c* antibody to visualize mitochondria. We observed a clear increase in mitochondrial mass during adipogenesis (manuscript 1: Fig. 4). Under the microscope mitochondria appeared as long structures which became highly networked during differentiation and arranged tightly around the lipid droplets (manuscript 1: Fig. 5).
Wilson-Fritch *et al.* [289] reported an increase in mitochondrial mass in 3T3-L1 derived adipocytes compared to the undifferentiated cells. They saw a very similar morphology than we did with our primary cells. In addition Lu *et al.* reported that mitochondrial mass increases during differentiation of primary rat adipocytes [228]. Therefore, these publications support our results.

To examine whether the morphological changes and the increase in ROS production alters cristae structure, transmission electron microscopy was performed during the differentiation process. We did not see any changes in the inner mitochondrial morphology or a loss of cristae structures (manuscript 1: Fig. 6). In contrast to our results, Sarsour *et al.* [229] reported loss of cristae in quiescent fibroblasts after a prolonged culture period. As cristea could be preserved by over-expressing MnSOD, their loss seems to be a result of ROS exposure. Thus, resistance of mitochondria to ROS induced damage may differ among cell types.

In our differentiation protocol we added rosiglitazone, an insulin sensitizer that activates PPARγ, to the medium in order to achieve efficient adipocytes

differentiation. However, there are some reports that rosiglitazone influences mitochondrial mass and morphology. Wilson-Fritch *et al.* observed fragmentation of mitochondria in 3T3-L1 derived adipocytes in response to rosiglitazone [289]. The mitochondria of untreated adipocytes showed a similar morphology as the mitochondria of our cells, while their cells treated with rosiglitazone did not. Later, the same group examined the effects of rosiglitazone on fat tissue of genetically obese *ob/ob* mice. They observed an increase in total body weight but no alteration in the epididymal fat pad. Cell fluorescence intensity of the mitochondrial protein mHsp60 was higher in adipocytes from rosiglitazone treated animals. They saw droplet-like structures within the mitochondrial staining which we interpret as lipid droplets. With Affimetrix assays they showed that 12% of all genes and 32% of mitochondrial genes were expressed differently in adipocytes of rosiglitazone treated animals. The expression of almost all of them was up-regulated. The adipocyte-specific transcription factor PGC-1α was up-regulated at the protein level. Furthermore, oxygen consumption of adipocytes from *ob/ob* mice was increased in response to rosiglitazone treatment. The longer the treatment lasted, the smaller the difference between treated and untreated cells was [56]. Elabd *et al.* [291] reported that pre-adipocytes from human white adipose tissue not only express the WAT marker ucoupling protein 2 (UCP2) but also the brown adipocytes markers UCP1 and cell death activator (CIDEA). Oxygen consumption and mitochondrial uncoupling increased in dependence of treatment duration. They concluded that rosiglitazone causes trans-differentiation of white into brown adipocytes [291].

Although the addition of rosiglitazone to the differentiation medium may have influenced parts of our results, our observations are still in agreement with other studies where no rosiglitazone was used [225, 228, 279, 283, 289].

7 Conclusion

In our studies, we characterized hBM-MSCs as an *in vitro* model for adipocytes. These cells differentiated efficiently into adipocytes after induction with adipogenic medium. They show fat accumulation, increase in ROS production as well as in mitochondrial mass and oxygen consumption during adipogenesis. These results are

in agreement with reports about 3T3 cells. However, in contrast to 3T3 cells, hBM-MSCs do not undergo any cell division after induction of adipogenesis. Compared to well-established cell lines such as 3T3-L1 cells, hBM-MSCs have the advantage to be of primary human origin. Thus, human bone marrow derived mesenchymal stem cells are an interesting model for adipocytes *in vitro*.

The effects of the antioxidants MitoQ, resveratrol and curcumin on adipocytes were also elucidated. All three compounds lowered intracellular ROS production. Resveratrol and curcumin slightly impaired state 3 respiration upon immediate addition but no effect on basal respiration was seen after 24 h. However, MitoQ decreased coupled respiration upon immediate treatment only little while a strong effect on basal and uncoupled respiration was seen after an incubation time of 24 h. The reason of this inhibition of oxygen consumption may be a competition between MitoQ and ubiquinone. None of the three antioxidants tested had any effect on intracellular ATP content. MitoQ did not impair ATP levels despite the finding that oxygen consumption was decreased and glycolysis was not altered. The reason of this observation needs further investigation. I conclude that MitoQ, resveratrol and curcumin are interesting candidates for treatment of elevated oxidative stress in tissues and organs of obese people, thus possibly lowering their risk to develop insulin resistance and diabetes.

References

1. Flegal, K.M., et al., *Prevalence and trends in obesity among US adults, 1999-2008.* Jama, 2010. **303**(3): p. 235-41.
2. Ahima, R.S., ed. *Metabolic Basis of Obesity*. 2011, Springer Science+Business Media: New York. 359-360.
3. Guh, D.P., et al., *The incidence of co-morbidities related to obesity and overweight: a systematic review and meta-analysis.* BMC Public Health, 2009. **9**: p. 88.
4. *Symptoms and Diagnosis of Metabolic Syndrome*. 2011.
5. Cannon, B. and J. Nedergaard, *Brown adipose tissue: function and physiological significance.* Physiol Rev, 2004. **84**(1): p. 277-359.
6. Frontini, A. and S. Cinti, *Distribution and development of brown adipocytes in the murine and human adipose organ.* Cell Metab, 2010. **11**(4): p. 253-6.
7. Lean, M.E., et al., *Brown adipose tissue uncoupling protein content in human infants, children and adults.* Clin Sci (Lond), 1986. **71**(3): p. 291-7.
8. Cypess, A.M., et al., *Identification and importance of brown adipose tissue in adult humans.* N Engl J Med, 2009. **360**(15): p. 1509-17.
9. van Marken Lichtenbelt, W.D., et al., *Cold-activated brown adipose tissue in healthy men.* N Engl J Med, 2009. **360**(15): p. 1500-8.
10. Virtanen, K.A., et al., *Functional brown adipose tissue in healthy adults.* N Engl J Med, 2009. **360**(15): p. 1518-25.
11. Koppen, A. and E. Kalkhoven, *Brown vs white adipocytes: the PPARgamma coregulator story.* FEBS Lett, 2010. **584**(15): p. 3250-9.
12. Picard, F., et al., *SRC-1 and TIF2 control energy balance between white and brown adipose tissues.* Cell, 2002. **111**(7): p. 931-41.
13. Louet, J.F., et al., *Oncogenic steroid receptor coactivator-3 is a key regulator of the white adipogenic program.* Proc Natl Acad Sci U S A, 2006. **103**(47): p. 17868-73.
14. Leone, T.C., et al., *PGC-1alpha deficiency causes multi-system energy metabolic derangements: muscle dysfunction, abnormal weight control and hepatic steatosis.* PLoS Biol, 2005. **3**(4): p. e101.
15. Lin, J., et al., *Defects in adaptive energy metabolism with CNS-linked hyperactivity in PGC-1alpha null mice.* Cell, 2004. **119**(1): p. 121-35.
16. Puigserver, P., et al., *A cold-inducible coactivator of nuclear receptors linked to adaptive thermogenesis.* Cell, 1998. **92**(6): p. 829-39.
17. Hondares, E., et al., *Thiazolidinediones and rexinoids induce peroxisome proliferator-activated receptor-coactivator (PGC)-1alpha gene transcription: an autoregulatory loop controls PGC-1alpha expression in adipocytes via peroxisome proliferator-activated receptor-gamma coactivation.* Endocrinology, 2006. **147**(6): p. 2829-38.
18. Camp, H.S., D. Ren, and T. Leff, *Adipogenesis and fat-cell function in obesity and diabetes.* Trends Mol Med, 2002. **8**(9): p. 442-7.
19. Rocha, V.Z. and P. Libby, *Obesity, inflammation, and atherosclerosis.* Nat Rev Cardiol, 2009. **6**(6): p. 399-409.
20. Fantuzzi, G., *Adipose tissue, adipokines, and inflammation.* J Allergy Clin Immunol, 2005. **115**(5): p. 911-9; quiz 920.
21. Hotamisligil, G.S., N.S. Shargill, and B.M. Spiegelman, *Adipose expression of tumor necrosis factor-alpha: direct role in obesity-linked insulin resistance.* Science, 1993. **259**(5091): p. 87-91.

22. Aggarwal, B.B., *Targeting inflammation-induced obesity and metabolic diseases by curcumin and other nutraceuticals.* Annu Rev Nutr, 2010. **30**: p. 173-99.
23. Green, A., et al., *Tumor necrosis factor increases the rate of lipolysis in primary cultures of adipocytes without altering levels of hormone-sensitive lipase.* Endocrinology, 1994. **134**(6): p. 2581-8.
24. Petruschke, T. and H. Hauner, *Tumor necrosis factor-alpha prevents the differentiation of human adipocyte precursor cells and causes delipidation of newly developed fat cells.* J Clin Endocrinol Metab, 1993. **76**(3): p. 742-7.
25. Tilg, H. and A.R. Moschen, *Adipocytokines: mediators linking adipose tissue, inflammation and immunity.* Nat Rev Immunol, 2006. **6**(10): p. 772-83.
26. Kern, P.A., et al., *The expression of tumor necrosis factor in human adipose tissue. Regulation by obesity, weight loss, and relationship to lipoprotein lipase.* J Clin Invest, 1995. **95**(5): p. 2111-9.
27. Uysal, K.T., et al., *Protection from obesity-induced insulin resistance in mice lacking TNF-alpha function.* Nature, 1997. **389**(6651): p. 610-4.
28. Nisoli, E., et al., *Tumor necrosis factor alpha mediates apoptosis of brown adipocytes and defective brown adipocyte function in obesity.* Proc Natl Acad Sci U S A, 2000. **97**(14): p. 8033-8.
29. Kirchgessner, T.G., et al., *Tumor necrosis factor-alpha contributes to obesity-related hyperleptinemia by regulating leptin release from adipocytes.* J Clin Invest, 1997. **100**(11): p. 2777-82.
30. Croker, B.A., et al., *SOCS3 negatively regulates IL-6 signaling in vivo.* Nat Immunol, 2003. **4**(6): p. 540-5.
31. Kaminski, T., et al., *Leptin and long form of leptin receptor genes expression in the hypothalamus and pituitary during the luteal phase and early pregnancy in pigs.* J Physiol Pharmacol, 2006. **57**(1): p. 95-108.
32. Konturek, S.J., et al., *Brain-gut axis and its role in the control of food intake.* J Physiol Pharmacol, 2004. **55**(1 Pt 2): p. 137-54.
33. Montague, C.T., et al., *Congenital leptin deficiency is associated with severe early-onset obesity in humans.* Nature, 1997. **387**(6636): p. 903-8.
34. La Cava, A. and G. Matarese, *The weight of leptin in immunity.* Nat Rev Immunol, 2004. **4**(5): p. 371-9.
35. Winters, B., et al., *Reduction of obesity, as induced by leptin, reverses endothelial dysfunction in obese (Lep(ob)) mice.* J Appl Physiol, 2000. **89**(6): p. 2382-90.
36. Gainsford, T., et al., *Leptin can induce proliferation, differentiation, and functional activation of hemopoietic cells.* Proc Natl Acad Sci U S A, 1996. **93**(25): p. 14564-8.
37. Yoon, M.J., et al., *Adiponectin increases fatty acid oxidation in skeletal muscle cells by sequential activation of AMP-activated protein kinase, p38 mitogen-activated protein kinase, and peroxisome proliferator-activated receptor alpha.* Diabetes, 2006. **55**(9): p. 2562-70.
38. Kubota, N., et al., *Disruption of adiponectin causes insulin resistance and neointimal formation.* J Biol Chem, 2002. **277**(29): p. 25863-6.
39. Bruun, J.M., et al., *Regulation of adiponectin by adipose tissue-derived cytokines: in vivo and in vitro investigations in humans.* Am J Physiol Endocrinol Metab, 2003. **285**(3): p. E527-33.
40. Maeda, N., et al., *Diet-induced insulin resistance in mice lacking adiponectin/ACRP30.* Nat Med, 2002. **8**(7): p. 731-7.

41. Guzik, T.J., D. Mangalat, and R. Korbut, *Adipocytokines - novel link between inflammation and vascular function?* J Physiol Pharmacol, 2006. **57**(4): p. 505-28.
42. Nishimura, K., et al., *Endogenous prostaglandins E2 and F 2alpha serve as an anti-apoptotic factor against apoptosis induced by tumor necrosis factor-alpha in mouse 3T3-L1 preadipocytes.* Biosci Biotechnol Biochem, 2006. **70**(9): p. 2145-53.
43. Ibrahim, M.M., *Subcutaneous and visceral adipose tissue: structural and functional differences.* Obes Rev, 2010. **11**(1): p. 11-8.
44. Wajchenberg, B.L., *Subcutaneous and visceral adipose tissue: their relation to the metabolic syndrome.* Endocr Rev, 2000. **21**(6): p. 697-738.
45. Marin, P., et al., *The morphology and metabolism of intraabdominal adipose tissue in men.* Metabolism, 1992. **41**(11): p. 1242-8.
46. Misra, A. and N.K. Vikram, *Clinical and pathophysiological consequences of abdominal adiposity and abdominal adipose tissue depots.* Nutrition, 2003. **19**(5): p. 457-66.
47. Dolinkova, M., et al., *The endocrine profile of subcutaneous and visceral adipose tissue of obese patients.* Mol Cell Endocrinol, 2008. **291**(1-2): p. 63-70.
48. Fox, C.S., et al., *Abdominal visceral and subcutaneous adipose tissue compartments: association with metabolic risk factors in the Framingham Heart Study.* Circulation, 2007. **116**(1): p. 39-48.
49. Frederiksen, L., et al., *Subcutaneous rather than visceral adipose tissue is associated with adiponectin levels and insulin resistance in young men.* J Clin Endocrinol Metab, 2009. **94**(10): p. 4010-5.
50. Fridlyand, L.E. and L.H. Philipson, *Oxidative reactive species in cell injury: Mechanisms in diabetes mellitus and therapeutic approaches.* Ann N Y Acad Sci, 2005. **1066**: p. 136-51.
51. Fridlyand, L.E. and L.H. Philipson, *Reactive species and early manifestation of insulin resistance in type 2 diabetes.* Diabetes Obes Metab, 2006. **8**(2): p. 136-45.
52. McGarry, J.D., *Banting lecture 2001: dysregulation of fatty acid metabolism in the etiology of type 2 diabetes.* Diabetes, 2002. **51**(1): p. 7-18.
53. Randle, P.J., et al., *The glucose fatty-acid cycle. Its role in insulin sensitivity and the metabolic disturbances of diabetes mellitus.* Lancet, 1963. **1**(7285): p. 785-9.
54. Lowell, B.B. and G.I. Shulman, *Mitochondrial dysfunction and type 2 diabetes.* Science, 2005. **307**(5708): p. 384-7.
55. Watson, R.T., M. Kanzaki, and J.E. Pessin, *Regulated membrane trafficking of the insulin-responsive glucose transporter 4 in adipocytes.* Endocr Rev, 2004. **25**(2): p. 177-204.
56. Wilson-Fritch, L., et al., *Mitochondrial remodeling in adipose tissue associated with obesity and treatment with rosiglitazone.* J Clin Invest, 2004. **114**(9): p. 1281-9.
57. Spiegelman, B.M., *Transcriptional control of mitochondrial energy metabolism through the PGC1 coactivators.* Novartis Found Symp, 2007. **287**: p. 60-3; discussion 63-9.
58. Semple, R.K., et al., *Expression of the thermogenic nuclear hormone receptor coactivator PGC-1alpha is reduced in the adipose tissue of morbidly obese subjects.* Int J Obes Relat Metab Disord, 2004. **28**(1): p. 176-9.

59. Uldry, M., et al., *Complementary action of the PGC-1 coactivators in mitochondrial biogenesis and brown fat differentiation.* Cell Metab, 2006. **3**(5): p. 333-41.
60. Song, F., et al., *Oxidative stress, antioxidant status and DNA damage in patients with impaired glucose regulation and newly diagnosed Type 2 diabetes.* Clin Sci (Lond), 2007. **112**(12): p. 599-606.
61. Zick, M., R. Rabl, and A.S. Reichert, *Cristae formation-linking ultrastructure and function of mitochondria.* Biochim Biophys Acta, 2009. **1793**(1): p. 5-19.
62. Bibb, M.J., et al., *Sequence and gene organization of mouse mitochondrial DNA.* Cell, 1981. **26**(2 Pt 2): p. 167-80.
63. Macreadie, I.G., et al., *Biogenesis of mitochondria: the mitochondrial gene (aap1) coding for mitochondrial ATPase subunit 8 in Saccharomyces cerevisiae.* Nucleic Acids Res, 1983. **11**(13): p. 4435-51.
64. Chomyn, A., et al., *Six unidentified reading frames of human mitochondrial DNA encode components of the respiratory-chain NADH dehydrogenase.* Nature, 1985. **314**(6012): p. 592-7.
65. Chomyn, A., et al., *URF6, last unidentified reading frame of human mtDNA, codes for an NADH dehydrogenase subunit.* Science, 1986. **234**(4776): p. 614-8.
66. Bologna Biocomputing Group, U.o.B., Italy, *Eukaryotic Subcellular Localization DataBase*. August 2011.
67. Frey, T.G. and C.A. Mannella, *The internal structure of mitochondria.* Trends Biochem Sci, 2000. **25**(7): p. 319-24.
68. Palade, G.E., *An electron microscope study of the mitochondrial structure.* J Histochem Cytochem, 1953. **1**(4): p. 188-211.
69. Munn, E.A., *The Structure of Mitochondria*. 1974, London, New York: Academic Press.
70. Palade, G.E., *The fine structure of mitochondria.* Anat Rec, 1952. **114**(3): p. 427-51.
71. Sjostrand, F.S., *Electron microscopy of mitochondria and cytoplasmic double membranes.* Nature, 1953. **171**(4340): p. 30-2.
72. Mannella, C.A., et al., *The internal compartmentation of rat-liver mitochondria: tomographic study using the high-voltage transmission electron microscope.* Microsc Res Tech, 1994. **27**(4): p. 278-83.
73. Mannella, C.A., M. Marko, and K. Buttle, *Reconsidering mitochondrial structure: new views of an old organelle.* Trends Biochem Sci, 1997. **22**(2): p. 37-8.
74. Mannella, C.A., et al., *Topology of the mitochondrial inner membrane: dynamics and bioenergetic implications.* IUBMB Life, 2001. **52**(3-5): p. 93-100.
75. Perkins, G.A., M.H. Ellisman, and D.A. Fox, *Three-dimensional analysis of mouse rod and cone mitochondrial cristae architecture: bioenergetic and functional implications.* Mol Vis, 2003. **9**: p. 60-73.
76. Nicastro, D., et al., *Cryo-electron tomography of neurospora mitochondria.* J Struct Biol, 2000. **129**(1): p. 48-56.
77. Williams, R.J., *Mitochondria and chloroplasts: localized and delocalized bioenergetic transduction.* Trends Biochem Sci, 2000. **25**(10): p. 479.
78. Tedeschi, H., *Old and new data, new issues: the mitochondrial DeltaPsi.* Biochim Biophys Acta, 2005. **1709**(3): p. 195-202.
79. Mitchell, P., *Keilin's respiratory chain concept and its chemiosmotic consequences.* Science, 1979. **206**(4423): p. 1148-59.

80. Mannella, C.A., *Structure and dynamics of the mitochondrial inner membrane cristae.* Biochim Biophys Acta, 2006. **1763**(5-6): p. 542-8.
81. Hackenbrock, C.R., *Ultrastructural bases for metabolically linked mechanical activity in mitochondria. I. Reversible ultrastructural changes with change in metabolic steady state in isolated liver mitochondria.* J Cell Biol, 1966. **30**(2): p. 269-97.
82. Mannella, C.A., *The relevance of mitochondrial membrane topology to mitochondrial function.* Biochim Biophys Acta, 2006. **1762**(2): p. 140-7.
83. Kane, L.A. and R.J. Youle, *Mitochondrial fission and fusion and their roles in the heart.* J Mol Med, 2010. **88**(10): p. 971-9.
84. Chen, H., et al., *Mitofusins Mfn1 and Mfn2 coordinately regulate mitochondrial fusion and are essential for embryonic development.* J Cell Biol, 2003. **160**(2): p. 189-200.
85. Ishihara, N., et al., *Mitochondrial fission factor Drp1 is essential for embryonic development and synapse formation in mice.* Nat Cell Biol, 2009. **11**(8): p. 958-66.
86. Detmer, S.A. and D.C. Chan, *Functions and dysfunctions of mitochondrial dynamics.* Nat Rev Mol Cell Biol, 2007. **8**(11): p. 870-9.
87. Tatsuta, T. and T. Langer, *Quality control of mitochondria: protection against neurodegeneration and ageing.* EMBO J, 2008. **27**(2): p. 306-14.
88. Twig, G., et al., *Fission and selective fusion govern mitochondrial segregation and elimination by autophagy.* EMBO J, 2008. **27**(2): p. 433-46.
89. Meeusen, S., J.M. McCaffery, and J. Nunnari, *Mitochondrial fusion intermediates revealed in vitro.* Science, 2004. **305**(5691): p. 1747-52.
90. Smirnova, E., et al., *A human dynamin-related protein controls the distribution of mitochondria.* J Cell Biol, 1998. **143**(2): p. 351-8.
91. Lackner, L.L., J.S. Horner, and J. Nunnari, *Mechanistic analysis of a dynamin effector.* Science, 2009. **325**(5942): p. 874-7.
92. Otsuga, D., et al., *The dynamin-related GTPase, Dnm1p, controls mitochondrial morphology in yeast.* J Cell Biol, 1998. **143**(2): p. 333-49.
93. Mozdy, A.D., J.M. McCaffery, and J.M. Shaw, *Dnm1p GTPase-mediated mitochondrial fission is a multi-step process requiring the novel integral membrane component Fis1p.* J Cell Biol, 2000. **151**(2): p. 367-80.
94. Gandre-Babbe, S. and A.M. van der Bliek, *The novel tail-anchored membrane protein Mff controls mitochondrial and peroxisomal fission in mammalian cells.* Mol Biol Cell, 2008. **19**(6): p. 2402-12.
95. Yoon, Y., et al., *Mitochondrial dynamics in diabetes.* Antioxid Redox Signal, 2011. **14**(3): p. 439-57.
96. Brooks, C., et al., *Bak regulates mitochondrial morphology and pathology during apoptosis by interacting with mitofusins.* Proc Natl Acad Sci U S A, 2007. **104**(28): p. 11649-54.
97. Autret, A. and S.J. Martin, *Emerging role for members of the Bcl-2 family in mitochondrial morphogenesis.* Mol Cell, 2009. **36**(3): p. 355-63.
98. Mitchell, P., *Coupling of phosphorylation to electron and hydrogen transfer by a chemi-osmotic type of mechanism.* Nature, 1961. **191**: p. 144-8.
99. Saraste, M., *Oxidative phosphorylation at the fin de siecle.* Science, 1999. **283**(5407): p. 1488-93.
100. Grigorieff, N., *Three-dimensional structure of bovine NADH:ubiquinone oxidoreductase (complex I) at 22 A in ice.* J Mol Biol, 1998. **277**(5): p. 1033-46.
101. Hagerhall, C., *Succinate: quinone oxidoreductases. Variations on a conserved theme.* Biochim Biophys Acta, 1997. **1320**(2): p. 107-41.

102. Braun, H.P. and U.K. Schmitz, *Are the 'core' proteins of the mitochondrial bc1 complex evolutionary relics of a processing protease?* Trends Biochem Sci, 1995. **20**(5): p. 171-5.
103. Xia, D., et al., *Crystal structure of the cytochrome bc1 complex from bovine heart mitochondria.* Science, 1997. **277**(5322): p. 60-6.
104. Bottcher, B., L. Schwarz, and P. Graber, *Direct indication for the existence of a double stalk in CF0F1.* J Mol Biol, 1998. **281**(5): p. 757-62.
105. Schnitzer, M.J., *Molecular motors. Doing a rotary two-step.* Nature, 2001. **410**(6831): p. 878-9, 881.
106. Rees, D.M., A.G. Leslie, and J.E. Walker, *The structure of the membrane extrinsic region of bovine ATP synthase.* Proc Natl Acad Sci U S A, 2009. **106**(51): p. 21597-601.
107. Boyer, P.D., *The binding change mechanism for ATP synthase--some probabilities and possibilities.* Biochim Biophys Acta, 1993. **1140**(3): p. 215-50.
108. Yasuda, R., et al., *F1-ATPase is a highly efficient molecular motor that rotates with discrete 120 degree steps.* Cell, 1998. **93**(7): p. 1117-24.
109. Yu, B.P., *Cellular defenses against damage from reactive oxygen species.* Physiol Rev, 1994. **74**(1): p. 139-62.
110. Turrens, J.F., et al., *The effect of hyperoxia on superoxide production by lung submitochondrial particles.* Arch Biochem Biophys, 1982. **217**(2): p. 401-10.
111. Fischer, L.J. and S.A. Hamburger, *Inhibition of alloxan action in isolated pancreatic islets by superoxide dismutase, catalase, and a metal chelator.* Diabetes, 1980. **29**(3): p. 213-6.
112. Vincent, H.K. and A.G. Taylor, *Biomarkers and potential mechanisms of obesity-induced oxidant stress in humans.* Int J Obes (Lond), 2006. **30**(3): p. 400-18.
113. Villalba, J.M., et al., *Therapeutic use of coenzyme Q10 and coenzyme Q10-related compounds and formulations.* Expert Opin Investig Drugs, 2010. **19**(4): p. 535-54.
114. McCord, J.M. and I. Fridovich, *Superoxide dismutase. An enzymic function for erythrocuprein (hemocuprein).* J Biol Chem, 1969. **244**(22): p. 6049-55.
115. McCay, P., ed. *Enzyme-generated free radicals and singlet oxygen as promoters of lipid peroxidation in cell membranes*. Lipids, ed. P. R. Vol. 1. 1976, Raven: New York. 157-168.
116. De Pauw, A., et al., *Mitochondrial (dys)function in adipocyte (de)differentiation and systemic metabolic alterations.* Am J Pathol, 2009. **175**(3): p. 927-39.
117. Murphy, M.P., *Selective targeting of bioactive compounds to mitochondria.* Trends Biotechnol, 1997. **15**(8): p. 326-30.
118. Liberman, E.A., et al., *Mechanism of coupling of oxidative phosphorylation and the membrane potential of mitochondria.* Nature, 1969. **222**(5198): p. 1076-8.
119. Smith, R.A., et al., *Delivery of bioactive molecules to mitochondria in vivo.* Proc Natl Acad Sci U S A, 2003. **100**(9): p. 5407-12.
120. Kelso, G.F., et al., *Selective targeting of a redox-active ubiquinone to mitochondria within cells: antioxidant and antiapoptotic properties.* J Biol Chem, 2001. **276**(7): p. 4588-96.
121. Burns, R.J. and M.P. Murphy, *Labeling of mitochondrial proteins in living cells by the thiol probe thiobutyltriphenylphosphonium bromide.* Arch Biochem Biophys, 1997. **339**(1): p. 33-9.
122. James, A.M., et al., *Interactions of mitochondria-targeted and untargeted ubiquinones with the mitochondrial respiratory chain and reactive oxygen*

species. Implications for the use of exogenous ubiquinones as therapies and experimental tools. J Biol Chem, 2005. **280**(22): p. 21295-312.
123. Smith, R.A., et al., *Selective targeting of an antioxidant to mitochondria.* Eur J Biochem, 1999. **263**(3): p. 709-16.
124. Asin-Cayuela, J., et al., *Fine-tuning the hydrophobicity of a mitochondria-targeted antioxidant.* FEBS Lett, 2004. **571**(1-3): p. 9-16.
125. Ng, Y., et al., *The role of docosahexaenoic acid in mediating mitochondrial membrane lipid oxidation and apoptosis in colonocytes.* Carcinogenesis, 2005. **26**(11): p. 1914-21.
126. Schafer, M., et al., *Role of redox signaling in the autonomous proliferative response of endothelial cells to hypoxia.* Circ Res, 2003. **92**(9): p. 1010-5.
127. Dhanasekaran, A., et al., *Supplementation of endothelial cells with mitochondria-targeted antioxidants inhibit peroxide-induced mitochondrial iron uptake, oxidative damage, and apoptosis.* J Biol Chem, 2004. **279**(36): p. 37575-87.
128. Saretzki, G., M.P. Murphy, and T. von Zglinicki, *MitoQ counteracts telomere shortening and elongates lifespan of fibroblasts under mild oxidative stress.* Aging Cell, 2003. **2**(2): p. 141-3.
129. Barhoumi, R., et al., *Manganese potentiates lipopolysaccharide-induced expression of NOS2 in C6 glioma cells through mitochondrial-dependent activation of nuclear factor kappaB.* Brain Res Mol Brain Res, 2004. **122**(2): p. 167-79.
130. Siler-Marsiglio, K.I., et al., *Mitochondrially targeted vitamin E and vitamin E mitigate ethanol-mediated effects on cerebellar granule cell antioxidant defense systems.* Brain Res, 2005. **1052**(2): p. 202-11.
131. Alleva, R., et al., *Coenzyme Q blocks biochemical but not receptor-mediated apoptosis by increasing mitochondrial antioxidant protection.* FEBS Lett, 2001. **503**(1): p. 46-50.
132. Hughes, G., M.P. Murphy, and E.C. Ledgerwood, *Mitochondrial reactive oxygen species regulate the temporal activation of nuclear factor kappaB to modulate tumour necrosis factor-induced apoptosis: evidence from mitochondria-targeted antioxidants.* Biochem J, 2005. **389**(Pt 1): p. 83-9.
133. Chen, K., et al., *Mitochondrial function is required for hydrogen peroxide-induced growth factor receptor transactivation and downstream signaling.* J Biol Chem, 2004. **279**(33): p. 35079-86.
134. Jauslin, M.L., et al., *Mitochondria-targeted antioxidants protect Friedreich Ataxia fibroblasts from endogenous oxidative stress more effectively than untargeted antioxidants.* FASEB J, 2003. **17**(13): p. 1972-4.
135. King, A., et al., *Mitochondria-derived reactive oxygen species mediate blue light-induced death of retinal pigment epithelial cells.* Photochem Photobiol, 2004. **79**(5): p. 470-5.
136. Galeotti, T., et al., *Protective role of MnSOD and redox regulation of neuronal cell survival.* Biomed Pharmacother, 2005. **59**(4): p. 197-203.
137. Wang, X.F., et al., *Vitamin E analogs trigger apoptosis in HER2/erbB2-overexpressing breast cancer cells by signaling via the mitochondrial pathway.* Biochem Biophys Res Commun, 2005. **326**(2): p. 282-9.
138. Hwang, P.M., et al., *Ferredoxin reductase affects p53-dependent, 5-fluorouracil-induced apoptosis in colorectal cancer cells.* Nat Med, 2001. **7**(10): p. 1111-7.
139. Fink, B.D., et al., *Mitochondrial targeted coenzyme Q, superoxide, and fuel selectivity in endothelial cells.* PLoS One, 2009. **4**(1): p. e4250.

140. Adlam, V.J., et al., *Targeting an antioxidant to mitochondria decreases cardiac ischemia-reperfusion injury.* FASEB J, 2005. **19**(9): p. 1088-95.
141. Graham, D., et al., *Mitochondria-targeted antioxidant MitoQ10 improves endothelial function and attenuates cardiac hypertrophy.* Hypertension, 2009. **54**(2): p. 322-8.
142. Supinski, G.S., M.P. Murphy, and L.A. Callahan, *MitoQ administration prevents endotoxin-induced cardiac dysfunction.* Am J Physiol Regul Integr Comp Physiol, 2009. **297**(4): p. R1095-102.
143. Hobbs, C.E., et al., *Neonatal rat hypoxia-ischemia: Effect of the anti-oxidant mitoquinol, and S-PBN.* Pediatr Int, 2008. **50**(4): p. 481-8.
144. Rodriguez-Cuenca, S., et al., *Consequences of long-term oral administration of the mitochondria-targeted antioxidant MitoQ to wild-type mice.* Free Radic Biol Med, 2010. **48**(1): p. 161-72.
145. Snow, B.J., et al., *A double-blind, placebo-controlled study to assess the mitochondria-targeted antioxidant MitoQ as a disease-modifying therapy in Parkinson's disease.* Mov Disord, 2010. **25**(11): p. 1670-4.
146. Smith, R.A. and M.P. Murphy, *Animal and human studies with the mitochondria-targeted antioxidant MitoQ.* Ann N Y Acad Sci, 2010. **1201**: p. 96-103.
147. Gane, E.J., et al., *The mitochondria-targeted anti-oxidant mitoquinone decreases liver damage in a phase II study of hepatitis C patients.* Liver Int, 2010. **30**(7): p. 1019-26.
148. Lancon, A., et al., *Human hepatic cell uptake of resveratrol: involvement of both passive diffusion and carrier-mediated process.* Biochem Biophys Res Commun, 2004. **316**(4): p. 1132-7.
149. Fischer-Posovszky, P., et al., *Resveratrol regulates human adipocyte number and function in a Sirt1-dependent manner.* Am J Clin Nutr, 2010. **92**(1): p. 5-15.
150. Rayalam, S., et al., *Resveratrol induces apoptosis and inhibits adipogenesis in 3T3-L1 adipocytes.* Phytother Res, 2008. **22**(10): p. 1367-71.
151. Mingrone, G., et al., *Could the low level of expression of the gene encoding skeletal muscle mitofusin-2 account for the metabolic inflexibility of obesity?* Diabetologia, 2005. **48**(10): p. 2108-14.
152. Baile, C.A., et al., *Effect of resveratrol on fat mobilization.* Ann N Y Acad Sci, 2011. **1215**: p. 40-7.
153. Ferry-Dumazet, H., et al., *Resveratrol inhibits the growth and induces the apoptosis of both normal and leukemic hematopoietic cells.* Carcinogenesis, 2002. **23**(8): p. 1327-33.
154. Liang, Y.C., et al., *Resveratrol-induced G2 arrest through the inhibition of CDK7 and p34CDC2 kinases in colon carcinoma HT29 cells.* Biochem Pharmacol, 2003. **65**(7): p. 1053-60.
155. Delmas, D., et al., *Transport, stability, and biological activity of resveratrol.* Ann N Y Acad Sci, 2011. **1215**: p. 48-59.
156. Hoshino, J., et al., *Selective synthesis and biological evaluation of sulfate-conjugated resveratrol metabolites.* J Med Chem, 2010. **53**(13): p. 5033-43.
157. Robb, E.L., et al., *Molecular mechanisms of oxidative stress resistance induced by resveratrol: Specific and progressive induction of MnSOD.* Biochem Biophys Res Commun, 2008. **367**(2): p. 406-12.
158. Mokni, M., et al., *Effect of resveratrol on antioxidant enzyme activities in the brain of healthy rat.* Neurochem Res, 2007. **32**(6): p. 981-7.

159. Robb, E.L., et al., *Dietary resveratrol administration increases MnSOD expression and activity in mouse brain.* Biochem Biophys Res Commun, 2008. **372**(1): p. 254-9.
160. Szkudelska, K., L. Nogowski, and T. Szkudelski, *Resveratrol, a naturally occurring diphenolic compound, affects lipogenesis, lipolysis and the antilipolytic action of insulin in isolated rat adipocytes.* J Steroid Biochem Mol Biol, 2009. **113**(1-2): p. 17-24.
161. Arichi, H., et al., *Effects of stilbene components of the roots of Polygonum cuspidatum Sieb. et Zucc. on lipid metabolism.* Chem Pharm Bull (Tokyo), 1982. **30**(5): p. 1766-70.
162. Baur, J.A., et al., *Resveratrol improves health and survival of mice on a high-calorie diet.* Nature, 2006. **444**(7117): p. 337-42.
163. Su, H.C., L.M. Hung, and J.K. Chen, *Resveratrol, a red wine antioxidant, possesses an insulin-like effect in streptozotocin-induced diabetic rats.* Am J Physiol Endocrinol Metab, 2006. **290**(6): p. E1339-46.
164. Schmatz, R., et al., *Effects of resveratrol on nucleotide degrading enzymes in streptozotocin-induced diabetic rats.* Life Sci, 2009. **84**(11-12): p. 345-50.
165. Penumathsa, S.V., et al., *Resveratrol enhances GLUT-4 translocation to the caveolar lipid raft fractions through AMPK/Akt/eNOS signalling pathway in diabetic myocardium.* J Cell Mol Med, 2008. **12**(6A): p. 2350-61.
166. Chi, T.C., et al., *Phosphatidylinositol-3-kinase is involved in the antihyperglycemic effect induced by resveratrol in streptozotocin-induced diabetic rats.* Life Sci, 2007. **80**(18): p. 1713-20.
167. Petrovski, G., N. Gurusamy, and D.K. Das, *Resveratrol in cardiovascular health and disease.* Ann N Y Acad Sci, 2011. **1215**: p. 22-33.
168. Liu, Z., et al., *Effects of trans-resveratrol on hypertension-induced cardiac hypertrophy using the partially nephrectomized rat model.* Clin Exp Pharmacol Physiol, 2005. **32**(12): p. 1049-54.
169. Thandapilly, S.J., et al., *Resveratrol prevents the development of pathological cardiac hypertrophy and contractile dysfunction in the SHR without lowering blood pressure.* Am J Hypertens, 2010. **23**(2): p. 192-6.
170. Markus, M.A. and B.J. Morris, *Resveratrol in prevention and treatment of common clinical conditions of aging.* Clin Interv Aging, 2008. **3**(2): p. 331-9.
171. Gurusamy, N., et al., *Red wine antioxidant resveratrol-modified cardiac stem cells regenerate infarcted myocardium.* J Cell Mol Med, 2010. **14**(9): p. 2235-9.
172. Fremont, L., L. Belguendouz, and S. Delpal, *Antioxidant activity of resveratrol and alcohol-free wine polyphenols related to LDL oxidation and polyunsaturated fatty acids.* Life Sci, 1999. **64**(26): p. 2511-21.
173. Jang, M., et al., *Cancer chemopreventive activity of resveratrol, a natural product derived from grapes.* Science, 1997. **275**(5297): p. 218-20.
174. Gupta, S.C., et al., *Chemosensitization of tumors by resveratrol.* Ann N Y Acad Sci, 2011. **1215**: p. 150-60.
175. Fulda, S. and K.M. Debatin, *Sensitization for anticancer drug-induced apoptosis by the chemopreventive agent resveratrol.* Oncogene, 2004. **23**(40): p. 6702-11.
176. Zhao, W., et al., *Resveratrol down-regulates survivin and induces apoptosis in human multidrug-resistant SPC-A-1/CDDP cells.* Oncol Rep, 2010. **23**(1): p. 279-86.
177. Gatouillat, G., et al., *Resveratrol induces cell-cycle disruption and apoptosis in chemoresistant B16 melanoma.* J Cell Biochem, 2010. **110**(4): p. 893-902.

178. Epstein, J., I.R. Sanderson, and T.T. Macdonald, *Curcumin as a therapeutic agent: the evidence from in vitro, animal and human studies.* Br J Nutr, 2010. **103**(11): p. 1545-57.
179. Walle, T., et al., *High absorption but very low bioavailability of oral resveratrol in humans.* Drug Metab Dispos, 2004. **32**(12): p. 1377-82.
180. Lu, Z., et al., *Transport of a cancer chemopreventive polyphenol, resveratrol: interaction with serum albumin and hemoglobin.* J Fluoresc, 2007. **17**(5): p. 580-7.
181. Cruz, M.N., et al., *Acute responses to phytoestrogens in small arteries from men with coronary heart disease.* Am J Physiol Heart Circ Physiol, 2006. **290**(5): p. H1969-75.
182. Rakici, O., et al., *Effects of resveratrol on vascular tone and endothelial function of human saphenous vein and internal mammary artery.* Int J Cardiol, 2005. **105**(2): p. 209-15.
183. Brasnyo, P., et al., *Resveratrol improves insulin sensitivity, reduces oxidative stress and activates the Akt pathway in type 2 diabetic patients.* Br J Nutr, 2011. **106**(3): p. 383-9.
184. Shishodia, S., et al., *Curcumin (diferuloylmethane) inhibits constitutive NF-kappaB activation, induces G1/S arrest, suppresses proliferation, and induces apoptosis in mantle cell lymphoma.* Biochem Pharmacol, 2005. **70**(5): p. 700-13.
185. Bharti, A.C., N. Donato, and B.B. Aggarwal, *Curcumin (diferuloylmethane) inhibits constitutive and IL-6-inducible STAT3 phosphorylation in human multiple myeloma cells.* J Immunol, 2003. **171**(7): p. 3863-71.
186. Mackenzie, G.G., et al., *Curcumin induces cell-arrest and apoptosis in association with the inhibition of constitutively active NF-kappaB and STAT3 pathways in Hodgkin's lymphoma cells.* Int J Cancer, 2008. **123**(1): p. 56-65.
187. Epstein, J., et al., *Curcumin suppresses p38 mitogen-activated protein kinase activation, reduces IL-1beta and matrix metalloproteinase-3 and enhances IL-10 in the mucosa of children and adults with inflammatory bowel disease.* Br J Nutr, 2010. **103**(6): p. 824-32.
188. Choudhuri, T., et al., *Curcumin selectively induces apoptosis in deregulated cyclin D1-expressed cells at G2 phase of cell cycle in a p53-dependent manner.* J Biol Chem, 2005. **280**(20): p. 20059-68.
189. Han, S.S., et al., *Curcumin causes the growth arrest and apoptosis of B cell lymphoma by downregulation of egr-1, c-myc, bcl-XL, NF-kappa B, and p53.* Clin Immunol, 1999. **93**(2): p. 152-61.
190. Moos, P.J., et al., *Curcumin impairs tumor suppressor p53 function in colon cancer cells.* Carcinogenesis, 2004. **25**(9): p. 1611-7.
191. Tsvetkov, P., et al., *Inhibition of NAD(P)H:quinone oxidoreductase 1 activity and induction of p53 degradation by the natural phenolic compound curcumin.* Proc Natl Acad Sci U S A, 2005. **102**(15): p. 5535-40.
192. Pender, S.L. and T.T. MacDonald, *Matrix metalloproteinases and the gut - new roles for old enzymes.* Curr Opin Pharmacol, 2004. **4**(6): p. 546-50.
193. Vihinen, P., R. Ala-aho, and V.M. Kahari, *Matrix metalloproteinases as therapeutic targets in cancer.* Curr Cancer Drug Targets, 2005. **5**(3): p. 203-20.
194. Woo, M.S., et al., *Curcumin suppresses phorbol ester-induced matrix metalloproteinase-9 expression by inhibiting the PKC to MAPK signaling pathways in human astroglioma cells.* Biochem Biophys Res Commun, 2005. **335**(4): p. 1017-25.

195. Lee, Y.K., et al., *Curcumin exerts antidifferentiation effect through AMPKalpha-PPAR-gamma in 3T3-L1 adipocytes and antiproliferatory effect through AMPKalpha-COX-2 in cancer cells.* J Agric Food Chem, 2009. **57**(1): p. 305-10.
196. Kuroda, M., et al., *Hypoglycemic effects of turmeric (Curcuma longa L. rhizomes) on genetically diabetic KK-Ay mice.* Biol Pharm Bull, 2005. **28**(5): p. 937-9.
197. Weisberg, S.P., R. Leibel, and D.V. Tortoriello, *Dietary curcumin significantly improves obesity-associated inflammation and diabetes in mouse models of diabesity.* Endocrinology, 2008. **149**(7): p. 3549-58.
198. Ejaz, A., et al., *Curcumin inhibits adipogenesis in 3T3-L1 adipocytes and angiogenesis and obesity in C57/BL mice.* J Nutr, 2009. **139**(5): p. 919-25.
199. Suryanarayana, P., et al., *Effect of turmeric and curcumin on oxidative stress and antioxidant enzymes in streptozotocin-induced diabetic rat.* Med Sci Monit, 2007. **13**(12): p. BR286-92.
200. Chan, M.M., *Inhibition of tumor necrosis factor by curcumin, a phytochemical.* Biochem Pharmacol, 1995. **49**(11): p. 1551-6.
201. Wang, S.L., et al., *Curcumin, a potential inhibitor of up-regulation of TNF-alpha and IL-6 induced by palmitate in 3T3-L1 adipocytes through NF-kappaB and JNK pathway.* Biomed Environ Sci, 2009. **22**(1): p. 32-9.
202. Woo, H.M., et al., *Active spice-derived components can inhibit inflammatory responses of adipose tissue in obesity by suppressing inflammatory actions of macrophages and release of monocyte chemoattractant protein-1 from adipocytes.* Life Sci, 2007. **80**(10): p. 926-31.
203. Jain, S.K., et al., *Curcumin supplementation lowers TNF-alpha, IL-6, IL-8, and MCP-1 secretion in high glucose-treated cultured monocytes and blood levels of TNF-alpha, IL-6, MCP-1, glucose, and glycosylated hemoglobin in diabetic rats.* Antioxid Redox Signal, 2009. **11**(2): p. 241-9.
204. Morimoto, T., et al., *The dietary compound curcumin inhibits p300 histone acetyltransferase activity and prevents heart failure in rats.* J Clin Invest, 2008. **118**(3): p. 868-78.
205. Carroll, R.E., et al., *Phase IIa clinical trial of curcumin for the prevention of colorectal neoplasia.* Cancer Prev Res (Phila), 2011. **4**(3): p. 354-64.
206. Dhillon, N., et al., *Phase II trial of curcumin in patients with advanced pancreatic cancer.* Clin Cancer Res, 2008. **14**(14): p. 4491-9.
207. Usharani, P., et al., *Effect of NCB-02, atorvastatin and placebo on endothelial function, oxidative stress and inflammatory markers in patients with type 2 diabetes mellitus: a randomized, parallel-group, placebo-controlled, 8-week study.* Drugs R D, 2008. **9**(4): p. 243-50.
208. Baum, L., et al., *Curcumin effects on blood lipid profile in a 6-month human study.* Pharmacol Res, 2007. **56**(6): p. 509-14.
209. Schenk, S., M. Saberi, and J.M. Olefsky, *Insulin sensitivity: modulation by nutrients and inflammation.* J Clin Invest, 2008. **118**(9): p. 2992-3002.
210. Xu, H., et al., *Chronic inflammation in fat plays a crucial role in the development of obesity-related insulin resistance.* J Clin Invest, 2003. **112**(12): p. 1821-30.
211. Weisberg, S.P., et al., *Obesity is associated with macrophage accumulation in adipose tissue.* J Clin Invest, 2003. **112**(12): p. 1796-808.
212. Brownlee, M., *The pathobiology of diabetic complications: a unifying mechanism.* Diabetes, 2005. **54**(6): p. 1615-25.

213. Haber, C.A., et al., *N-acetylcysteine and taurine prevent hyperglycemia-induced insulin resistance in vivo: possible role of oxidative stress.* Am J Physiol Endocrinol Metab, 2003. **285**(4): p. E744-53.
214. Bindokas, V.P., et al., *Visualizing superoxide production in normal and diabetic rat islets of Langerhans.* J Biol Chem, 2003. **278**(11): p. 9796-801.
215. Talior, I., et al., *Increased glucose uptake promotes oxidative stress and PKC-delta activation in adipocytes of obese, insulin-resistant mice.* Am J Physiol Endocrinol Metab, 2003. **285**(2): p. E295-302.
216. Evans, J.L., et al., *Oxidative stress and stress-activated signaling pathways: a unifying hypothesis of type 2 diabetes.* Endocr Rev, 2002. **23**(5): p. 599-622.
217. Turrens, J.F., *Mitochondrial formation of reactive oxygen species.* J Physiol, 2003. **552**(Pt 2): p. 335-44.
218. Skulachev, V.P., *Mitochondrial physiology and pathology; concepts of programmed death of organelles, cells and organisms.* Mol Aspects Med, 1999. **20**(3): p. 139-84.
219. Green, K., M.D. Brand, and M.P. Murphy, *Prevention of mitochondrial oxidative damage as a therapeutic strategy in diabetes.* Diabetes, 2004. **53 Suppl 1**: p. S110-8.
220. Droge, W., *Free radicals in the physiological control of cell function.* Physiol Rev, 2002. **82**(1): p. 47-95.
221. Lu, B., et al., *Enhanced sensitivity of insulin-resistant adipocytes to vanadate is associated with oxidative stress and decreased reduction of vanadate (+5) to vanadyl (+4).* J Biol Chem, 2001. **276**(38): p. 35589-98.
222. Tirosh, A., et al., *Oxidative stress disrupts insulin-induced cellular redistribution of insulin receptor substrate-1 and phosphatidylinositol 3-kinase in 3T3-L1 adipocytes. A putative cellular mechanism for impaired protein kinase B activation and GLUT4 translocation.* J Biol Chem, 1999. **274**(15): p. 10595-602.
223. Hoch, M., et al., *Weak functional coupling of the melanocortin-1 receptor expressed in human adipocytes.* J Recept Signal Transduct Res, 2008. **28**(5): p. 485-504.
224. Grimaldi, P.A., *The roles of PPARs in adipocyte differentiation.* Prog Lipid Res, 2001. **40**(4): p. 269-81.
225. Saitoh, Y., et al., *Novel polyhydroxylated fullerene suppresses intracellular oxidative stress together with repression of intracellular lipid accumulation during the differentiation of OP9 preadipocytes into adipocytes.* Free Radic Res, 2010. **44**(9): p. 1072-81.
226. Lee, H., et al., *Reactive oxygen species facilitate adipocyte differentiation by accelerating mitotic clonal expansion.* J Biol Chem, 2009. **284**(16): p. 10601-9.
227. Ducluzeau, P.H., et al., *Dynamic regulation of mitochondrial network and oxidative functions during 3T3-L1 fat cell differentiation.* J Physiol Biochem, 2011.
228. Lu, R.H., et al., *Mitochondrial development and the influence of its dysfunction during rat adipocyte differentiation.* Mol Biol Rep, 2010. **37**(5): p. 2173-82.
229. Sarsour, E.H., et al., *MnSOD activity protects mitochondrial morphology of quiescent fibroblasts from age associated abnormalities.* Mitochondrion, 2010. **10**(4): p. 342-9.
230. Hoch, M., et al., *LPS induces interleukin-6 and interleukin-8 but not tumor necrosis factor-alpha in human adipocytes.* Cytokine, 2008. **41**(1): p. 29-37.
231. Juge-Aubry, C.E., et al., *Adipose tissue is a regulated source of interleukin-10.* Cytokine, 2005. **29**(6): p. 270-4.

232. Fain, J.N., *Release of interleukins and other inflammatory cytokines by human adipose tissue is enhanced in obesity and primarily due to the nonfat cells.* Vitam Horm, 2006. **74**: p. 443-77.
233. Finkel, T., *Oxidant signals and oxidative stress.* Curr Opin Cell Biol, 2003. **15**(2): p. 247-54.
234. Appel K, H.H., *Reactive oxygen species: metabolism, oxidative stress and signal transduction.* Annu Rev Plant Biol, 2004. **55**: p. 373-399.
235. Finkel, T., *Signal transduction by reactive oxygen species.* J Cell Biol, 2011. **194**(1): p. 7-15.
236. Andriantsitohaina, R., et al., *Systems biology of antioxidants.* Clin Sci (Lond), 2012. **123**(3): p. 173-92.
237. Sena, L.A. and N.S. Chandel, *Physiological roles of mitochondrial reactive oxygen species.* Mol Cell, 2012. **48**(2): p. 158-67.
238. D'Autreaux, B. and M.B. Toledano, *ROS as signalling molecules: mechanisms that generate specificity in ROS homeostasis.* Nat Rev Mol Cell Biol, 2007. **8**(10): p. 813-24.
239. Tormos, K.V., et al., *Mitochondrial complex III ROS regulate adipocyte differentiation.* Cell Metab, 2011. **14**(4): p. 537-44.
240. Furukawa, S., et al., *Increased oxidative stress in obesity and its impact on metabolic syndrome.* J Clin Invest, 2004. **114**(12): p. 1752-61.
241. Krawczyk, S.A., et al., *Reactive oxygen species facilitate translocation of hormone sensitive lipase to the lipid droplet during lipolysis in human differentiated adipocytes.* PLoS One, 2012. **7**(4): p. e34904.
242. Naviaux, R.K., *Oxidative shielding or oxidative stress?* J Pharmacol Exp Ther, 2012. **342**(3): p. 608-18.
243. Riccioni, G., et al., *Carotenoids and vitamins C and E in the prevention of cardiovascular disease.* Int J Vitam Nutr Res, 2012. **82**(1): p. 15-26.
244. Lo Surdo, J. and S.R. Bauer, *Quantitative approaches to detect donor and passage differences in adipogenic potential and clonogenicity in human bone marrow-derived mesenchymal stem cells.* Tissue Eng Part C Methods, 2012. **18**(11): p. 877-89.
245. Gaiba, S., et al., *Characterization of human adipose-derived stem cells.* Acta Cir Bras, 2012. **27**(7): p. 471-6.
246. Hirzel, E., et al., *Characterization of human bone marrow-derived mesenchymal stem cells as model for adipogenesis and adipocytes.* Manuscript submitted.
247. Lowes, D.A., et al., *The mitochondria-targeted antioxidant MitoQ protects against organ damage in a lipopolysaccharide-peptidoglycan model of sepsis.* Free Radic Biol Med, 2008. **45**(11): p. 1559-65.
248. Lowes, D.A., et al., *A double-blind, placebo-controlled study to assess the mitochondria-targeted antioxidant MitoQ as a disease-modifying therapy in Parkinson's disease.* Mov Disord, 2010. **25**: p. 1670-1674.
249. Pervaiz, S. and A.L. Holme, *Resveratrol: its biologic targets and functional activity.* Antioxid Redox Signal, 2009. **11**(11): p. 2851-97.
250. Alappat, L. and A.B. Awad, *Curcumin and obesity: evidence and mechanisms.* Nutr Rev, 2010. **68**(12): p. 729-38.
251. Weber, W.M., et al., *TPA-induced up-regulation of activator protein-1 can be inhibited or enhanced by analogs of the natural product curcumin.* Biochem Pharmacol, 2006. **72**(8): p. 928-40.
252. Chun, K.S., et al., *Curcumin inhibits phorbol ester-induced expression of cyclooxygenase-2 in mouse skin through suppression of extracellular signal-*

regulated kinase activity and NF-kappaB activation. Carcinogenesis, 2003. **24**(9): p. 1515-24.
253. Zheng, S., F. Yumei, and A. Chen, *De novo synthesis of glutathione is a prerequisite for curcumin to inhibit hepatic stellate cell (HSC) activation.* Free Radic Biol Med, 2007. **43**(3): p. 444-53.
254. Jang, E.M., et al., *Beneficial effects of curcumin on hyperlipidemia and insulin resistance in high-fat-fed hamsters.* Metabolism, 2008. **57**(11): p. 1576-83.
255. Ramirez-Bosca, A., et al., *An hydroalcoholic extract of curcuma longa lowers the apo B/apo A ratio. Implications for atherogenesis prevention.* Mech Ageing Dev, 2000. **119**(1-2): p. 41-7.
256. Ramirez Bosca, A., et al., *An hydroalcoholic extract of Curcuma longa lowers the abnormally high values of human-plasma fibrinogen.* Mech Ageing Dev, 2000. **114**(3): p. 207-10.
257. Srinivasan, M., *Effect of curcumin on blood sugar as seen in a diabetic subject.* Indian J Med Sci, 1972. **26**(4): p. 269-70.
258. James, A.M., H.M. Cocheme, and M.P. Murphy, *Mitochondria-targeted redox probes as tools in the study of oxidative damage and ageing.* Mech Ageing Dev, 2005. **126**(9): p. 982-6.
259. James, A.M., et al., *Interaction of the mitochondria-targeted antioxidant MitoQ with phospholipid bilayers and ubiquinone oxidoreductases.* J Biol Chem, 2007. **282**(20): p. 14708-18.
260. Biswas, S.K., et al., *Curcumin induces glutathione biosynthesis and inhibits NF-kappaB activation and interleukin-8 release in alveolar epithelial cells: mechanism of free radical scavenging activity.* Antioxid Redox Signal, 2005. **7**(1-2): p. 32-41.
261. Beeson, C.C., G.C. Beeson, and R.G. Schnellmann, *A high-throughput respirometric assay for mitochondrial biogenesis and toxicity.* Anal Biochem, 2010. **404**(1): p. 75-81.
262. Lagouge, M., et al., *Resveratrol improves mitochondrial function and protects against metabolic disease by activating SIRT1 and PGC-1alpha.* Cell, 2006. **127**(6): p. 1109-22.
263. Ligeret, H., et al., *Fluoride curcumin derivatives: new mitochondrial uncoupling agents.* FEBS Lett, 2004. **569**(1-3): p. 37-42.
264. Szkudelska, K., L. Nogowski, and T. Szkudelski, *Resveratrol and genistein as adenosine triphosphate-depleting agents in fat cells.* Metabolism, 2011. **60**(5): p. 720-9.
265. Li, H., S. Horke, and U. Forstermann, *Oxidative stress in vascular disease and its pharmacological prevention.* Trends Pharmacol Sci, 2013. **34**(6): p. 313-9.
266. Mitchell, T., et al., *The mitochondria-targeted antioxidant mitoquinone protects against cold storage injury of renal tubular cells and rat kidneys.* J Pharmacol Exp Ther, 2011. **336**(3): p. 682-92.
267. Pung, Y.F., et al., *Resolution of mitochondrial oxidative stress rescues coronary collateral growth in Zucker obese fatty rats.* Arterioscler Thromb Vasc Biol, 2012. **32**(2): p. 325-34.
268. Gruber, J., et al., *Mitochondria-targeted antioxidants and metabolic modulators as pharmacological interventions to slow ageing.* Biotechnol Adv, 2012. **31**: p. in press.
269. He, H.J., et al., *Curcumin attenuates Nrf2 signaling defect, oxidative stress in muscle and glucose intolerance in high fat diet-fed mice.* World J Diabetes, 2012. **3**(5): p. 94-104.

270. Paravicini, T.M. and R.M. Touyz, *NADPH oxidases, reactive oxygen species, and hypertension: clinical implications and therapeutic possibilities.* Diabetes Care, 2008. **31 Suppl 2**: p. S170-80.
271. Waris, G. and H. Ahsan, *Reactive oxygen species: role in the development of cancer and various chronic conditions.* J Carcinog, 2006. **5**: p. 14.
272. Choi, S.W. and S. Friso, *Epigenetics: A New Bridge between Nutrition and Health.* Adv Nutr, 2010. **1**(1): p. 8-16.
273. Gerhauser, C., *Cancer chemoprevention and nutriepigenetics: state of the art and future challenges.* Top Curr Chem, 2013. **329**: p. 73-132.
274. Cantone, I. and A.G. Fisher, *Epigenetic programming and reprogramming during development.* Nat Struct Mol Biol, 2013. **20**(3): p. 282-9.
275. Shao, W., et al., *Curcumin prevents high fat diet induced insulin resistance and obesity via attenuating lipogenesis in liver and inflammatory pathway in adipocytes.* PLoS One, 2012. **7**(1): p. e28784.
276. Abdel Aziz, M.T., et al., *Effect of novel water soluble curcumin derivative on experimental type- 1 diabetes mellitus (short term study).* Diabetol Metab Syndr, 2012. **4**(1): p. 30.
277. Lim, S., et al., *Mitochondria-targeted antioxidants protect pancreatic beta-cells against oxidative stress and improve insulin secretion in glucotoxicity and glucolipotoxicity.* Cell Physiol Biochem, 2011. **28**(5): p. 873-86.
278. Chacko, B.K., et al., *Prevention of diabetic nephropathy in Ins2(+/)(-)(AkitaJ) mice by the mitochondria-targeted therapy MitoQ.* Biochem J, 2010. **432**(1): p. 9-19.
279. Qian, S.W., et al., *Characterization of adipocyte differentiation from human mesenchymal stem cells in bone marrow.* BMC Dev Biol, 2010. **10**: p. 47.
280. Di Girolamo, M. and D. Rudman, *Species differences in glucose metabolism and insulin responsiveness of adipose tissue.* Am J Physiol, 1966. **210**(4): p. 721-7.
281. Imhoff, B.R. and J.M. Hansen, *Extracellular redox environments regulate adipocyte differentiation.* Differentiation, 2010. **80**(1): p. 31-9.
282. Lechpammer, S., et al., *Adipocyte differentiation in Sod2(-/-) and Sod2(+/+) murine bone marrow stromal cells is associated with low antioxidant pools.* Exp Hematol, 2005. **33**(10): p. 1201-8.
283. Gregoire, F.M., C.M. Smas, and H.S. Sul, *Understanding adipocyte differentiation.* Physiol Rev, 1998. **78**(3): p. 783-809.
284. Timchenko, N.A., et al., *CCAAT/enhancer-binding protein alpha (C/EBP alpha) inhibits cell proliferation through the p21 (WAF-1/CIP-1/SDI-1) protein.* Genes Dev, 1996. **10**(7): p. 804-15.
285. Altiok, S., M. Xu, and B.M. Spiegelman, *PPARgamma induces cell cycle withdrawal: inhibition of E2F/DP DNA-binding activity via down-regulation of PP2A.* Genes Dev, 1997. **11**(15): p. 1987-98.
286. Bjorntorp, P., *Effects of age, sex, and clinical conditions on adipose tissue cellularity in man.* Metabolism, 1974. **23**(11): p. 1091-102.
287. Kubota, N., et al., *PPAR gamma mediates high-fat diet-induced adipocyte hypertrophy and insulin resistance.* Mol Cell, 1999. **4**(4): p. 597-609.
288. Ducluzeau, P.H., et al., *Dynamic regulation of mitochondrial network and oxidative functions during 3T3-L1 fat cell differentiation.* J Physiol Biochem, 2011. **67**(3): p. 285-96.
289. Wilson-Fritch, L., et al., *Mitochondrial biogenesis and remodeling during adipogenesis and in response to the insulin sensitizer rosiglitazone.* Mol Cell Biol, 2003. **23**(3): p. 1085-94.

290. von Heimburg, D., et al., *Oxygen consumption in undifferentiated versus differentiated adipogenic mesenchymal precursor cells.* Respir Physiol Neurobiol, 2005. **146**(2-3): p. 107-16.
291. Elabd, C., et al., *Human multipotent adipose-derived stem cells differentiate into functional brown adipocytes.* Stem Cells, 2009. **27**(11): p. 2753-60.

Acknowledgements

I would like to address my special thanks to Prof. Alex N. Eberle who gave me the opportunity to work in this interesting field. He gave me the chance to develop a critical, scientific way of thinking and to broaden my knowledge. You allowed me to make my own experiences and to work in great latitude. Thank you for your support and advice during the thesis and for your encouragement and patience during the very difficult times I also encountered. You still believed in me when I was close to give up. I would also like to thank Dr. Peter Lindinger for his practical help and teaching in the lab. He showed me so many important techniques and always encouraged me when an experiment failed. You were always present for answering questions, giving advice and for helpful discussions. I also thank Dr. Martine Calame, Heidi Tanner, Verena Jäggin and Jean-Philippe Bapst for the pleasant atmosphere during work. I'm looking forward to the next time of our traditional "Ueli Bier" meeting.

My special thanks go the Prof. Stephan Krähenbühl who gave me the opportunity to finish my thesis in his lab. His advice and fair comment allowed me to critically analyze my work. In particular I thank him for his help in the last phase of the thesis, for guiding me to a successful end. Thank you for all your time you invested in my work, your support and for accepting the co-report.

I also thank all the lab members of the group for Clinical Pharmacology and Toxicology. You were always willingly to help when I needed you. Thank you Swarna, Réjane, Linda, Andrea, Pete, Annalisa, Anja, Massimiliano, Bea and Karin for the nice atmosphere during work. We had a great time together, not only in the lab but also during free time. I enjoyed playing squash, savoring Indian dinners and doing many other things with you.